Reconstitution of bacterial lipopolysaccharide transport from purified components

Reconstitution of bacterial lipopolysaccharide transport from purified components

A dissertation presented

by

David Joseph Sherman

to

The Department of Chemistry and Chemical Biology

in partial fulfillment of the requirements
for the degree of
Doctor of Philosophy
in the subject of

Chemistry

Harvard University
Cambridge, Massachusetts
May 2015

Dissertation Advisor: Professor Daniel Kahne David Joseph Sherman

Reconstitution of bacterial lipopolysaccharide transport from purified components

Abstract

The surface of Gram-negative bacteria is largely composed of lipopolysaccharide (LPS), a complex glycolipid that contains multiple fatty acyl chains and up to hundreds of sugars. LPS is transported from its site of synthesis at the cytoplasmic inner membrane (IM), across an aqueous compartment (the periplasm), and through the outer membrane (OM) to the cell surface. LPS is essential for the survival of most Gram-negative bacteria. Seven essential and conserved lipopolysaccharide transport (Lpt) proteins in *Escherichia coli* are responsible for assembling LPS. These proteins form a continuous bridge from the IM to the OM, but it is unknown how they function in LPS transport.

This dissertation describes the development of a reconstitution of LPS transport using purified Lpt proteins. The first two steps of this process are extraction of LPS from the IM by LptBFGC and transport along the periplasmic bridge comprising LptA. We obtained high-resolution crystal structures of the ATPase LptB, which taught us how to overexpress and purify LptBFGC as a stable complex that is highly active in proteoliposomes. Crystallographic snapshots of LptB bound to ATP and ADP provided insight into how energy is used to extract the fatty acyl chains of LPS from the IM. Using site-specific photocrosslinking, we monitored ATP-dependent extraction of LPS from proteoliposomes by LptC and release to LptA. This reconstitution of LptBFGC led to a hypothesis about a role for LptC in regulating the activity of

the Lpt IM complex. We also developed methods to reconstitute the late steps of transport by monitoring LPS transit from LptA to the OM components, LptDE, contained in a different proteoliposome. One important observation from this reconstitution is that it appears as though the OM translocon can change activity depending on the amount of LPS in the OM. These studies provide us with the first clues as to how the cell might regulate LPS flux to the cell surface. This reconstitution will allow for mechanistic studies of LPS transport and will aid in the discovery and development of antibiotics targeting this essential process.

Table of Contents

List of Figures

Acknowledgements

Graduate school does not happen in a vacuum, and I am very appreciative of the kind and generous support of so many people. I am grateful for the unconditional encouragement of my advisor, Dan Kahne. Dan is an inspiring mentor, and I admire his creativity and ability to think outside of the box about scientific problems. He has given me enough freedom to take my project in new directions while remaining interested and encouraging. Dan has been helpful and thoughtful both academically and personally. It is unusual to have a graduate advisor who cares so much about his students as people, and I look forward to my continuing friendship with Dan.

I have also been fortunate to have the support of other great faculty members, from Harvard and elsewhere. Chris Walsh, Rachelle Gaudet, and Greg Verdine have served on my graduate advising committee over the years, and they have offered a lot of valuable advice about the overall direction of my project as well as other possible interpretations of my data. I am thankful that Chris Walsh agreed to stay on my committee, attending my annual committee meetings and final defense, after retiring. I am also indebted to Suzanne Walker and Natacha Ruiz (OSU), who have been innovative collaborators on various projects. They are critical within reason and always honest when discussing science. I really appreciate these qualities, as I do all of their advice and encouragement over the years.

I was fortunate to work closely with Suguru Okuda, a former post-doc in the lab. I respect Suguru tremendously as a scientist, and he had a huge influence on my approach to lab research. I enjoyed working with Suguru on the Lpt IM complex for some time, and I feel lucky to have inherited the Lpt reconstitution project from him. He has been helpful and patient with

me over the years, and I look forward to our continuing friendship, even though he is back in Japan now.

There have been many other former graduate students in the Kahne Lab who have been very influential. Mike Lazarus was fun to work with when I started to crystallize LptB. Mike was the "resident crystallographer" in the lab, and he was also very patient with me as I began to tackle a technique that I knew nothing about at the time. Likewise, Luisa Gronenberg was helpful in getting me started with my project in the lab. Luisa was fun to be around, so I was happy to originally learn the ropes around lab from her.

Helen Corriero and Mike Quinn have also been instrumental in my experience in the Kahne Lab (and in graduate school in general). They keep the lab operating everyday, and Helen has become my "Lab Mum," as she says. I am incredibly grateful for all that they have done to help me over the years, as well as for their kind encouragement and support. Helen has helped me during particularly challenging times.

More recently, I have been fortunate to work with a close friend in the lab, Janine May. Janine and I have been friends at Harvard since even before she joined the Kahne Lab five years ago, and she is a huge support. She has kept me sane during otherwise insane times. In the last few years, she began working with me on the Lpt IM complex, and it has been a pleasure to do experiments with her now, too!

Tania Lupoli and Christine Hagan are former graduate students in the Kahne Lab who inspired me, mentored me in various ways, and have also been good friends. Outside of lab, I was fortunate to make many great friends in the graduate school community. These friends have been instrumental in shaping my graduate school experience and have been there for me when

I've really needed them. It has been very special to have a community to escape to outside of the department.

I am fortunate to remain in touch with many supportive friends from other times in my life. These friends are very important to me and have helped me get through difficult times in graduate school, even if they were not physically in Cambridge (though many visited!).

Finally, I would like to acknowledge my amazing family. My parents, Nancy and Jerry, have always been encouraging and loving. I couldn't be where I am today without their constant support. I am also grateful for my two fantastic brothers, Josh and Michael, who are caring, fun, and motivating. I am incredibly thankful to have such a good family. My grandparents, Bud, Essie, Ruth, and Morris, were loving and supportive over the years. I wish that all four of them could be here with me today to celebrate the finishing of my PhD. My grandmother, Essie, passed away from a bacterial infection while I was in graduate school, and this loss added a deep personal component to my desire to establish the Lpt pathway as an antibiotic target.

Chapter One

Introduction to Lipopolysaccharide Transport and Assembly in *Escherichia coli*

1.1 The Cell Envelope of Gram-Negative Bacteria

Gram-negative bacteria such as *Escherichia coli* are faced with the problem of surviving in unpredictable and often hostile environments, such as the mammalian gut (1). These organisms have therefore evolved a protective cell envelope that allows for clear separation between the intracellular space and the outside environment. The Gram-negative cell envelope consists of three compartments. The inner membrane (IM) is a traditional phospholipid bilayer enclosing the aqueous cytoplasm of the cell (Figure 1.1). The IM contains integral α-helical membrane proteins and lipoproteins that serve important roles in transport and cellular processes such as oxidative phosphorylation and lipid biosynthesis (2). This membrane also maintains a proton motive force and functions in ATP synthesis, like the eukaryotic plasma membrane (3). Outside the IM is the aqueous periplasmic compartment. The periplasm contains a thin peptidoglycan layer, commonly known as the cell wall, which is essential for maintaining the cell's shape and for survival under osmotic stress (4). Notably, the periplasm is devoid of any apparent chemical energy source, such as adenosine triphosphate (ATP); therefore, all processes that occur in the periplasm must either have no chemical energy requirement or be coupled to intracellular processes. The periplasmic compartment is enclosed by the outer membrane (OM), which serves as the final interface between the cell and the external environment.

The main function of the OM is to provide a selective permeability barrier, controlling traffic into and out of the cell (5). Like most biological membranes, the OM prevents passage of large, hydrophilic molecules into the cell; however, unlike most membranes, the OM also prevents the rapid diffusion of small hydrophobic molecules. Therefore, this membrane does not allow for entry of most clinically used antibiotics into Gram-negative cells (2).

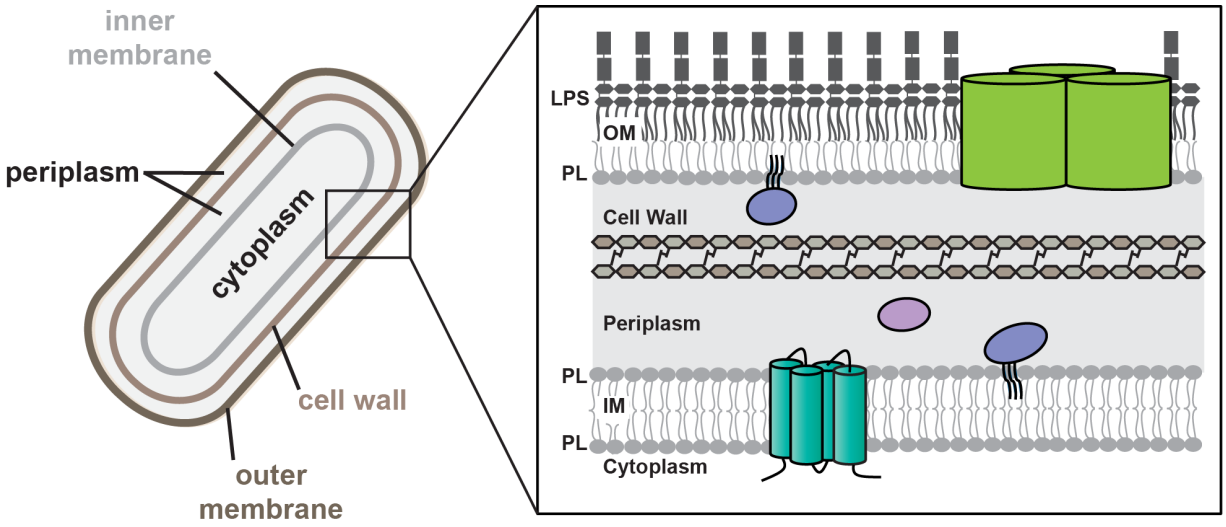

Figure 1.1. Gram-negative bacteria possess a double-membrane architecture. Surrounding the cytoplasm is the inner membrane (IM), which contains α-helical membrane proteins and lipoproteins. Outside the IM is the aqueous periplasm, which contains soluble proteins and the cell wall (made of peptidoglycan). The periplasm is enclosed by the OM, an asymmetric lipid bilayer with phospholipids (PL) in the inner leaflet and lipopolysaccharide (LPS) in the outer leaflet. The OM also contains β-barrel membrane proteins and lipoproteins.

The unusual barrier function of the OM is a result of its structure (Figure 1.1). Unlike most biological membranes, the OM is an asymmetric lipid bilayer with phospholipids in its inner leaflet and lipopolysaccharide (LPS) in its outer leaflet (6, 7). In *E. coli*, LPS occupies nearly three fourths of the outer cell surface area (8). LPS is a complex glycolipid containing fatty acyl chains that anchor it to the membrane and up to hundreds of sugar residues (Figure 1.2). Lipid A is the glucosamine-based lipid anchor of LPS that is conserved across most Gram-negative organisms (9). Lipid A is also known as endotoxin because it is responsible for activation of the mammalian innate immune response (9, 10). Overall, the biosynthetic pathway of lipid A is highly conserved, but modifying enzymes exist that create diversity in lipid A structures depending on the environmental circumstances of specific organisms (9-11). In *E. coli*, lipid A is typically bound to two Kdo (3-deoxy-D-*manno*-oct-2-ulosonic acid) sugars (9). In many strains, Kdo_2-lipid A (also known as Re-LPS) is further glycosylated with a core

oligosaccharide, which can also be glycosylated with an O-antigenic polysaccharide (O-antigen) (8, 9). The more variable O-antigen is responsible for interactions of the organisms with their environments, including host defenses. Genetic mutations affecting O-antigen biosynthesis in Gram-negative bacteria have been shown to result in loss of virulence (8, 9).

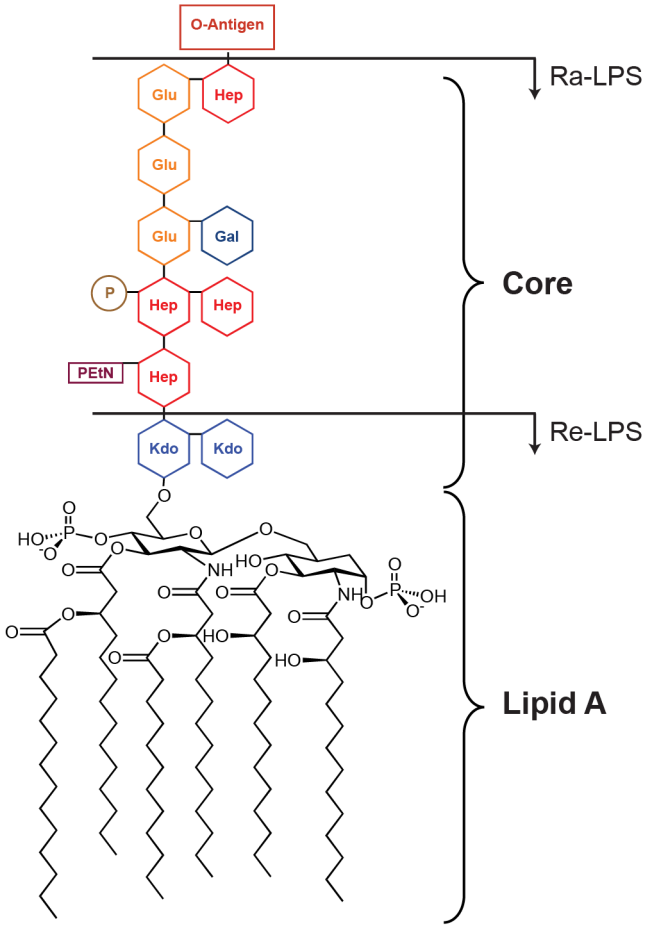

Figure 1.2. LPS from *E. coli* K-12 is composed of lipid A (endotoxin) and the core oligosaccharide. LPS is first synthesized as Re-LPS. The addition of the core sugars results in Ra-LPS, which can be further modified with an O-antigen (not present in *E. coli* K-12). EtN, ethanolamine; Gal, D-galactose; Glu, D-glucose; Hep, L-glycero-D-mannoheptose; Kdo, 3-deoxy-D-*manno*-oct-2-ulosonic acid; P, phosphate.

Lipid A and the inner core residues of LPS are primarily responsible for creating the barrier-like quality of the OM. There is remarkable diversity in O-antigen structures between

strains, largely predicted to be the result of different selective pressures (8). Many laboratory strains of *E. coli*, such as K-12, contain LPS lacking the O-antigen, a form called rough LPS (Figure 1.2). Therefore, the more conserved portions of LPS provide it with the physical properties necessary to establish a permeability barrier. Lipid A generally contains more fatty acyl chains than phospholipids; in *E. coli*, this number is usually six or seven (Figure 1.2). Negatively charged phosphate groups in lipid A are bridged by metal cations, such as magnesium and calcium, which prevent electrostatic repulsion between individual molecules (5, 12, 13). These properties allow LPS to form a tightly packed polyelectrolyte mesh at the cell surface of Gram-negative bacteria.

The Gram-negative cell envelope consists of three major compartments (IM, periplasm, and OM), each of which has a unique composition. All components of these compartments are biosynthesized entirely in the cytoplasm or at the IM. Therefore, an interesting question is how the OM is properly assembled with all of the correct components and the proper asymmetry (phospholipids in the inner leaflet and LPS in the outer leaflet). It is unclear how LPS, which contains multiple lipids and up to hundreds of sugar residues, is transported from its site of synthesis inside the cell against a concentration gradient to the cell surface.

1.2 Outer Membrane Biogenesis in *E. coli*

The OM is composed primarily of phospholipids, LPS, and two types of OM proteins (OMPs): lipoproteins and integral membrane proteins. Unlike integral IM proteins, which span the membrane with hydrophobic α-helices, OMPs adopt a structure in which antiparallel, amphipathic β-strands fold into a barrel-like structure with hydrophilic residues facing the lumen of the barrel and hydrophobic residues facing the lipidic membrane environment. OMPs serve a

variety of functions, including passive diffusion of nutrients (5), drug efflux (14), and assembly of the OM itself (15, 16). Each OM component must somehow be transported from the IM to its final destination at the OM. Although there is no known pathway for transporting phospholipids from the IM to the OM (3), pathways responsible for transporting and assembling lipoproteins (2, 17-25), β-barrel membrane proteins (2, 26-35), and LPS (2, 15, 16, 36-42), have been identified and characterized (Figure 1.3). Because an intact OM is essential for the survival of Gram-negative bacteria, these pathways must be carefully coordinated to generate an effective permeability barrier during each cell division cycle.

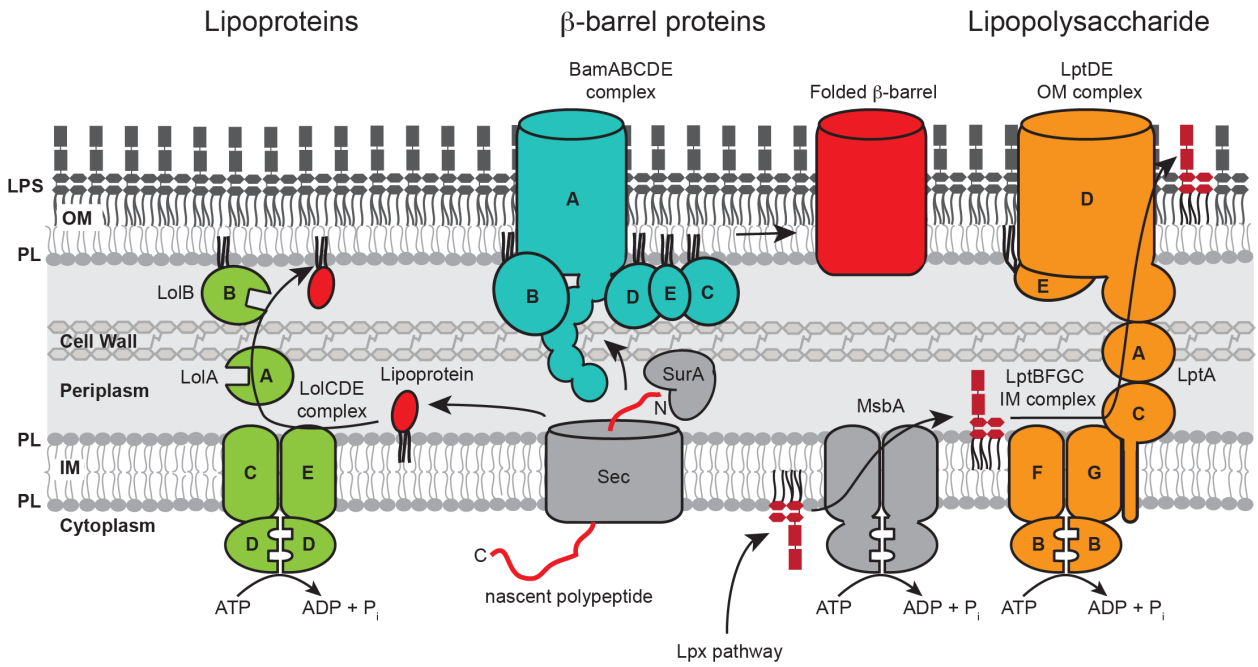

Figure 1.3. The pathways responsible for OM biogenesis in *E. coli* are integrated. Both lipoproteins and β-barrel OMPs are synthesized in the cytoplasm and transported across the IM by the secretory (Sec) machinery. At this point, nascent OM lipoproteins are further processed and transported to the OM by the Lol pathway (*left*), and unfolded β-barrel proteins are translocated across the periplasm by soluble chaperone proteins (mainly SurA) (*center*). β-barrels are folded and assembled into the OM by the Bam complex. LPS is synthesized in the cytoplasm by the Lpx proteins; it is subsequently flipped to the outer leaflet of the IM by MsbA and translocated to the cell surface by the Lpt pathway (*right*).

1.2.1 Outer Membrane Protein Assembly in *E. coli*

OMPs are either lipoproteins or β-barrel integral membrane proteins. All integral membrane proteins, both in the IM and the OM, must internally satisfy the hydrogen bonds of their amide backbones to exist in a hydrophobic, lipidic environment. Unlike the α-helical membrane proteins found in the IM, which form hydrogen bonds between proximal amino acids, β-barrel OMPs must form hydrogen bonds between distal residues in order to close into a cylindrical barrel. Lipoproteins are soluble proteins with fatty acyl chains on their N-terminal cysteine residues that anchor them to the membrane (43). Lipoproteins are processed to their mature form at the IM, requiring them to be chaperoned to the OM and then inserted into the membrane, facing the periplasm (19, 43). Every protein destined for the OM is synthesized by the ribosome in the cytoplasm as a precursor with an N-terminal signal peptide and is post-translationally transported across the IM by the secretory (Sec) machinery (44-49). OMP translocation through the Sec machinery is energized by the ATPase SecB (50). Once translocated to the periplasmic side of the IM, OM-destined lipoproteins and β-barrel proteins are transported and assembled by distinct pathways.

1.2.1.1 Lipoprotein Transport

Bacterial OM lipoproteins have a variety of cellular functions, including assembling and maintaining the OM (2, 33, 41). Because lipoproteins serve important roles, the proteins responsible for processing, transporting, and assembling them are essential for growth in *E. coli* and are highly conserved in Gram-negative bacteria (17, 18). Lipoprotein precursors synthesized in the cytoplasm contain a consensus sequence near their signal peptide cleavage site called a lipobox (17). After lipoproteins are processed into their mature form on the periplasmic side of

the IM, they are recognized and transported to the OM by the Lol (localization of lipoprotein) machinery (18). The Lol system in *E. coli* consists of five proteins, LolABCDE (Figure 1.3). These proteins are responsible for releasing lipoproteins from the periplasmic face of the IM in an ATP-dependent manner, chaperoning them to the OM, and inserting them into the inner leaflet of the OM (21-23).

ATP hydrolysis in the cytoplasm is coupled to release of lipoproteins from the opposite side of the IM. This process is catalyzed by the ATP-binding cassette (ABC) transporter LolCDE (20, 22). LolD is a cytoplasmic membrane-associated protein responsible for ATP binding and hydrolysis, and LolC and LolE are integral membrane proteins that interact with two copies of LolD to couple cytoplasmic ATP hydrolysis to lipoprotein release. This nucleotide-binding domain/transmembrane domain architecture is typical for ABC transporters, which comprise one of the largest protein superfamilies across all domains of life (51, 52); these systems will be discussed in more detail in later sections. An aspartate residue at the second position of mature lipoproteins in *E. coli* serves as a LolCDE-avoidance signal, indicating that the lipoprotein should be retained in the IM (17, 53).

The current model for lipoprotein transport and assembly begins with lipoproteins on the periplasmic side of the IM interacting with the ABC transporter LolCDE. Lipoprotein interaction with LolCDE increases the binding affinity of LolD for ATP. LolA, a soluble periplasmic chaperone protein, interacts with LolCDE. ATP binding to LolD decreases the affinity of the complex for the bound lipoprotein, and ATP hydrolysis by LolD allows for the lipoprotein to be transferred to LolA (19, 21, 22, 54). Despite dissimilar primary amino acid sequences, LolA and the OM receptor protein LolB have similar secondary structures consisting of incomplete β-barrels with α-helical lids (55). The structures reveal a hydrophobic channel for

these proteins to bind the fatty acyl chains of lipoproteins (55). Site-specific crosslinking studies guided by these crystal structures led to the model that LolA and the final protein in the pathway, LolB, interact in a "mouth-to-mouth" manner in which lipoproteins are transferred from the hydrophobic cavity of LolA to the hydrophobic cavity of LolB (18, 24). Differential affinity for lipoproteins is thought to drive passive transport of lipoproteins from LolA to LolB (56). LolB is then responsible for inserting lipoproteins into the inner leaflet of the OM by an unknown mechanism (18). The first of the three OM biogenesis pathways to be studied, the Lol system proves to be important not only for the existence of the pathway itself, as LolB is a lipoprotein, but also for the existence of the other two major pathways involved in OM biogenesis, which assemble β-barrels and LPS.

1.2.1.2 β-Barrel Transport and Assembly

β-barrels serve important functions in the OM as channels through which solutes and nutrients can pass into the cell and waste products can exit the cell. Unfolded β-barrel proteins are translocated through the Sec machinery, their signal sequences are cleaved by the signal peptidase, and they are transported across the aqueous periplasm in a folding-competent state by chaperone proteins (33, 57). The chaperone responsible for transporting the majority of β-barrel proteins is SurA, with periplasmic proteins Skp and DegP believed to compensate for SurA deficiencies and for substrates that have fallen off the SurA pathway (58).

The next step of β-barrel assembly was less well understood until the last decade or so, when the major complex that catalyzes this process was discovered in *E. coli*. The five proteins responsible for β-barrel assembly are collectively called the Bam (β-barrel assembly machine) complex, comprising BamABCDE (Figure 1.3). The central component of the pathway, BamA,

is itself an essential β-barrel protein conserved in all Gram-negative organisms, with orthologs in the mitochondria and chloroplasts of higher eukaryotes (27, 31, 33, 59, 60). BamA contains a soluble periplasmic domain comprised of five polypeptide transport-associated (POTRA) domains. These allow for BamA to interact with the other Bam components and are thought to play roles in recognizing unfolded OMPs and aiding with membrane assembly (27, 33, 61-63). BamA stably associates with four lipoproteins (BamB, -C, -D, and -E), only one of which (BamD) is essential in *E. coli* (29, 30, 32-34). Considering that β-barrel recognition, folding, and insertion into the OM must be a complex, multi-step process, it is not surprising that although there are only two essential Bam components, deletions of BamB, BamC, or BamE result in lower levels of folded OMPs, an OM stress response, and increased membrane permeability to antibiotics (30, 32, 33).

Since the identification of the Bam components, remarkable progress has been made in understanding β-barrel folding and insertion into the OM. A major advance in this area was the development of an *in vitro* reconstitution of β-barrel assembly into proteoliposomes, which was used to demonstrate that there is no energy requirement for β-barrel folding and insertion into a membrane in the presence of an intact Bam complex, as long as a soluble chaperone delivers unfolded polypeptides to Bam (64, 65). Although the individual steps required for assembly remain unclear, progress has been made towards understanding the functions of specific components, specifically how Bam lipoproteins assemble BamA (66). The other essential β-barrel protein assembled by the Bam complex, LptD, is a component of the LPS assembly pathway, described below.

1.2.2 Overview of LPS Biogenesis in *E. coli*

1.2.2.1 Kdo_2-Lipid A Biosynthesis

The development of sucrose density gradient centrifugation allowed for Mary Jane Osborn and colleagues to separate the IM and OM fractions of *Salmonella typhimurium* and to initially assign the location of ninety percent of the total membrane LPS to the OM (67). In combination with pulse-chase experiments, this technique also allowed them to be the first to suggest that LPS is synthesized at the IM and transported unidirectionally to the OM by some unknown mechanism (68). Following these seminal discoveries in the early 1970's, Osborn, Raetz, and colleagues spent the following decades elucidating the conserved pathway required for Kdo_2-lipid A biosynthesis in *E. coli* and *S. typhimurium* (8, 9, 69-86).

The Kdo_2-lipid A biosynthetic pathway involves nine enzymatic steps catalyzed by Lpx proteins. The first enzyme in the pathway, LpxA, is responsible for acylating the 3-hydroxyl group of uridine diphosphate-*N*-acetylglucosamine (UDP-GlcNAc) (74, 86). The first four pathway steps, including this initial acylation step, result in the production of 2,3-diacylglucosamine-1-phosphate, or lipid X. Lipid X is subsequently condensed with a molecule of UDP-2,3-diacylglucosmine (the precursor to lipid X), which is phosphorylated to form lipid IV_A (8, 9). There is evidence that challenges the long-standing belief that Kdo_2-lipid A is the minimal LPS requirement for *E. coli* viability, as a strain was constructed that transports lipid IV_A, lacking the Kdo sugars, to the cell surface (87). In fact, lipid IV_A has been demonstrated to have some of the same endotoxin effects as Kdo_2-lipid A (9). The remaining steps in the pathway result in the glycosylated product Kdo_2-lipid IV_A, which is acylated twice to form Kdo_2-lipid A (8, 9).

Considering their essentiality, conservation, and lack of mammalian homologs, the enzymes in the Raetz pathway are viable targets for antibiotic development. There has been considerable effort to develop inhibitors of LpxC (88-94), the second enzyme in the pathway that catalyzes the first committed step of Kdo_2-lipid A biosynthesis (9, 73, 75). LpxC is a zinc metalloenzyme that does not contain characteristic zinc-binding motifs. The three-dimensional structure of LpxC has been resolved by X-ray crystallography, greatly aiding in the development and validation of this enzyme as a drug target (95).

Following Kdo_2-lipid A biosynthesis, which occurs on the cytoplasmic face of the IM, inner and outer core oligosaccharides are added sequentially by glycosyltransferases to form Ra-LPS (8, 9). The final component of LPS to be added in its biosynthesis is the O-antigen polysaccharide. Early evidence from immuno-electron microscopy suggested that the O-antigen is ligated to rough LPS on the periplasmic face of the IM (96). Therefore, rough LPS must be flipped across the IM to the outer leaflet prior to O-antigen ligation. Flipping a large glycolipid across the IM for O-antigen ligation and then transport is an energetically unfavorable process because the core sugar residues prefer to be exposed to water than to the hydrophobic membrane environment. Therefore, there must be energy input for this step (97).

1.2.2.2 LPS Flipping Across the IM

The homodimeric ABC transporter MsbA is now known to be responsible for flipping rough LPS across the IM (8, 9, 41). The gene encoding MsbA was first discovered as a multicopy suppressor of *lpxL* (formerly *htrB*) mutations (98). It was identified as an essential gene in *E. coli* encoding an ABC transporter thought to be involved in LPS and glycerophospholipid transport, as MsbA depletion results in a buildup of these components in the

IM (98-100). Importantly, *msbA* does not suppress null mutations in *lpxL* by performing the same lauroyl transferase function as LpxL; rather, the suppression results in an increase in immature, tetra-acylated lipid A at the cell surface. Therefore, MsbA was thought to play a role in LPS transport. The role of MsbA in phospholipid transport was challenged soon after this function was initially proposed (101-103). Overexpression, purification, and reconstitution of MsbA *in vitro* demonstrated that it exhibits ATPase activity both in detergent solution and in proteoliposomes, as expected for an ABC transporter (104). In a reconstituted system, hexa-acylated Kdo_2-lipid A stimulated its ATPase activity four- to five-fold. These results provided the first *in vitro* evidence that MsbA is a lipid A-stimulated ATPase.

In vivo experiments utilizing covalent lipid A modifications that only occur on the periplasmic side of the IM provided the first evidence that MsbA functions specifically as the lipid A flippase in the IM (105). Multiple crystal structures of MsbA in the apo state and bound to nucleotides, obtained from three closely related bacterial orthologs, reveal major conformational changes of the flippase that might correspond to structural changes necessary to flip a large glycolipid (106). Biophysical studies suggest that MsbA samples even more conformations during its catalytic cycle (107-109). Functional studies have also characterized the interaction of MsbA with nucleotides and substrates, and how these interactions might relate to conformational changes of the transporter (110-113). Like other ABC transporters, MsbA contains one polypeptide chain with a nucleotide-binding domain (NBD) fused to a transmembrane domain (TMD) with six α-helices, which dimerizes to form the functional transporter (52). There has been much interest in studying the function and mechanism of MsbA because it shows high primary sequence identity with the human multidrug resistance transporter 1 (P-glycoprotein) and with a transporter responsible for multidrug resistance in *Lactococcus*

lactis (LmrA) (52, 106, 114). The MsbA structure also shows similarity to structures of other human and bacterial multidrug exporters (52, 115, 116). Therefore, it is not surprising that MsbA has been found to transport drugs *in vitro*, with overlapping substrate specificity with LmrA (114, 117, 118). The abundance of work related to the ubiquitous ABC transporter family of proteins to which MsbA belongs will be discussed more in Chapter 2.

1.2.2.3 O-Antigen Ligation and Lipid A Modifications

In bacterial strains that contain LPS with an O-antigen, the O-antigen is biosynthesized separately from the rest of the LPS molecule in the cytoplasm and flipped independently to the outer leaflet of the IM. Synthesis of the O-antigen occurs by one of three pathways: the Wzy-, ABC transporter-, or synthase-dependent pathway. Each of these pathways culminates in the glycosylation of Ra-LPS with the O-antigen in the periplasm by the O-antigen ligase, WaaL (8, 9). In addition to modification with the O-antigen, the lipid A core of LPS can be covalently modified to preserve OM integrity and to counter the host immune response in different bacterial species (10). Many of the enzymes involved in modifying lipid A reside on the periplasmic side of the IM or at the OM (8, 9). These modifications provide an additional level of diversity amongst Gram-negative organisms, contribute to their pathogenicity, and allow for greater adaptability under a variety of conditions. These modifications can also be used as biological tools to study the localization of LPS in different compartments or leaflets of a membrane.

1.2.2.4 LPS Transport to the Cell Surface

It was only in the last decade or so, well after the discovery of the Raetz pathway and MsbA, that the proteins responsible for transporting LPS to the cell surface were identified in *E.*

coli by Kahne, Silhavy, and colleagues. These seven proteins are essential and conserved in most Gram-negative organisms (41, 42). They are known as the lipopolysaccharide transport (Lpt) proteins, and they comprise a distinct pathway from the Lpx biosynthetic pathway described above. The fact that LPS biosynthesis and transport/assembly are separated into different pathways allows for multiple levels of regulation and coordination, which is likely necessary to ensure proper assembly of millions of LPS molecules on the cell surface during each division cycle. The Lpt components reside in every cell envelope compartment: the IM, periplasm, and OM (41, 42). It is not surprising that a pathway exists to transport and assemble LPS on the cell surface, as such a process cannot occur passively. The steps involved in this process are: extraction of a large amphipathic molecule from one membrane, passage through a soluble compartment, and insertion across another membrane. Additionally, because there is no ATP present in the periplasm, LPS transport is believed to be coupled to ATP hydrolysis in the cytoplasm (41, 42). Originally, the major question in the field of LPS biogenesis was: what are the protein components involved in LPS biogenesis, and how do they interact? Now, it is believed that the proteins responsible for LPS transport and assembly have all been identified, and we have a model and structural information to help us understand how they interact. Therefore, the current big question is: how do these proteins work to transport and assemble LPS? We now have a model to explain the role of ATP in LPS transport (119), but there is no clear model to explain how this complex process works.

1.3 Discovery of the Lpt Pathway

The Lpt proteins were discovered using a combination of genetic, biochemical, and bioinformatic approaches (41). LptD was the first Lpt component to be identified in 1989; the

gene encoding this protein was found in a genetic selection that took advantage of the barrier function of the OM (120). The selection was designed to find mutations that allow for *E. coli* to grow on large maltodextrins in the absence of a functional OM maltodextrin transporter, LamB. Two mutations were identified that mapped to a locus that they called *imp* (increased membrane permeability), which was later renamed *lptD*. In addition to allowing for entry of large maltodextrins, these mutations increased the cell's permeability to detergents, antibiotics, and dyes that normally cannot penetrate the OM. Therefore, it appeared that mutations in this newly identified essential gene result in perturbations in OM integrity. It was not until 2002 that it was shown that *lptD* is involved in cell envelope biogenesis (16). The observations that led to this initial hypothesis were that *lptD* is located upstream of *surA*, the gene encoding a chaperone involved in OMP biogenesis, and the two are co-transcribed. Additionally, *lptD* is under control of the σ^E regulon, which is typically activated in times of periplasmic stress (121). LptD was confirmed to be an essential OMP that, when depleted, causes accumulation of lipids and OMPs in a novel membrane fraction denser than the OM (16).

Soon after it was suggested that LptD is involved in OM biogenesis, a role for LptD in LPS biogenesis at the cell surface was identified (15). This initial discovery was made in *Neisseria meningitidis*, which is a unique Gram-negative organism that can survive without LPS (122). Therefore, phenotypes can be observed in strains lacking LPS biogenesis factors. After establishing that *lptD* is not essential in *N. meningitidis*, it was shown that strains lacking the LptD ortholog do not localize LPS to the cell surface based on a series of experiments involving LPS-modifying enzymes in the OM or added in the extracellular medium (15).

Biochemical studies showed that LptD forms a stable complex with the outer membrane lipoprotein LptE (formerly RlpB) (40). An affinity tag purification of LptD indicated that it pulls

down LptE; additionally, an affinity tag on LptE pulls down LptD. The *lptE* gene is essential in *E. coli*, and cells depleted of LptD or LptE result in similar phenotypes, including the formation of abnormal membrane structures and buildup of phospholipids in the outer leaflet of the OM. Finally, using a pulse-labeling experiment, it was found that newly synthesized LPS does not reach the cell surface in LptD- or LptE-depleted cells (40). Because OmpA and LamB are found at the OM in these depletion strains, OMP and LPS biogenesis must occur independently, even though there is likely coordination to ensure proper envelope assembly during each cell division cycle. Therefore, LptD and LptE co-purify as a complex that must function in what might be the final step of LPS assembly at the OM (40).

The genes encoding LptA and LptB (formerly YhbN and YhbG, respectively) were initially discovered because they are part of a conserved locus with genes responsible for Kdo biosynthesis (39). These genes are essential and co-transcribed, and their depletion results in increased membrane permeability to hydrophobic molecules that ordinarily cannot penetrate the OM. This phenotype is typical of cells with a defective OM; therefore, it was suggested that these proteins are involved in cell envelope biogenesis. Although its function was unknown, LptB was identified as a soluble protein associated with other, unidentified IM proteins (123), and LptA was identified as a periplasmic protein (37). Like *lptD*, *lptA* and *lptB* are under σ^E regulation. Additionally, pulse-labeling of LPS indicated that newly synthesized LPS does not reach the OM in strains depleted of LptA and LptB, or either individual protein (37). In these depletion strains, electron micrographs revealed membrane aberrations and newly synthesized proteins and lipids accumulated in a novel membrane fraction. Sequence analysis suggested that LptB belongs to the ABC transporter family, and it contains an ATP-binding fold but not a TMD (37, 123). An early model was proposed in which LptB and LptA form an IM complex with an

as-yet unidentified transmembrane protein, which powers extraction of LPS from the IM and transit across the periplasm to LptDE (37). The IM protein encoded by the gene *yrbK*, which is located immediately upstream of *lptA*, was potentially proposed to be the missing transmembrane component of the ABC transporter.

The protein of unknown function encoded by the gene *yrbK*, renamed *lptC*, was characterized (38). It was found that *lptC* is an essential gene in *E. coli* (39), and the gene product, LptC, is an IM protein predicted to contain a single transmembrane helix. Genetic studies showed that isogenic LptA, LptB, LptC, LptD, and LptE depletion strains all have a similar phenotype: the presence of unusual membrane structures in the periplasm, the inability to transport *de novo*-synthesized LPS as judged by pulse-labeling experiments, and the accumulation of LPS covalently modified with repeating colanic acid units (38). It had previous been shown that LPS can be modified with colanic acid by WaaL, the O-antigen ligase (124); because WaaL is located on the periplasmic side of the IM, such a modification in these depletion strains indicates that defects in any of these Lpt components results in accumulation of LPS on the outer leaflet of the IM. This work established that there are Lpt components in the cytoplasm, IM, periplasm, and OM, which makes sense considering that LPS needs to be transported through each of these compartments, presumably with energy input from the cytoplasm.

LptB shows high sequence homology to NBDs of ABC transporters. Although LptC could be the missing TMD for this ABC transporter, LptC was predicted to be a bitopic protein with a single transmembrane helix at its N-terminus (38). ABC transporters typically contain two TMDs with six transmembrane helices each (125). Therefore, it seemed probable that there was at least one more necessary Lpt protein. Using a reductionist bioinformatic approach, two

new genes involved in this pathway were identified: *lptF* and *lptG* (formerly *yjgP* and *yjgQ*, respectively), which encode for two predicted IM six-transmembrane helix proteins (36). LptF and LptG are essential proteins, and depleting them causes increased sensitivity to hydrophobic antibiotics, indicative of an OM defect. Furthermore, cells depleted of LptF and LptG contain LPS covalently modified with a palmitate group, making it hepta-acylated instead of hexa-acylated (36). This covalent modification occurs when there is a defect in LPS assembly and the outer leaflet of the OM contains phospholipids in addition to LPS. The movement of phospholipids to the outer leaflet of the OM activates the OMP PagP, which catalyzes the transfer of palmitate from phospholipids to lipid A (126). This has served as a useful covalent modification of LPS to indicate defects in LPS biogenesis, and it was used to demonstrate that LPS synthesized after LptFG depletion does not reach the cell surface (36). Therefore, LptFG were believed to be the missing TMDs in the ABC transporter containing LptB as the NBD. At this point, all of the essential LPS biogenesis components were thought to be identified.

1.4 Structure of the Lpt Pathway

There are Lpt pathway components in the cytoplasm (LptB), IM (LptF/G/C), periplasm (LptA), and OM (LptD/E). Therefore, there must be a specific and selective process for coordinating these components to transport and assemble LPS directly in the outer leaflet of the OM. Defects in the LPS biogenesis machinery all result in buildup of LPS in the outer leaflet of the IM, before membrane extraction (38). This suggests that the Lpt proteins must all be coordinated, as LPS is either found in the inner leaflet of the IM prior to flipping, the outer leaflet of the IM after flipping (or with defects in Lpt components), or in the outer leaflet of the OM (its final destination). There is never LPS mislocalized in the inner leaflet of the OM. This

raises the question: how are the Lpt proteins arranged to allow for direct passage of LPS to the cell surface?

1.4.1 OM Complex LptDE

It is unclear how the OM LPS translocon, comprised of LptD and LptE, functions to assemble LPS in the outer leaflet of the OM. LptD is an ~ 87 kDa β-barrel OMP targeted to the OM by the Bam complex, and LptE is a ~ 20 kDa lipoprotein targeted to the OM by the Lol pathway. Biochemical studies have shown that LptD and LptE can be overexpressed and purified together, and they associate in a very stable one-to-one complex that remains intact following size-exclusion chromatography (127). Additionally, the C-terminal β-barrel domain of LptD and LptE form a trypsin-resistant complex. LptD has a soluble N-terminal domain that is cleaved by trypsin; however, the β-barrel of LptD alone, lacking the soluble domain, does not support *E. coli* growth (127). In fact, in order for LptD to be functional *in vivo*, at least one of two possible nonconsecutive disulfide bonds connecting the N-terminal soluble domain and the C-terminal β-barrel must be present (128). The fact that LptE alone is susceptible to proteolytic degradation, but LptE in complex with LptD is resistant to degradation, suggested that LptD somehow protects LptE from degradation.

The logical next step in understanding this translocon was to gain insight into the structure of the stable LptDE complex. The fact that LptD could not be overexpressed without LptE suggested that LptE might serve a structural role in LptD biogenesis (127). LptE is required for proper disulfide bond formation in LptD, providing even more evidence for this hypothesis (128). Genetic suppressors of a mutant allele of *lptE* that lacks two amino acids further suggested a role of LptE in the assembly of LptD by the Bam complex (129). Data

showing that LptE can bind and disaggregate LPS *in vitro* suggest that LptE might also have a functional role in assembling LPS (127, 130). Site-specific *in vivo* photocrosslinking studies showed that LptE has multiple interaction sites with LptD on different surfaces, suggesting that LptE forms a plug inside the β-barrel of LptD (131). This would explain how the β-barrel of LptD protects LptE from proteolytic digestion. Furthermore, mass spectrometric analysis of crosslinked LptD/E species showed that LptE interacts with a putative extracellular loop of LptD, and deletion of this loop in LptD results in OM permeability defects and problems with LptDE biogenesis (131).

Two recent crystal structures of LptDE from *Shigella flexneri* and *Salmonella typhimurium* confirm the unprecedented plug-and-barrel architecture of this complex (132, 133). LptD has a soluble N-terminal periplasmic domain and a C-terminal kidney-shaped β-barrel with twenty-six antiparallel β-strands, the largest single-protein β-barrel in Gram-negative bacteria (132). A possible model for how LptDE work, based on a previous prediction (131), is that LPS is inserted through a lateral opening of the β-barrel between the first and last β-strands, which are distorted by the presence of proline residues and therefore do not have as many hydrogen bonds holding them together (132, 133). Such a lateral diffusion mechanism has been proposed for fatty acid diffusion into the β-barrels of bacterial OMPs PagP and FadL (126, 134-138). Therefore, a possible model for LPS assembly on the cell surface is that LPS first binds to the N-terminal periplasmic domain of LptD, which somehow triggers the unplugging of LptE from the barrel of LptD. This unplugging event allows for LPS to be inserted into the lumen of LptD, perhaps aided by LptE, and then transferred to the outer leaflet through a lateral opening in the β-barrel. This model is mostly based on structural evidence, but there is no structural information

about how LPS is oriented in the translocon. Further mechanistic studies are necessary to understand how these proteins actually function together.

1.4.2 The Lpt Proteins Form a Transenvelope Bridge

LPS must transit the aqueous periplasmic compartment and associate with LptDE in order to be properly assembled on the cell surface. A big question for many years was how LPS is transported through the periplasm. The hydrophobic lipid A moiety must be sequestered to allow for diffusion through the aqueous compartment. Therefore, there were two models to explain the transit of LPS across the periplasm: the soluble chaperone model and the transenvelope bridge model (Figure 1.4) (26, 41, 42).

The chaperone model is analogous to how lipoproteins transit the periplasm in Gram-negative bacteria (17, 18). In such a system, LPS would be released from the IM, and its fatty acyl chains would reside within LptA. An LptA-LPS complex would then freely diffuse through the periplasm and deliver LPS to LptDE at the OM. There are many similarities between the Lol and Lpt systems, making this an attractive model. For example, both pathways involve an IM ABC transporter to provide energy, one periplasmic component (LolA and LptA), and an OM receptor. Additionally, studies suggesting that LptA binds to the lipid A domain of LPS *in vitro* lent support to a chaperone model (139).

In the bridge model, LPS is transported from the IM to the OM through points of contact between the two membranes. The first evidence for this model came from pulse-labeling and electron microscopy experiments indicating that newly synthesized LPS localizes around apparent zones of adhesion between the IM and the OM in *S. typhimurium* (140). These membranous zones of adhesion were initially observed in the late 1960's (141), but the nature of

them has since been disputed (142, 143). However, newly synthesized LPS was found to pass through a membrane fraction less dense than the OM, called the OM_L, which appears to contain both IM and the cell wall/OM, providing further support for a bridge model (144).

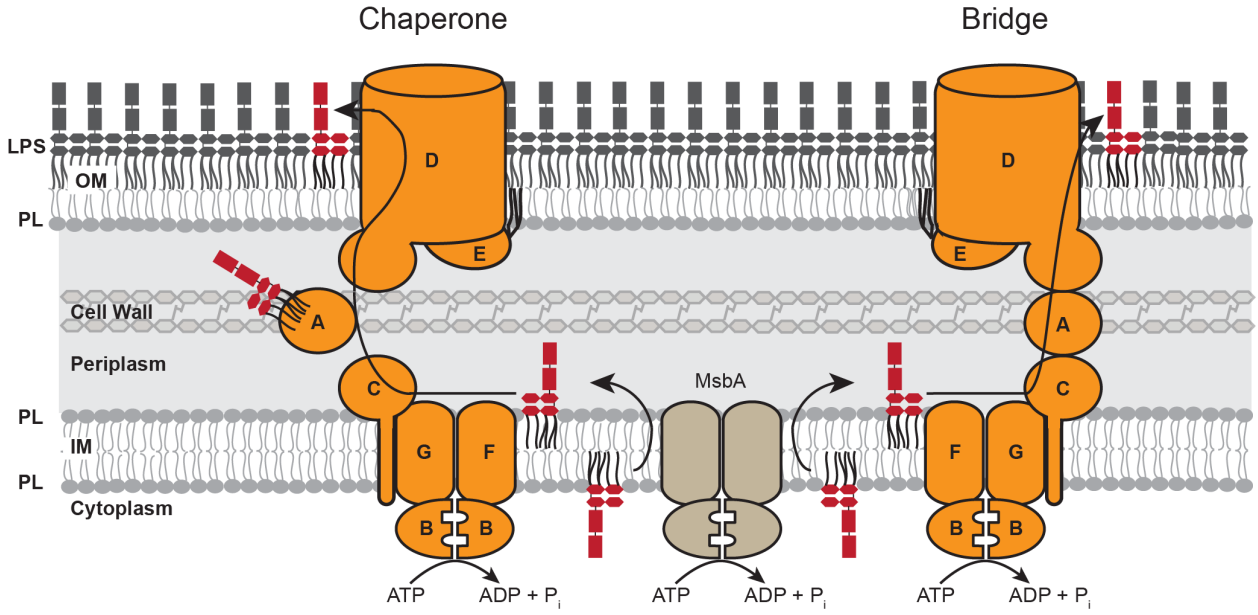

Figure 1.4. Models for LPS transport across the periplasm. LPS can be transit the periplasm bound to LptA as a soluble chaperone (*left*) or in a transenvelope bridge (*right*).

More convincing evidence for the bridge model was that newly synthesized LPS could not be released from spheroplasts, which are plasmolyzed cells with digested cell walls (145, 146). Spheroplasts lack soluble periplasmic components. Lipoproteins can be released from spheroplasts upon addition of the periplasmic fraction, which is now known to contain the chaperone LolA (19). LPS remained in the spheroplasts and was transported from the IM to the OM in sites of membrane adhesion. This transport depended on MsbA and was independent of any periplasmic factor (145). Therefore, the machinery required to transport LPS must remain intact in spheroplasts. The first biochemical evidence that the Lpt proteins form a bridge came from affinity tag purification experiments demonstrating that affinity tagged LptF, LptB, or LptC co-purify with Lpt components in other compartments, suggesting that they form a stable

complex (147). Additionally, all Lpt proteins can be found in the OM_L fraction described above, which contains both the IM and the OM; LptA is also found associated with the membrane and not in the soluble fraction (147).

Further support for the bridge model came from the crystal structure of *E. coli* LptA. LptA has a unique twisted β-jellyroll structure, and addition of LPS to the crystallization condition induced formation of long fibrils of LptA, stacked in a head-to-tail manner (the C-terminus of one LptA molecule interacting with the N-terminus of the adjacent molecule) (148). Although there was no clear electron density for LPS, the head-to-tail stacking suggests a mechanism by which LptA can bridge the IM and the OM. The interior of the β-jellyroll is hydrophobic, supporting the idea that the lipid A acyl chains are sequestered in the interior of the β-jellyroll, allowing for passage through the aqueous periplasm. Moreover, the soluble C-terminal periplasmic domain of *E. coli* LptC was crystallized and found to have a similar twisted β-jellyroll structure to LptA, despite low sequence similarity (149). Together with the head-to-tail oligomerization of LptA, evidence that the C-terminus of LptC binds LPS *in vitro* and interacts with LptA *in vivo* and *in vitro* suggested that LptC might be a docking point for LptA, which forms a bridge across the periplasm (149-152).

In vivo photocrosslinking was used to investigate the architecture of the transenvelope bridge (153). A photocrosslinkable amino acid, *p*-benzyol-L-phenylalanine (*p*BPA), was incorporated at specific positions throughout LptC, LptA, and LptD to determine if and where these proteins interact in cells. The results confirmed that the edge of the β-jellyroll at the C-terminus of LptC interacts with the N-terminus of LptA; additionally, the C-terminus of LptA interacts with the N-terminus of LptD (153). No interaction between LptA and LptE could previously be detected *in vitro*, supporting the notion that LptA interacts with LptD at the OM

(151). The N-terminus of LptD contains a β-jellyroll and is a member of the same OstA structural superfamily as LptC and LptA (26, 132, 148, 149). The N-terminus of LptD also has a very hydrophobic interior cavity that is bound by two ordered detergent molecules in the crystal structure, suggesting that it might be able to bind LPS in a similar manner (132). It is unclear how many molecules of LptA are necessary to form a bridge, and it is possible that bridges of multiple lengths can form depending on specific conditions (Figure 1.5A) (153).

1.4.3 Assembly of the Transenvelope Bridge

There must be a mechanism to ensure that LPS is not transported across the periplasm unless the OM translocon, LptDE, is properly assembled. In other words, before building a transenvelope bridge, the cell needs to ensure that it is not building a "bridge to nowhere." In order to function properly, properly oxidized LptD and LptE must form a complex (40, 128). *E. coli* LptD contains four cysteine residues, two in the N-terminal domain (C31 and C173) and two in the C-terminal β-barrel (C724 and C725) (128). One of two non-consecutive disulfide bonds (C31-C724 or C173-C725) connecting the two domains is essential for function (128). Pulse-chase experiments allowed for the identification of *in vivo* folding intermediates along the oxidative folding pathway of LptD (154). Prior to folding and insertion into the membrane, LptD forms a non-native disulfide bond in the N-terminus (C31-C173) introduced by the periplasmic oxidase DsbA (155). In the presence of LptE, LptD forms a folded, pre-assembled complex with non-native disulfide bond C31-C173. There is subsequently a disulfide bond rearrangement to produce correctly assembled, mature LptD with non-consecutive disulfide bonds (154). This complex oxidative folding process is required to form a functional LPS OM translocon.

In vivo photocrosslinking experiments and affinity tag purification assays demonstrated that LptDE can properly assemble into a functional, mature translocon prior to formation of a transenvelope bridge (153). However, a functional OM translocon is necessary to form the transenvelope bridge, as LptA cannot crosslink to LptD *in vivo* without proper oxidation of LptD. A hypothesis is that proper disulfide bonding is necessary to orient the N-terminus of LptD in such a way that it can interact and function properly with LptA (153).

Formation of a transenvelope bridge solves the problem of selectively transporting LPS to its destination, as a soluble chaperone runs the risk of docking at the wrong location. Once the OM translocon is assembled, a transenvelope bridge can link the IM Lpt components with the OM components, allowing for convenient coordination of all proteins. This also explains why defects in any single Lpt component results in localization of LPS in the outer leaflet of the IM (38). Such an architecture for direct transit allows for LPS to be transported to the cell surface without ever residing in the inner leaflet of the IM. Additionally, it appears that only the C-terminal domain of LptC and not the transmembrane helix is essential in *E. coli* and is sufficient to interact with LptBFG (156). A specific variant of the C-terminal domain of LptC was identified that can interact with LptBFG but failed to form a transenvelope complex, further supporting the importance of this domain in bridge formation (156). LptA is the central component linking the membrane-bound Lpt machinery, and it has been found that depletion of Lpt components leads to degradation of LptA, perhaps serving as a mechanism to ensure bridge assembly only when all Lpt components are present (150). Taken together, all evidence suggests that the Lpt machinery forms a stable transenvelope complex to efficiently and selectively transport LPS to the cell surface.

1.4.4 IM Complex LptBFGC

As described above, LptBFGC constitute the IM Lpt complex. LptB is a ~ 27 kDa NBD thought to provide energy through ATP hydrolysis for LPS transport (37, 38). LptF and LptG are ~ 40 kDa proteins predicted to have six transmembrane helices each; therefore, they likely serve as the TMDs that interact with LptB to form an ABC transporter (36, 41, 125). It is unclear what role the bitopic IM protein LptC plays in relation to the ABC transporter, but its main function might be to link the IM with the OM through LptA (26, 41, 147, 149, 153, 156).

LptBFG can be overexpressed and purified as a complex with an affinity tag on LptB (157). Additionally, LptC co-purifies with the ABC transporter to form a stable complex, LptBFGC, that elutes as a single peak in size-exclusion chromatography. The stoichiometry of the LptBFGC complex was estimated to be 2:1:1:1, consistent with the model that LptBFG function as an ABC transporter with two NBDs and one of each TMD (52, 125, 157). This ABC transporter is unusual in that it is closely associated with the bitopic membrane protein LptC. The LptBFG and LptBFGC complexes were found to exhibit ATPase activity in detergent solution, and vanadate inhibits their ATPase activity. However, unlike other ABC systems, the ATPase activities of these complexes were not stimulated by their substrate, LPS (52, 157, 158). This could be physiologically relevant, or it can be due to the structures of the complexes in detergent solution.

It is unclear how an ABC transporter in the IM can power LPS transport to the cell surface. Are there specific steps that require ATP hydrolysis? What is the role of ATP hydrolysis, and how is ATP hydrolysis in the cytoplasm coupled to LPS transport through the periplasm?

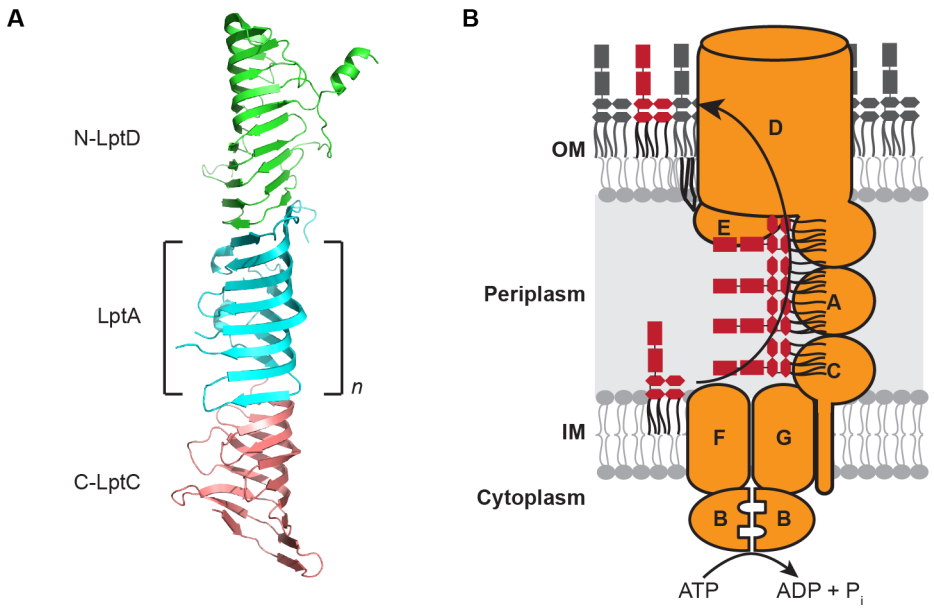

Figure 1.5. LPS is pushed against its concentration gradient by multiple rounds of ATP hydrolysis. *(A)* The N-terminus of LptD (PDB ID: 4q35), LptA (PDB ID: 2r19), and the C-terminus of LptC (PDB ID: 3my2) form a continuous bridge of structurally homologous domains to allow LPS to transit the aqueous periplasm. It is unclear how many LptA molecules are in the bridge. *(B)* The "PEZ" model of LPS transport describes a continuous stream of LPS molecules being pushed through the Lpt complex to the cell service, powered by ATP hydrolysis in the cytoplasm.

1.5 The "PEZ" Model for LPS Transport

In order to study the process of LPS transport, intermediates along the Lpt pathway must be observed in cells. To develop such a method, the unnatural amino acid *p*BPA, which photocrosslinks to nearby residues upon UV-irradiation, was incorporated at specific positions in Lpt proteins using amber codon suppression (159-162). Such a method allowed for direct observation of crosslinking products at various positions throughout LptC and LptA *in vivo* (119). By immunoblotting with antibodies against LPS, positions in LptC and LptA that exhibit UV-dependent crosslinking to LPS in *E. coli* were identified. All positions that crosslinked were inside the β-jellyrolls of these proteins, except for one position in LptC located in a disordered region of the crystal structure near the transmembrane helix (149). The identification of LPS

binding sites within the β-jellyrolls of LptC and LptA is consistent with the model that these domains form a continuous bridge to transport LPS (Figure 1.5A).

To ensure that the observed crosslinking events were on-pathway intermediates along the Lpt pathway, the dependence of these crosslinking products on the presence of other Lpt components was evaluated by altering the expression levels of individual proteins along with *p*BPA-containing LptA or LptC (119). Overexpressing LptBFGC, for example, would mean that most LPS would have nowhere to go after LptC, as the other Lpt components would be limiting. Crosslinking of LPS to LptA at specific binding sites increased substantially when LptBFGC were co-overexpressed. Only crosslinking at the one position in the disordered region of LptC increased with co-overexpression of LptBFG, suggesting that this might be a strong binding site. Therefore, LptA and LptC require LptBFGC and LptBFG, respectively, to bind LPS *in vivo*. These results also indicated that LPS can be transported in broken bridges in which the OM Lpt components are not present. This allowed for the development of a system to study the ATP requirement for LPS transport.

The early steps of LPS transport were reconstituted *in vitro* in right-side-out (RSO) membrane vesicles overexpressing Lpt components (119). Using the same positions in LptC and LptA that crosslink LPS *in vivo*, it was shown that LPS crosslinks to LptC and soluble LptA in an ATP- and IM complex-dependent manner. Additionally, time-dependent LPS transfer from LptC to LptA could be observed. Addition of the ATPase inhibitor vanadate after pre-loading LptC with LPS suggested that additional ATP hydrolysis is required to transfer LPS to LptA.

The fact that the levels of LPS crosslinking to LptC did not decrease with transfer to LptA in a time course suggested that LptC is always loaded with LPS. This result, in conjunction with the observation that an additional round of ATP hydrolysis is required to

transfer LPS from LptC to LptA, led to the development of the "PEZ" model for LPS transport (Figure 1.5B) (119). In this model, the Lpt pathway behaves much like a PEZ candy dispenser. As the head of a PEZ dispenser is opened, a candy is released from the top of a column of candies. Removal of each candy pushes the candy below it to the top position; a spring at the bottom of the dispenser keeps the candy moving. In a similar manner, LPS is constantly being shuttled into the Lpt pathway. Multiple rounds of ATP hydrolysis are required to push a stream of LPS to the cell surface; LPS leaves the pathway as it is assembled on the cell surface, keeping the stream of molecules flowing. ATP hydrolysis is necessary to efficiently transport LPS unidirectionally against its concentration gradient.

1.6 Mechanism of LPS Transport

The "PEZ" model provides a model for how ATP hydrolysis is used to continuously push LPS to the cell surface. The fact that millions of LPS molecules must be assembled on the cell surface during every division cycle necessitates an efficient transport process. Many questions still remain about how LPS transport occurs. Because there is no ATP present in the periplasm, all energy required for LPS transport must come from the cytoplasm. An intriguing question is specifically how ATP hydrolysis in the cytoplasm is coupled to extraction of LPS from the opposite side of the membrane. Additionally, ATPase LptB is an attractive antibiotic target because it is specific to Gram-negative bacteria and is the only Lpt protein with a known enzymatic activity. Chapter 2 will describe studies to characterize and understand the biological function of LptB in powering LPS transport and efforts to inhibit it. In order to learn about the role of the IM complex in relation to the entire pathway, it is necessary to have a biochemical assay to study the pathway in a pure system (without other proteins and cellular components).

Chapters 3 and 4 will describe the development of a reconstitution of LPS transport from purified Lpt proteins. These tools will be useful for understanding how LPS goes out of one membrane, through an aqueous compartment, and into another membrane. Additionally, reconstitution of just the IM complex allows for the role of LptC, associated with ABC transporter LptBFG, to be assessed. Additionally, nothing is known about the mechanism of the OM translocon LptDE and its role in LPS assembly, and the complete reconstitution of LPS transport will aid in studies of this complex. The development of these tools will help to begin to answer questions about how the Lpt pathway works. The reconstitution will also be essential for learning ways of inhibiting Lpt proteins with antibiotics.

1.7 References

1. Silhavy TJ, Kahne D, & Walker S (2010) The bacterial cell envelope. *Cold Spring Harb. Perspect. Biol.* 2(5):a000414.

2. Ruiz N, Kahne D, & Silhavy TJ (2006) Advances in understanding bacterial outer-membrane biogenesis. *Nat Rev Microbiol* 4(1):57-66.

3. Doerrler WT (2006) Lipid trafficking to the outer membrane of Gram-negative bacteria. *Mol Microbiol* 60(3):542-552.

4. Holtje JV (1998) Growth of the stress-bearing and shape-maintaining murein sacculus of Escherichia coli. *Microbiology and molecular biology reviews : MMBR* 62(1):181-203.

5. Nikaido H (2003) Molecular basis of bacterial outer membrane permeability revisited. *Microbiol. Mol. Biol. Rev.* 67(4):593-656.

6. Kamio Y & Nikaido H (1976) Outer membrane of Salmonella typhimurium: accessibility of phospholipid head groups to phospholipase c and cyanogen bromide activated dextran in the external medium. *Biochemistry* 15(12):2561-2570.

7. Muhlradt PF & Golecki JR (1975) Asymmetrical distribution and artifactual reorientation of lipopolysaccharide in the outer membrane bilayer of Salmonella typhimurium. *Eur J Biochem* 51(2):343-352.

8. Whitfield C & Trent MS (2014) Biosynthesis and export of bacterial lipopolysaccharides. *Annu Rev Biochem* 83:99-128.

9. Raetz CR & Whitfield C (2002) Lipopolysaccharide endotoxins. *Annu Rev Biochem* 71:635-700.

10. Raetz CR, Reynolds CM, Trent MS, & Bishop RE (2007) Lipid A modification systems in gram-negative bacteria. *Annu Rev Biochem* 76:295-329.

11. Trent MS, Stead CM, Tran AX, & Hankins JV (2006) Diversity of endotoxin and its impact on pathogenesis. *Journal of endotoxin research* 12(4):205-223.

12. Galanos C & Luderitz O (1975) Electrodialysis of lipopolysaccharides and their conversion to uniform salt forms. *Eur J Biochem* 54(2):603-610.

13. Schindler M & Osborn MJ (1979) Interaction of divalent cations and polymyxin B with lipopolysaccharide. *Biochemistry* 18(20):4425-4430.

14. Nikaido H (1998) Multiple antibiotic resistance and efflux. *Curr Opin Microbiol* 1(5):516-523.

15. Bos MP, Tefsen B, Geurtsen J, & Tommassen J (2004) Identification of an outer membrane protein required for the transport of lipopolysaccharide to the bacterial cell surface. *Proc. Natl. Acad. Sci. U. S. A.* 101(25):9417-9422.

16. Braun M & Silhavy TJ (2002) Imp/OstA is required for cell envelope biogenesis in Escherichia coli. *Mol. Microbiol.* 45(5):1289-1302.

17. Tokuda H & Matsuyama S (2004) Sorting of lipoproteins to the outer membrane in E. coli. *Biochim. Biophys. Acta* 1694(1-3):IN1-9.

18. Okuda S & Tokuda H (2011) Lipoprotein sorting in bacteria. *Annu. Rev. Microbiol.* 65:239-259.

19. Matsuyama S, Tajima T, & Tokuda H (1995) A novel periplasmic carrier protein involved in the sorting and transport of Escherichia coli lipoproteins destined for the outer membrane. *EMBO J.* 14(14):3365-3372.

20. Yakushi T, Masuda K, Narita S, Matsuyama S, & Tokuda H (2000) A new ABC transporter mediating the detachment of lipid-modified proteins from membranes. *Nat Cell Biol* 2(4):212-218.

21. Yakushi T, Yokota N, Matsuyama S, & Tokuda H (1998) LolA-dependent release of a lipid-modified protein from the inner membrane of Escherichia coli requires nucleoside triphosphate. *J Biol Chem* 273(49):32576-32581.

22. Ito Y, Kanamaru K, Taniguchi N, Miyamoto S, & Tokuda H (2006) A novel ligand bound ABC transporter, LolCDE, provides insights into the molecular mechanisms underlying membrane detachment of bacterial lipoproteins. *Mol Microbiol* 62(4):1064-1075.

23. Matsuyama S, Yokota N, & Tokuda H (1997) A novel outer membrane lipoprotein, LolB (HemM), involved in the LolA (p20)-dependent localization of lipoproteins to the outer membrane of Escherichia coli. *EMBO J* 16(23):6947-6955.

24. Okuda S & Tokuda H (2009) Model of mouth-to-mouth transfer of bacterial lipoproteins through inner membrane LolC, periplasmic LolA, and outer membrane LolB. *Proc Natl Acad Sci U S A* 106(14):5877-5882.

25. Ruiz N, Kahne D, & Silhavy TJ (2006) Advances in understanding bacterial outer-membrane biogenesis. *Nat. Rev. Microbiol.* 4(1):57-66.

26. Bos MP, Robert V, & Tommassen J (2007) Biogenesis of the gram-negative bacterial outer membrane. *Annu Rev Microbiol* 61:191-214.

27. Kim S*, et al.* (2007) Structure and function of an essential component of the outer membrane protein assembly machine. *Science* 317(5840):961-964.

28. Knowles TJ, Scott-Tucker A, Overduin M, & Henderson IR (2009) Membrane protein architects: the role of the BAM complex in outer membrane protein assembly. *Nat. Rev. Microbiol.* 7(3):206-214.

29. Ruiz N, Falcone B, Kahne D, & Silhavy TJ (2005) Chemical conditionality: a genetic strategy to probe organelle assembly. *Cell* 121(2):307-317.

30. Sklar JG*, et al.* (2007) Lipoprotein SmpA is a component of the YaeT complex that assembles outer membrane proteins in Escherichia coli. *Proc. Natl. Acad. Sci. U.S.A.* 104(15):6400-6405.

31. Voulhoux R, Bos MP, Geurtsen J, Mols M, & Tommassen J (2003) Role of a highly conserved bacterial protein in outer membrane protein assembly. *Science* 299(5604):262-265.

32. Wu T*, et al.* (2005) Identification of a multicomponent complex required for outer membrane biogenesis in Escherichia coli. *Cell* 121(2):235-245.

33. Hagan CL, Silhavy TJ, & Kahne D (2011) β-Barrel Membrane Protein Assembly by the Bam Complex. *Annu. Rev. Biochem.* 80:189-210.

34. Malinverni JC*, et al.* (2006) YfiO stabilizes the YaeT complex and is essential for outer membrane protein assembly in Escherichia coli. *Mol. Microbiol.* 61(1):151-164.

35. Eggert US*, et al.* (2001) Genetic basis for activity differences between vancomycin and glycolipid derivatives of vancomycin. *Science* 294(5541):361-364.

36. Ruiz N, Gronenberg LS, Kahne D, & Silhavy TJ (2008) Identification of two inner-membrane proteins required for the transport of lipopolysaccharide to the outer membrane of Escherichia coli. *Proc. Natl. Acad. Sci. U. S. A.* 105(14):5537-5542.

37. Sperandeo P*, et al.* (2007) Characterization of lptA and lptB, two essential genes implicated in lipopolysaccharide transport to the outer membrane of Escherichia coli. *J Bacteriol* 189(1):244-253.

38. Sperandeo P*, et al.* (2008) Functional analysis of the protein machinery required for transport of lipopolysaccharide to the outer membrane of Escherichia coli. *J Bacteriol* 190(13):4460-4469.

39. Sperandeo P, Pozzi C, Deho G, & Polissi A (2006) Non-essential KDO biosynthesis and new essential cell envelope biogenesis genes in the Escherichia coli yrbG-yhbG locus. *Research in microbiology* 157(6):547-558.

40. Wu T*, et al.* (2006) Identification of a protein complex that assembles lipopolysaccharide in the outer membrane of Escherichia coli. *Proc. Natl. Acad. Sci. U. S. A.* 103(31):11754-11759.

41. Ruiz N, Kahne D, & Silhavy TJ (2009) Transport of lipopolysaccharide across the cell envelope: the long road of discovery. *Nat Rev Microbiol* 7(9):677-683.

42. Sperandeo P, Deho G, & Polissi A (2009) The lipopolysaccharide transport system of Gram-negative bacteria. *Biochim Biophys Acta* 1791(7):594-602.

43. Sankaran K & Wu HC (1994) Lipid modification of bacterial prolipoprotein. Transfer of diacylglyceryl moiety from phosphatidylglycerol. *J Biol Chem* 269(31):19701-19706.

44. Driessen AJ & Nouwen N (2008) Protein translocation across the bacterial cytoplasmic membrane. *Annu. Rev. Biochem.* 77:643-667.

45. Rapoport TA (2007) Protein translocation across the eukaryotic endoplasmic reticulum and bacterial plasma membranes. *Nature* 450(7170):663-669.

46. Wickner W, Driessen AJ, & Hartl FU (1991) The enzymology of protein translocation across the Escherichia coli plasma membrane. *Annu. Rev. Biochem.* 60:101-124.

47. Danese PN & Silhavy TJ (1998) Targeting and assembly of periplasmic and outer-membrane proteins in Escherichia coli. *Annu. Rev. Genet.* 32:59-94.

48. Mori H & Ito K (2001) The Sec protein-translocation pathway. *Trends Microbiol* 9(10):494-500.

49. Pugsley AP (1993) The complete general secretory pathway in gram-negative bacteria. *Microbiological reviews* 57(1):50-108.

50. Zimmer J, Nam Y, & Rapoport TA (2008) Structure of a complex of the ATPase SecA and the protein-translocation channel. *Nature* 455(7215):936-943.

51. Dassa E & Bouige P (2001) The ABC of ABCS: a phylogenetic and functional classification of ABC systems in living organisms. *Research in microbiology* 152(3-4):211-229.

52. Davidson AL, Dassa E, Orelle C, & Chen J (2008) Structure, function, and evolution of bacterial ATP-binding cassette systems. *Microbiology and molecular biology reviews : MMBR* 72(2):317-364, table of contents.

53. Yamaguchi K, Yu F, & Inouye M (1988) A single amino acid determinant of the membrane localization of lipoproteins in E. coli. *Cell* 53(3):423-432.

54. Tajima T, Yokota N, Matsuyama S, & Tokuda H (1998) Genetic analyses of the in vivo function of LolA, a periplasmic chaperone involved in the outer membrane localization of Escherichia coli lipoproteins. *FEBS Lett* 439(1-2):51-54.

55. Takeda K*, et al.* (2003) Crystal structures of bacterial lipoprotein localization factors, LolA and LolB. *EMBO J* 22(13):3199-3209.

56. Taniguchi N, Matsuyama S, & Tokuda H (2005) Mechanisms underlying energy-independent transfer of lipoproteins from LolA to LolB, which have similar unclosed {beta}-barrel structures. *J Biol Chem* 280(41):34481-34488.

57. Zwizinski C & Wickner W (1980) Purification and characterization of leader (signal) peptidase from Escherichia coli. *J Biol Chem* 255(16):7973-7977.

58. Sklar JG, Wu T, Kahne D, & Silhavy TJ (2007) Defining the roles of the periplasmic chaperones SurA, Skp, and DegP in Escherichia coli. *Genes Dev.* 21(19):2473-2484.

59. Reumann S, Davila-Aponte J, & Keegstra K (1999) The evolutionary origin of the protein-translocating channel of chloroplastic envelope membranes: identification of a cyanobacterial homolog. *Proc. Natl. Acad. Sci. U.S.A.* 96(2):784-789.

60. Noinaj N*, et al.* (2013) Structural insight into the biogenesis of beta-barrel membrane proteins. *Nature* 501(7467):385-390.

61. Gatzeva-Topalova PZ, Walton TA, & Sousa MC (2008) Crystal structure of YaeT: conformational flexibility and substrate recognition. *Structure* 16(12):1873-1881.

62. Gatzeva-Topalova PZ, Warner LR, Pardi A, & Sousa MC (2010) Structure and flexibility of the complete periplasmic domain of BamA: the protein insertion machine of the outer membrane. *Structure* 18(11):1492-1501.

63. Knowles TJ*, et al.* (2008) Fold and function of polypeptide transport-associated domains responsible for delivering unfolded proteins to membranes. *Mol. Microbiol.* 68(5):1216-1227.

64. Hagan CL, Kim S, & Kahne D (2010) Reconstitution of outer membrane protein assembly from purified components. *Science* 328(5980):890-892.

65. Hagan CL & Kahne D (2011) The reconstituted Escherichia coli Bam complex catalyzes multiple rounds of β-barrel assembly. *Biochemistry* 50(35):7444-7446.

66. Hagan CL, Westwood DB, & Kahne D (2013) Bam Lipoproteins Assemble BamA in vitro. *Biochemistry* 52(35):6108-6113.

67. Osborn MJ, Gander JE, Parisi E, & Carson J (1972) Mechanism of assembly of the outer membrane of Salmonella typhimurium. Isolation and characterization of cytoplasmic and outer membrane. *J Biol Chem* 247(12):3962-3972.

68. Osborn MJ, Gander JE, & Parisi E (1972) Mechanism of assembly of the outer membrane of Salmonella typhimurium. Site of synthesis of lipopolysaccharide. *J Biol Chem* 247(12):3973-3986.

69. Rick PD, Fung LW, Ho C, & Osborn MJ (1977) Lipid A mutants of Salmonella typhimurium. Purification and characterization of a lipid A precursor produced by a mutant in 3-deoxy-D-mannooctulosonate-8-phosphate synthetase. *J Biol Chem* 252(14):4904-4912.

70. Rick PD & Osborn MJ (1977) Lipid A mutants of Salmonella typhimurium. Characterization of a conditional lethal mutant in 3-deoxy-D-mannooctulosonate-8-phosphate synthetase. *J Biol Chem* 252(14):4895-4903.

71. Crowell DN, Anderson MS, & Raetz CR (1986) Molecular cloning of the genes for lipid A disaccharide synthase and UDP-N-acetylglucosamine acyltransferase in Escherichia coli. *J Bacteriol* 168(1):152-159.

72. Kelly TM, Stachula SA, Raetz CR, & Anderson MS (1993) The firA gene of Escherichia coli encodes UDP-3-O-(R-3-hydroxymyristoyl)-glucosamine N-acyltransferase. The third step of endotoxin biosynthesis. *J Biol Chem* 268(26):19866-19874.

73. Young K*, et al.* (1995) The envA permeability/cell division gene of Escherichia coli encodes the second enzyme of lipid A biosynthesis. UDP-3-O-(R-3-hydroxymyristoyl)-N-acetylglucosamine deacetylase. *J Biol Chem* 270(51):30384-30391.

74. Anderson MS & Raetz CR (1987) Biosynthesis of lipid A precursors in Escherichia coli. A cytoplasmic acyltransferase that converts UDP-N-acetylglucosamine to UDP-3-O-(R-3-hydroxymyristoyl)-N-acetylglucosamine. *J Biol Chem* 262(11):5159-5169.

75. Anderson MS*, et al.* (1993) UDP-N-acetylglucosamine acyltransferase of Escherichia coli. The first step of endotoxin biosynthesis is thermodynamically unfavorable. *J Biol Chem* 268(26):19858-19865.

76. Anderson MS, Robertson AD, Macher I, & Raetz CR (1988) Biosynthesis of lipid A in Escherichia coli: identification of UDP-3-O-[(R)-3-hydroxymyristoyl]-alpha-D-glucosamine as a precursor of UDP-N2,O3-bis[(R)-3-hydroxymyristoyl]-alpha-D-glucosamine. *Biochemistry* 27(6):1908-1917.

77. Babinski KJ, Ribeiro AA, & Raetz CR (2002) The Escherichia coli gene encoding the UDP-2,3-diacylglucosamine pyrophosphatase of lipid A biosynthesis. *J Biol Chem* 277(29):25937-25946.

78. Babinski KJ, Kanjilal SJ, & Raetz CR (2002) Accumulation of the lipid A precursor UDP-2,3-diacylglucosamine in an Escherichia coli mutant lacking the lpxH gene. *J Biol Chem* 277(29):25947-25956.

79. Ray BL, Painter G, & Raetz CR (1984) The biosynthesis of gram-negative endotoxin. Formation of lipid A disaccharides from monosaccharide precursors in extracts of Escherichia coli. *J Biol Chem* 259(8):4852-4859.

80. Garrett TA, Kadrmas JL, & Raetz CR (1997) Identification of the gene encoding the Escherichia coli lipid A 4'-kinase. Facile phosphorylation of endotoxin analogs with recombinant LpxK. *J Biol Chem* 272(35):21855-21864.

81. Clementz T & Raetz CR (1991) A gene coding for 3-deoxy-D-manno-octulosonic-acid transferase in Escherichia coli. Identification, mapping, cloning, and sequencing. *J Biol Chem* 266(15):9687-9696.

82. Belunis CJ & Raetz CR (1992) Biosynthesis of endotoxins. Purification and catalytic properties of 3-deoxy-D-manno-octulosonic acid transferase from Escherichia coli. *J Biol Chem* 267(14):9988-9997.

83. Brozek KA & Raetz CR (1990) Biosynthesis of lipid A in Escherichia coli. Acyl carrier protein-dependent incorporation of laurate and myristate. *J Biol Chem* 265(26):15410-15417.

84. Six DA, Carty SM, Guan Z, & Raetz CR (2008) Purification and mutagenesis of LpxL, the lauroyltransferase of Escherichia coli lipid A biosynthesis. *Biochemistry* 47(33):8623-8637.

85. Clementz T, Zhou Z, & Raetz CR (1997) Function of the Escherichia coli msbB gene, a multicopy suppressor of htrB knockouts, in the acylation of lipid A. Acylation by MsbB follows laurate incorporation by HtrB. *J Biol Chem* 272(16):10353-10360.

86. Anderson MS, Bulawa CE, & Raetz CR (1985) The biosynthesis of gram-negative endotoxin. Formation of lipid A precursors from UDP-GlcNAc in extracts of Escherichia coli. *J Biol Chem* 260(29):15536-15541.

87. Meredith TC, Aggarwal P, Mamat U, Lindner B, & Woodard RW (2006) Redefining the requisite lipopolysaccharide structure in Escherichia coli. *ACS Chem Biol* 1(1):33-42.

88. Onishi HR*, et al.* (1996) Antibacterial agents that inhibit lipid A biosynthesis. *Science* 274(5289):980-982.

89. Caughlan RE*, et al.* (2011) Mechanisms decreasing in vitro susceptibility to the LpxC inhibitor CHIR-090 in the gram-negative pathogen Pseudomonas aeruginosa. *Antimicrob Agents Chemother* 56(1):17-27.

90. Barb AW*, et al.* (2009) Uridine-based inhibitors as new leads for antibiotics targeting Escherichia coli LpxC. *Biochemistry* 48(14):3068-3077.

91. Clements JM*, et al.* (2002) Antibacterial activities and characterization of novel inhibitors of LpxC. *Antimicrob Agents Chemother* 46(6):1793-1799.

92. Mdluli KE*, et al.* (2006) Molecular validation of LpxC as an antibacterial drug target in Pseudomonas aeruginosa. *Antimicrob Agents Chemother* 50(6):2178-2184.

93. Mochalkin I, Knafels JD, & Lightle S (2008) Crystal structure of LpxC from Pseudomonas aeruginosa complexed with the potent BB-78485 inhibitor. *Protein Sci* 17(3):450-457.

94. Montgomery JI*, et al.* (2012) Pyridone methylsulfone hydroxamate LpxC inhibitors for the treatment of serious gram-negative infections. *J Med Chem* 55(4):1662-1670.

95. Whittington DA, Rusche KM, Shin H, Fierke CA, & Christianson DW (2003) Crystal structure of LpxC, a zinc-dependent deacetylase essential for endotoxin biosynthesis. *Proc Natl Acad Sci U S A* 100(14):8146-8150.

96. Mulford CA & Osborn MJ (1983) An intermediate step in translocation of lipopolysaccharide to the outer membrane of Salmonella typhimurium. *Proc Natl Acad Sci U S A* 80(5):1159-1163.

97. Marino PA, Phan KA, & Osborn MJ (1985) Energy dependence of lipopolysaccharide translocation in Salmonella typhimurium. *J Biol Chem* 260(28):14965-14970.

98. Karow M & Georgopoulos C (1993) The essential Escherichia coli msbA gene, a multicopy suppressor of null mutations in the htrB gene, is related to the universally conserved family of ATP-dependent translocators. *Mol Microbiol* 7(1):69-79.

99. Polissi A & Georgopoulos C (1996) Mutational analysis and properties of the msbA gene of Escherichia coli, coding for an essential ABC family transporter. *Mol Microbiol* 20(6):1221-1233.

100. Zhou Z, White KA, Polissi A, Georgopoulos C, & Raetz CR (1998) Function of Escherichia coli MsbA, an essential ABC family transporter, in lipid A and phospholipid biosynthesis. *J Biol Chem* 273(20):12466-12475.

101. Huijbregts RP, de Kroon AI, & de Kruijff B (1998) Rapid transmembrane movement of newly synthesized phosphatidylethanolamine across the inner membrane of Escherichia coli. *J Biol Chem* 273(30):18936-18942.

102. Kol MA, van Dalen A, de Kroon AI, & de Kruijff B (2003) Translocation of phospholipids is facilitated by a subset of membrane-spanning proteins of the bacterial cytoplasmic membrane. *J Biol Chem* 278(27):24586-24593.

103. Tefsen B, Bos MP, Beckers F, Tommassen J, & de Cock H (2005) MsbA is not required for phospholipid transport in Neisseria meningitidis. *J Biol Chem* 280(43):35961-35966.

104. Doerrler WT & Raetz CR (2002) ATPase activity of the MsbA lipid flippase of Escherichia coli. *J Biol Chem* 277(39):36697-36705.

105. Doerrler WT, Gibbons HS, & Raetz CR (2004) MsbA-dependent translocation of lipids across the inner membrane of Escherichia coli. *J Biol Chem* 279(43):45102-45109.

106. Ward A, Reyes CL, Yu J, Roth CB, & Chang G (2007) Flexibility in the ABC transporter MsbA: Alternating access with a twist. *Proc Natl Acad Sci U S A* 104(48):19005-19010.

107. Dong J, Yang G, & McHaourab HS (2005) Structural basis of energy transduction in the transport cycle of MsbA. *Science* 308(5724):1023-1028.

108. Zou P & McHaourab HS (2009) Alternating access of the putative substrate-binding chamber in the ABC transporter MsbA. *J Mol Biol* 393(3):574-585.

109. Zou P, Bortolus M, & McHaourab HS (2009) Conformational cycle of the ABC transporter MsbA in liposomes: detailed analysis using double electron-electron resonance spectroscopy. *J Mol Biol* 393(3):586-597.

110. Eckford PD & Sharom FJ (2008) Functional characterization of Escherichia coli MsbA: interaction with nucleotides and substrates. *J Biol Chem* 283(19):12840-12850.

111. Doshi R & van Veen HW (2013) Substrate binding stabilizes a pre-translocation intermediate in the ATP-binding cassette transport protein MsbA. *J Biol Chem* 288(30):21638-21647.

112. Doshi R*, et al.* (2013) Molecular disruption of the power stroke in the ATP-binding cassette transport protein MsbA. *J Biol Chem* 288(10):6801-6813.

113. Siarheyeva A & Sharom FJ (2009) The ABC transporter MsbA interacts with lipid A and amphipathic drugs at different sites. *The Biochemical journal* 419(2):317-328.

114. van Veen HW*, et al.* (1998) A bacterial antibiotic-resistance gene that complements the human multidrug-resistance P-glycoprotein gene. *Nature* 391(6664):291-295.

115. Aller SG*, et al.* (2009) Structure of P-glycoprotein reveals a molecular basis for poly-specific drug binding. *Science* 323(5922):1718-1722.

116. Dawson RJ & Locher KP (2006) Structure of a bacterial multidrug ABC transporter. *Nature* 443(7108):180-185.

117. Reuter G*, et al.* (2003) The ATP binding cassette multidrug transporter LmrA and lipid transporter MsbA have overlapping substrate specificities. *J Biol Chem* 278(37):35193-35198.

118. Woebking B*, et al.* (2005) Drug-lipid A interactions on the Escherichia coli ABC transporter MsbA. *J Bacteriol* 187(18):6363-6369.

119. Okuda S, Freinkman E, & Kahne D (2012) Cytoplasmic ATP hydrolysis powers transport of lipopolysaccharide across the periplasm in E. coli. *Science* 338(6111):1214-1217.

120. Sampson BA, Misra R, & Benson SA (1989) Identification and characterization of a new gene of Escherichia coli K-12 involved in outer membrane permeability. *Genetics* 122(3):491-501.

121. Dartigalongue C, Missiakas D, & Raina S (2001) Characterization of the Escherichia coli sigma E regulon. *J Biol Chem* 276(24):20866-20875.

122. Steeghs L*, et al.* (1998) Meningitis bacterium is viable without endotoxin. *Nature* 392(6675):449-450.

123. Stenberg F*, et al.* (2005) Protein complexes of the Escherichia coli cell envelope. *J. Biol. Chem.* 280(41):34409-34419.

124. Meredith TC*, et al.* (2007) Modification of lipopolysaccharide with colanic acid (M-antigen) repeats in Escherichia coli. *J Biol Chem* 282(11):7790-7798.

125. Higgins CF (1992) ABC transporters: from microorganisms to man. *Annual review of cell biology* 8:67-113.

126. Bishop RE*, et al.* (2000) Transfer of palmitate from phospholipids to lipid A in outer membranes of gram-negative bacteria. *EMBO J* 19(19):5071-5080.

127. Chng SS, Ruiz N, Chimalakonda G, Silhavy TJ, & Kahne D (2010) Characterization of the two-protein complex in Escherichia coli responsible for lipopolysaccharide assembly at the outer membrane. *Proc. Natl. Acad. Sci. U. S. A.* 107(12):5363-5368.

128. Ruiz N, Chng SS, Hiniker A, Kahne D, & Silhavy TJ (2010) Nonconsecutive disulfide bond formation in an essential integral outer membrane protein. *Proc Natl Acad Sci U S A* 107(27):12245-12250.

129. Chimalakonda G*, et al.* (2011) Lipoprotein LptE is required for the assembly of LptD by the beta-barrel assembly machine in the outer membrane of Escherichia coli. *Proc. Natl. Acad. Sci. U. S. A.* 108(6):2492-2497.

130. Malojcic G*, et al.* (2014) LptE binds to and alters the physical state of LPS to catalyze its assembly at the cell surface. *Proc Natl Acad Sci U S A* 111(26):9467-9472.

131. Freinkman E, Chng SS, & Kahne D (2011) The complex that inserts lipopolysaccharide into the bacterial outer membrane forms a two-protein plug-and-barrel. *Proc. Natl. Acad. Sci. U. S. A.* 108(6):2486-2491.

132. Qiao S, Luo Q, Zhao Y, Zhang XC, & Huang Y (2014) Structural basis for lipopolysaccharide insertion in the bacterial outer membrane. *Nature* 511(7507):108-111.

133. Dong H*, et al.* (2014) Structural basis for outer membrane lipopolysaccharide insertion. *Nature* 511(7507):52-56.

134. Khan MA & Bishop RE (2009) Molecular mechanism for lateral lipid diffusion between the outer membrane external leaflet and a beta-barrel hydrocarbon ruler. *Biochemistry* 48(41):9745-9756.

135. Bishop RE (2005) The lipid A palmitoyltransferase PagP: molecular mechanisms and role in bacterial pathogenesis. *Mol. Microbiol.* 57(4):900-912.

136. Hearn EM, Patel DR, Lepore BW, Indic M, & van den Berg B (2009) Transmembrane passage of hydrophobic compounds through a protein channel wall. *Nature* 458(7236):367-370.

137. van den Berg B (2010) Going forward laterally: transmembrane passage of hydrophobic molecules through protein channel walls. *Chembiochem* 11(10):1339-1343.

138. van den Berg B, Black PN, Clemons WM, Jr., & Rapoport TA (2004) Crystal structure of the long-chain fatty acid transporter FadL. *Science* 304(5676):1506-1509.

139. Tran AX, Trent MS, & Whitfield C (2008) The LptA protein of Escherichia coli is a periplasmic lipid A-binding protein involved in the lipopolysaccharide export pathway. *J Biol Chem* 283(29):20342-20349.

140. Muhlradt PF, Menzel J, Golecki JR, & Speth V (1973) Outer membrane of salmonella. Sites of export of newly synthesised lipopolysaccharide on the bacterial surface. *Eur J Biochem* 35(3):471-481.

141. Bayer ME (1968) Areas of adhesion between wall and membrane of Escherichia coli. *Journal of general microbiology* 53(3):395-404.

142. Kellenberger E (1990) The 'Bayer bridges' confronted with results from improved electron microscopy methods. *Mol Microbiol* 4(5):697-705.

143. Bayer ME (1991) Zones of membrane adhesion in the cryofixed envelope of Escherichia coli. *Journal of structural biology* 107(3):268-280.

144. Ishidate K*, et al.* (1986) Isolation of differentiated membrane domains from Escherichia coli and Salmonella typhimurium, including a fraction containing attachment sites between the inner and outer membranes and the murein skeleton of the cell envelope. *J Biol Chem* 261(1):428-443.

145. Tefsen B, Geurtsen J, Beckers F, Tommassen J, & de Cock H (2005) Lipopolysaccharide transport to the bacterial outer membrane in spheroplasts. *J Biol Chem* 280(6):4504-4509.

146. Birdsell DC & Cota-Robles EH (1967) Production and ultrastructure of lysozyme and ethylenediaminetetraacetate-lysozyme spheroplasts of Escherichia coli. *J. Bacteriol.* 93(1):427-437.

147. Chng SS, Gronenberg LS, & Kahne D (2010) Proteins required for lipopolysaccharide assembly in Escherichia coli form a transenvelope complex. *Biochemistry* 49(22):4565-4567.

148. Suits MD, Sperandeo P, Deho G, Polissi A, & Jia Z (2008) Novel structure of the conserved gram-negative lipopolysaccharide transport protein A and mutagenesis analysis. *J Mol Biol* 380(3):476-488.

149. Tran AX, Dong C, & Whitfield C (2010) Structure and functional analysis of LptC, a conserved membrane protein involved in the lipopolysaccharide export pathway in Escherichia coli. *J Biol Chem* 285(43):33529-33539.

150. Sperandeo P*, et al.* (2011) New insights into the Lpt machinery for lipopolysaccharide transport to the cell surface: LptA-LptC interaction and LptA stability as sensors of a properly assembled transenvelope complex. *J Bacteriol* 193(5):1042-1053.

151. Bowyer A, Baardsnes J, Ajamian E, Zhang L, & Cygler M (2011) Characterization of interactions between LPS transport proteins of the Lpt system. *Biochemical and biophysical research communications* 404(4):1093-1098.

152. Sestito SE*, et al.* (2014) Functional characterization of E. coli LptC: interaction with LPS and a synthetic ligand. *Chembiochem* 15(5):734-742.

153. Freinkman E, Okuda S, Ruiz N, & Kahne D (2012) Regulated Assembly of the Transenvelope Protein Complex Required for Lipopolysaccharide Export. *Biochemistry* 51(24):4800-4806.

154. Chng SS*, et al.* (2012) Disulfide rearrangement triggered by translocon assembly controls lipopolysaccharide export. *Science* 337(6102):1665-1668.

155. Kadokura H, Tian H, Zander T, Bardwell JC, & Beckwith J (2004) Snapshots of DsbA in action: detection of proteins in the process of oxidative folding. *Science* 303(5657):534-537.

156. Villa R*, et al.* (2013) The Escherichia coli Lpt Transenvelope Protein Complex for Lipopolysaccharide Export Is Assembled via Conserved Structurally Homologous Domains. *J Bacteriol* 195(5):1100-1108.

157. Narita S & Tokuda H (2009) Biochemical characterization of an ABC transporter LptBFGC complex required for the outer membrane sorting of lipopolysaccharides. *FEBS Lett* 583(13):2160-2164.

158. Higgins CF & Linton KJ (2004) The ATP switch model for ABC transporters. *Nature structural & molecular biology* 11(10):918-926.

159. Wang L, Brock A, Herberich B, & Schultz PG (2001) Expanding the genetic code of Escherichia coli. *Science* 292(5516):498-500.

160. Chin JW, Martin AB, King DS, Wang L, & Schultz PG (2002) Addition of a photocrosslinking amino acid to the genetic code of Escherichiacoli. *Proc Natl Acad Sci U S A* 99(17):11020-11024.

161. Ryu Y & Schultz PG (2006) Efficient incorporation of unnatural amino acids into proteins in Escherichia coli. *Nat Methods* 3(4):263-265.

162. Liu CC & Schultz PG (2010) Adding new chemistries to the genetic code. *Annu Rev Biochem* 79:413-444.

Chapter Two

Structure, Function, and Inhibition of LptB, the ATPase that Powers LPS Transport

---

Much of this chapter is adapted/reproduced from:

Sherman, D.J., *et. al.* (2014) *Proc. Natl. Acad. Sci. U.S.A.* 111(13):4982-4987. (Ref. 6)

The chapter also contains some adapted material from:

Sherman, D.J., *et. al.* (2013) *Bioorg. Med. Chem.* 21(16): 4846-4851. (Ref. 28)

2.1 Why Study LptB?

ATP-binding cassette (ABC) systems represent one of the largest protein superfamilies across all domains of life (1, 2). Many of these systems are transporters that share a common architecture of two transmembrane domains (TMDs) and two cytoplasmic nucleotide-binding domains (NBDs), which bind and hydrolyze ATP. They couple the energy of ATP binding and hydrolysis to the transport of a variety of substrates against a concentration gradient. Although eukaryotic ABC transporters involved in human diseases have received much attention (3), the canonical ABC systems that have been most extensively studied are Gram-negative bacterial importers, notably the histidine and maltose importers (2).

As described in Chapter 1, three of the Lpt proteins responsible for the transport and assembly of LPS on the cell surface of *E. coli* form an ABC system composed of a heterodimeric TMD complex (LptF and LptG) and a homodimeric NBD complex (LptB). LptB, both alone and in a complex with LptF and LptG, has ATPase activity *in vitro* (4-6). In addition, the LptBFG complex is closely associated with the bitopic IM protein LptC, which binds LPS and is also part of the transenvelope bridge (5, 7-9). Based on these findings, the current model is that LptBFG extracts LPS from the outer leaflet of the IM and is the sole energy input responsible for the entire process of transport and assembly of LPS on the cell surface against a concentration gradient (Figure 2.1A) (8). Coupling this ABC transporter with the Lpt periplasmic bridge and OM translocon enables cytoplasmic ATP to drive periplasmic transit. Although its heteromeric architecture with separate NBDs and TMDs resembles that of bacterial importers, LptBFG has to perform a unique function that places it in a class distinct from traditional importers and exporters: LptB, the cytoplasmic ATPase, must power the extraction of a large glycolipid from the periplasmic face of the IM.

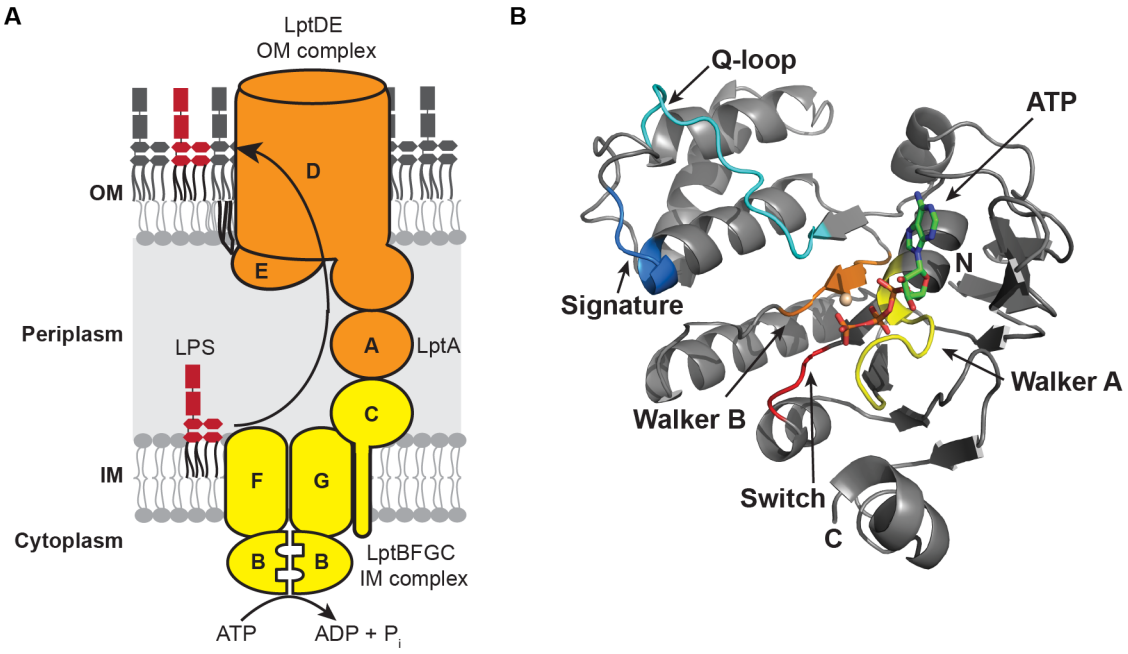

Figure 2.1. LptB is the NBD of the ABC transporter that powers LPS transport. *(A)* The Lpt pathway in *E. coli* is comprised of seven essential proteins that span the periplasm as a continuous bridge. LptBFGC (yellow) comprise the IM complex, which is responsible for powering all of LPS transport and assembly. *(B)* Cartoon rendering of LptB-E163Q bound to Na^+-ATP (pre-hydrolysis crystal structure), with conserved ATPase and ABC motifs indicated (Walker A, yellow; Walker B, orange; signature motif, blue; Q-loop, cyan; switch region, red). N- and C-termini are indicated.

Large conformational changes in the LptBFGC complex are likely required to transduce information about ATP hydrolysis in the cytoplasm to other Lpt components, and vice versa. Even years after its discovery, very little was known about this unusual ABC system other than that it is part of the Lpt pathway. This chapter describes the first structural and functional characterization of LptB, the only Lpt component with a known enzymatic activity (Figure 2.1B). High-resolution crystal structures of LptB in pre- and post-ATP hydrolysis states led to the identification of specific residues essential for catalytic function and interaction with the TMDs. These studies identify that inhibiting the function and assembly of LptB serve as promising strategies for blocking LPS biogenesis *in vivo*.

2.2 Crystal Structures of LptB Bound to ADP and ATP

To gain insight into the catalytic cycle of LptB and its function in powering LPS transport, we obtained crystal structures of LptB before and after ATP hydrolysis. LptB with a C-terminal polyhistidine tag (LptB-His) was overexpressed and purified, and crystals were obtained with both the native protein and a selenomethionine-derivate (to obtain phasing information for solving the crystal structure) after incubation with ATP/$MgCl_2$. There was unambiguous electron density for ADP-Mg^{2+}, indicating that ATP hydrolysis had occurred prior to or during crystallization. To solve the structure, experimental phasing was obtained by multiple isomorphous replacement with anomalous scattering using the selenomethionine derivative and a tantalum derivative (experimental details in Section 2.7). This 1.55-Å structure will hereafter be referred to as LptB-ADP (crystallographic details in Table 2.4).

To obtain a pre-hydrolysis structure of LptB bound to ATP, we overexpressed and purified a catalytically inactive variant LptB-E163Q-His (4). This protein crystallized in a different crystal form following incubation with ATP. The structure was solved by molecular replacement using the native LptB-ADP structure as the search model (details in Section 2.7). The resulting 1.65-Å structure will hereafter be referred to as LptB-ATP (Figure 2.1B, crystallographic details in Table 2.4). Examination of the active site showed clear electron density for an intact ATP molecule. The active site metal of the LptB-ATP structure was assigned as a sodium cation based on the distances between the metal and the coordinating water molecules (10). The high resolution of these crystallographic snapshots allowed us to look carefully at specific protein interactions that might be important for LptB function.

LptB possesses an overall fold resembling other NBDs structures (Figure 2.1B). It contains the canonical L-shaped architecture composed of a RecA-like α/β ATPase domain and a

structurally diverse α-helical domain (11). The RecA-like domain contains the Walker A and Walker B motifs present in many nucleoside triphosphate-binding proteins (12). This domain also contains magnesium- and nucleotide-binding motifs specific to ABC proteins, namely the Q-loop, which links this conserved domain with the α-helical domain, and the switch region, which contains the conserved histidine-195 (H195). As observed in other NBDs, the LSSG(E/Q) signature motif is found in the helical domain (Figure 2.1B) (13, 14).

Unlike the LptB-ADP structure, LptB-ATP crystallized as a canonical nucleotide-sandwich dimer, the expected closed conformation of NBDs when ATP is bound (Figure 2.2A) (2, 13). Secondary structure matching alignments of the LptB-ATP sandwich dimer with those of ATP-bound MalK, the NBD of the maltose/maltodextrin importer (PDB ID: 1q12), and *Methanocaldococcus jannaschii* MJ0796, a homolog of LolD, the NBD of the ABC system that powers lipoprotein transport (PDB ID: 1l2t), have RMSD values less than 1.75 Å (15). In all cases, ATP is sandwiched between the Walker A motif of one subunit and the signature motif of the opposing subunit (Figure 2.2B). The LptB dimer reveals an interface predicted to interact with TMDs LptF and LptG, based on comparisons with other NBD and full ABC transporter structures (Figure 2.2A). Molecular details of this interface will be described in later sections.

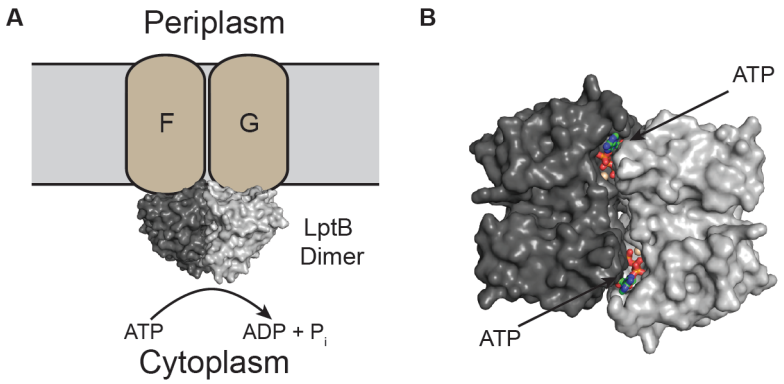

Figure 2.2. LptB-ATP crystallized as a canonical nucleotide-sandwich dimer. *(A)* Surface rendering of the LptB-ATP dimer. Based on comparisons with other NBD structures, it can be predicted where TMDs LptF and LptG might reside relative to the active LptB dimer. *(B)* Top view of the nucleotide-sandwich dimer, showing ATP molecules sandwiched between each protomer.

2.2.1 ATP Hydrolysis Induces Conformational Changes

Comparison of the pre- and post-hydrolysis complexes of LptB indicates considerable movement in a number of regions associated with binding and/or hydrolysis of the γ-phosphate (Figure 2.3A). Glutamate-163 (E163) is at the end of the Walker B motif and is essential for catalysis in other NBDs. This glutamate is the proposed general base that deprotonates the nucleophilic water molecule so that it can attack the γ-phosphate of ATP in the hydrolysis reaction (2, 13, 16). H195, mentioned above, is located in the conserved switch region adjacent to the active site in NBDs; it has been implicated in catalytic activity, but its specific function has been debated (2, 13, 17, 18). Examination of the crystal structures demonstrates conformational changes in the switch region and the region surrounding the Walker B motif (Figure 2.3A). These changes are apparently driven by reorganization of the active site following ATP hydrolysis, such that ATP-binding motifs reorient to stabilize the product, ADP. This reorganization is coupled to changes in the signature motif and the Q-loop, which links the active site with the structurally diverse region of NDBs that interacts with the TMDs to coordinate

catalysis and transport (Figure 2.3B) (2, 13, 19). The Q-look contains the conserved glutamine-85 (Q85), which coordinates with the active site cation (Figure 2.3A).

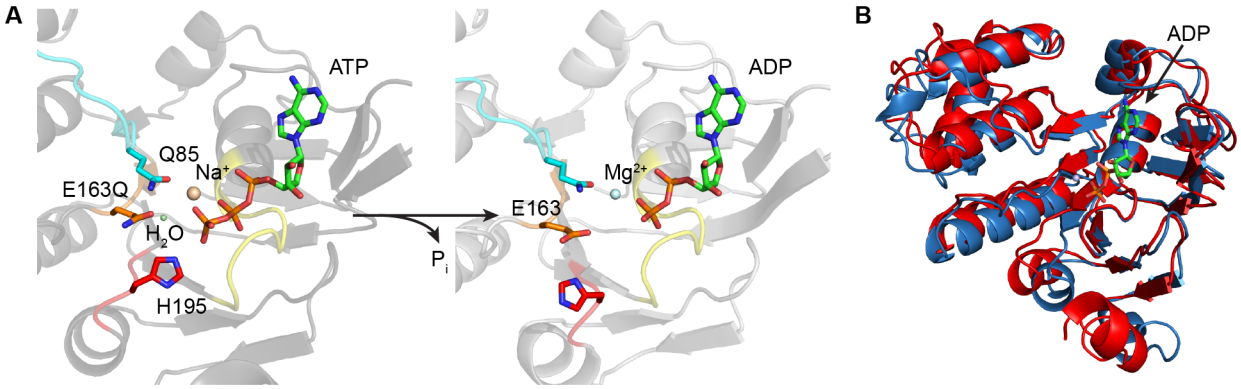

Figure 2.3. Conformational changes upon ATP hydrolysis show how reorganization of the active site causes changes in the region of LptB believed to interact with LptFG. *(A)* Close-up view of the active sites of the pre- and post-hydrolysis structures of LptB. Side chains of conserved residues in the Walker B, switch, and Q-loop regions are shown. The putative hydrolytic water is indicated in the ATP-bound active site. Motif coloring is the same as in Figure 2.1B. *(B)* Structural overlay of the LptB-ATP (red) and LptB-ADP (blue) structures shows conformational changes in the helical region upon ATP hydrolysis. The product, ADP, is shown in the active site.

E163 appears to be essential for catalysis. A closer look at the carbonyl oxygen in the side chain of residue 163 reveals that it is approximately 2.2 Å closer to the nucleotide in the post-hydrolysis structure based on a structural alignment of the Walker A motifs (36-GPNGAGKT-43) (Figure 2.3A). Through a bridging water molecule, this glutamate contacts the β-phosphate of the nucleotide. In LptB-ATP, Q163 is oriented slightly farther from the nucleotide because it is separated by both a bridging water molecule and the γ-phosphate. Based on structural alignments with *E. coli* MalK bound to transition-state mimics (ADP-vanadate and ADP-aluminum fluoride) (20), and by comparison with the ATP-bound MJ0796 structure (10), it appears that this water molecule is well positioned to be the nucleophilic water in the hydrolysis

reaction. Consistent with this hypothesis, this water molecule is not present in the post-hydrolysis structure (Figure 2.3A).

2.3 Characterization of LptB Residues Required for Cell Viability

Based on the crystal structures, E163, H195, and Q85 appear to be important for catalytic function. These residues are conserved in LptB orthologs in many Gram-negative organisms, including pathogens. Another residue that was analyzed, phenylalanine-90 (F90), is a Q-loop residue closer to the predicted LptF/G interface that is conserved in LptB orthologs. Because LptB is required for LPS transport and, consequently, cell viability in *E. coli*, the laboratory of collaborator Natividad Ruiz at The Ohio State University mutated *lptB* to assess the importance of these residues in LPS biogenesis in cells. To do so, they assessed the mutant strains for susceptibility to OM-impermeant antibiotics and cell viability.

Using a clever genetic approach, Ruiz and colleagues found that the E163Q, H195A, and F90A variants of LptB are all nonfunctional, and this loss of functionality is not due to reduced protein expression levels (6). The F90Y variant of LptB was also tested because an aromatic amino acid is found at this position in other NBDs based on primary sequence alignments (not shown). It was found that LptB-F90Y is functional. Interestingly, Ruiz and colleagues found that strains of *E. coli* containing plasmids encoding the E163Q and H195A variants of LptB increased membrane permeability to antibiotics, even with the presence of wild-type chromosomal *lptB*. This suggests that these nonfunctional variants of LptB can substitute for wild-type LptB *in vivo*, reducing the number of functional transporters. Such competition with active transporters results in LPS biogenesis defects. In contrast, strains harboring a plasmid

encoding the LptB-F90A variant did not show the same phenotype, suggesting that LptB-F90A cannot substitute for wild-type LptB in the IM complex.

To better understand the roles of these essential residues in LptB and to confirm hypotheses based on the crystal structures, first the ability of these LptB variants to form an intact IM complex *in vivo* was assessed. To do this, we performed affinity purifications with *E. coli* strains containing C-terminally polyhistidine-tagged LptB variants. The functionality of these tagged LptB variants *in vivo* was confirmed by the Ruiz laboratory to make sure that the presence of the affinity tag did not affect the results. As expected, wild-type LptB-His interacts with other components of the Lpt IM complex in cells, as it co-purifies with LptF and LptC (a lack of anti-LptG antiserum prevented detection of this component, but it is likely that both LptF and LptG are required to form an intact IM complex) (Figure 2.4A). The E163Q and H195A variants also pull down these components, but the F90A variant does not. This result is consistent with the interpretation of the phenotypes of strains harboring plasmids expressing LptB-F90A, LptB-E163Q and LptB-H195A. Because the F90A variant cannot form a stable complex with other IM components, it cannot substitute for wild-type LptB in cells, whereas LptB-E163Q and LptB-H195A can. LptB-F90Y-His does not co-purify with as much LptF and LptC compared to the E163Q and H195A variants (Figure 2.4A). This is consistent with the genetic observation by Ruiz and colleagues that a haploid strain containing only LptB-F90Y shows increased membrane permeability compared to the wild-type strain. Taken together, these results implicate F90 in the association with the Lpt IM complex. They additionally show that the essential role of E163 and H195 in LptB function is unrelated to IM complex formation.

The ATPase activity of the LptB variants was tested to gain more insight into the nature of their functional defects. We overexpressed and purified all LptB-His variants. As expected,

LptB-E163Q-His is catalytically inactive (Figure 2.4B). Because this variant forms a stable IM complex *in vivo*, its inability to support cell viability must be due to its defective catalytic activity. This result demonstrates that ATP hydrolysis by LptB is required for LPS transport in the cell, which had previously been an assumption. The LptB-F90Y-His and LptB-F90A-His variants show wild-type levels of ATPase activity. Even though these substitutions in LptB do not affect protein folding or catalytic activity, they affect protein function *in vivo*. Also, LptB-H195A-His does not support cell viability but only shows a ~ 60% reduction in ATPase activity compared to the wild-type protein (Figure 2.4B). This result was surprising considering that changing this conserved histidine in other ABC transporters results in complete loss of catalytic activity (17, 21-24).

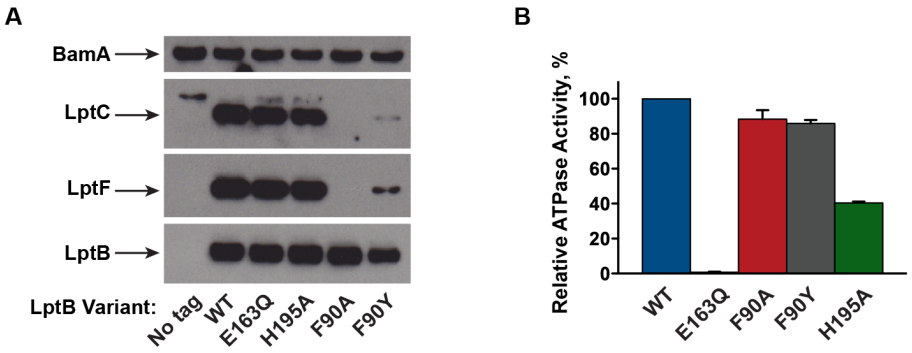

Figure 2.4. Biochemical studies indicate residues in LptB essential for catalysis and proper coupling with other Lpt components. *(A)* Western blots showing affinity purifications of LptB variants expressed in merodipoloid strains harboring plasmids expressing LptB variants. All plasmids express LptB-His, except for the untagged variant (labeled "No tag"). Levels of LptF and LptC that co-purify with LptB are shown. Levels of BamA, an outer-membrane protein that nonspecifically interacts with the purification resin, are shown as a sample preparation and loading control. *(B)* LptB-His variants were overexpressed and purified, and their ATPase activity with 5 mM ATP was measured using a molybdate detection method for inorganic phosphate release. Data represent the average and standard deviations of three experiments.

Comparison of the pre- and post-hydrolysis structures indicates that H195 in the switch region undergoes a major conformational change (Figure 2.3A). The imidazole side chain of H195 makes direct contact with the γ-phosphate in the ATP-bound structure, but its Cα shifts by ~ 4 Å in the ADP-bound structure. Not only does the switch region move, but the side chain of H195 flips. One important unanswered question is how inorganic phosphate (P_i) exits the active sites of NBDs. There is no clear electron density for a P_i group in the post-hydrolysis crystal structure, which is consistent with claims that P_i leaves the active site before ADP is released (10, 25, 26). Based on an electrostatic potential surface of LptB (27), the H195 side chain flips to face a negatively-charged part of the protein (Figure 2.5). It is possible that the γ-phosphate remains bound to H195, and that movement of the switch region forces out the P_i by electrostatic repulsion in this negatively-charged area. It is also possible that the dramatic movement of the switch region observed during ATP hydrolysis plays a critical role in communicating changes in the active site to changes in the TMDs.

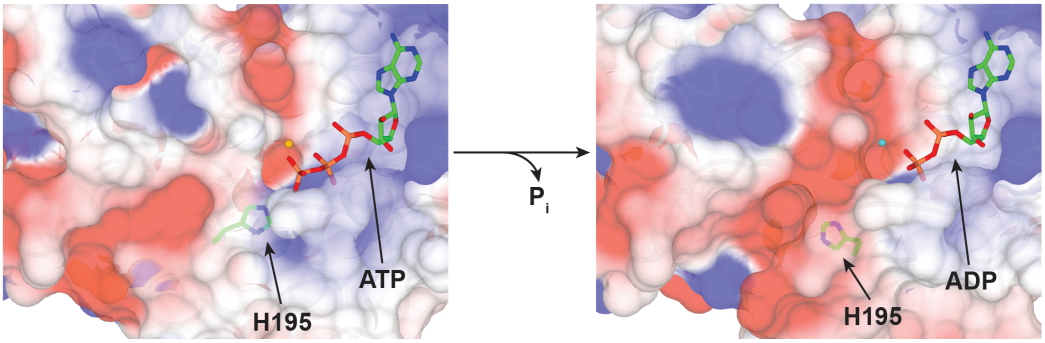

Figure 2.5. Electrostatic potential surface of LptB-ATP reveals a potential phosphate exit channel. Nucleotides and side chain of H195 are shown as sticks to indicate structural changes between ATP-bound and ADP-bound structures. Sodium and magnesium ions are depicted as light orange and light cyan spheres, respectively. Blue represents areas of positive charge and red represents areas of negative charge.

Because H195 is essential *in vivo* and the LptB-ATP structure shows that the imidazole side chain directly interacts with the γ-phosphate of ATP, the ATPase activity observed for the isolated LptB-H195A-His NBD might not report inaccurately on the activity of the full complex. In fact, a comparison of the ATPase activities of LptB-His and LptB-His-LptFGC purified in detergent indicates that the full complex is ten to twenty times more active at its maximal rate than the NBD alone (Figure 2.6A) (28). This suggests that interactions between the individual components of the transporter stabilize the proteins and promote formation of an active conformation of dimeric LptB. Therefore, we compared the ATPase activity of LptBFGC with that of complexes containing LptB-E163Q and LptB-H195A purified in detergent (Figure 2.6B). The complex containing LptB-E163Q is catalytically inactive, and the complex containing LptB-H195A has ~ 10% the ATPase activity of the wild-type complex. This confirms the hypothesis that, though H195 is not the sole catalytic residue, its positioning is important for some step of the catalytic cycle, as suggested by the crystal structures. Taken together, we have identified essential residues in LptB that serve different purposes, allowing for us to begin to learn how LptB works.

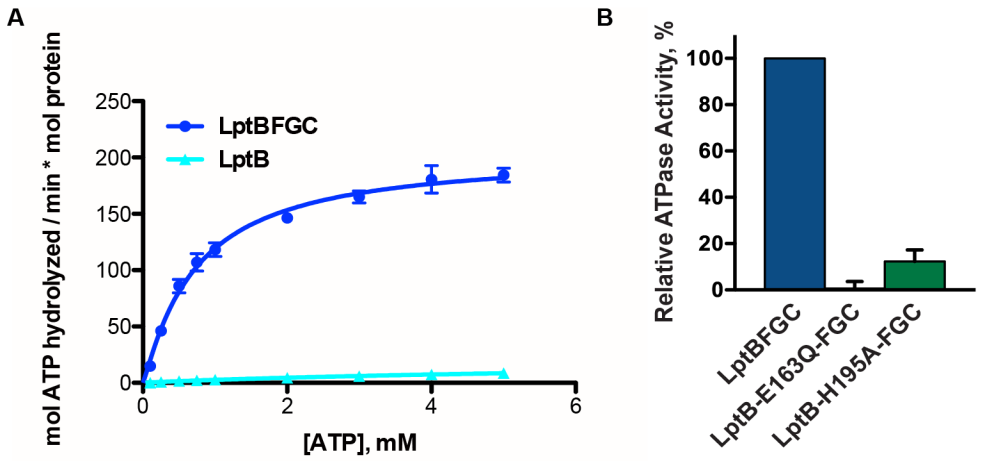

Figure 2.6. The ATPase activity of LptB by itself is much lower than that of the LptBFGC complex. *(A)* ATPase activity was measured using a modified molybdate method for detecting inorganic phosphate release. The following kinetic parameters for LptBFGC can be obtained from the graph (all values represent mean ± standard error): V_{max} = 203.3 ± 8.0 mol ATP hydrolyzed / min * mol LptBFGC, K' = 0.7 ± 0.1 mM, and h = 1.1 ± 0.1. *(B)* LptBFGC variants were overexpressed and purified, and their ATPase activity was measured with 5 mM ATP/$MgCl_2$. Bars represent the average of three experiments, with error bars indicating standard deviations.

2.4 The Groove Region of LptB is Essential for Interaction with TMDs

ATP hydrolysis appears to initiate global movement in LptB that couples changes in regions surrounding the active site (the switch and the Walker B regions) to changes in the structurally diverse helical domain (the signature motif and the Q-loop). These changes near the helical domain result in the shift in a groove located adjacent to the Q-loop (Figure 2.7). This groove could accommodate coupling helices of TMDs, which in other ABC transporters are involved in communication between the NBDs and TMDs (29, 30). Therefore, this coupling of ATP hydrolysis with movement in the groove region could be important for communicating with the TMDs, thereby affecting LPS transport. *In vivo* and biochemical results described above suggest that F90 in the Q-loop is important for binding to putative coupling helices of the TMDs of this ABC system. The side chain of F90 faces the interior of the groove opening in both the

ATP- and ADP-bound structures (Figure 2.7), suggesting this residue might be functionally important for interacting with the TMDs during part or all of the catalytic cycle. Indeed, this would explain why the *lptB-F90A* allele is nonfunctional (see above). The residue adjacent to F90, R91, has a side chain that faces away from the interior of the groove in both crystallographic snapshots (Figure 2.7). The Ruiz laboratory found that the *lptB-R91A* variant is functionally similar to wild-type *lptB*.

Taken together, these results support the hypothesis that residues in the Q-loop of LptB that face the interior of the groove are important for assembly of the complex, for its function, or for both. The high conservation of F90 in LptB orthologs combined with the fact that the *lptB-F90Y* allele confers mild OM permeability defects in haploid strains suggest that a conservative change from a phenylalanine to a tyrosine is tolerated, but not optimal, as LptB evolved to have a phenylalanine at this position. These experiments lead to the conclusion that F90 forms a critical part of the binding site for LptFG.

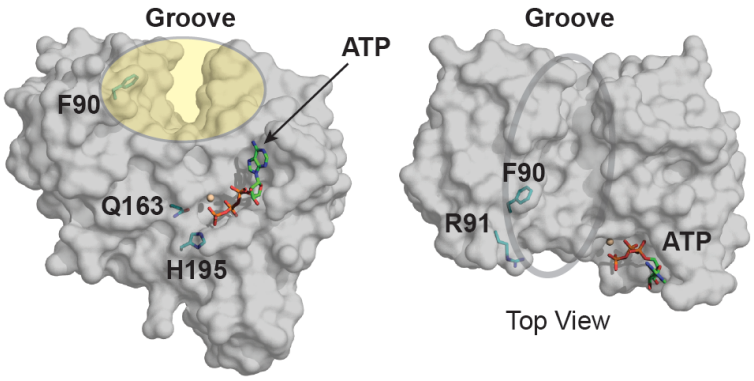

Figure 2.7. Structural observations of LptB implicate a key binding site for TMDs. Surface renderings of a monomer of LptB-ATP (front face and top views) showing residues Q163 and H195 near ATP, residue F90 facing the interior of the groove, and residue R91 facing away from the groove.

2.5 Relating LptB Structure to Function

With respect to the mode of catalysis, the observations described in previous sections are consistent with the prevailing general base catalysis model, in which a carboxylate side chain at the end of the Walker B motif (in residue E163) deprotonates a water molecule so that it can serve as a nucleophile in the hydrolysis reaction. The locations of the general base and potential nucleophile are also consistent with structures of the transition state of the *E. coli* maltose importer (20). The pre- and post-catalysis structures reveal that ATP hydrolysis induces conformational changes in LptB. The most dramatic conformational change in the structural snapshots is in the switch region. Not only does the switch loop move, but the imidazole side chain of the conserved H195 flips away from the active site towards a negatively-charged channel. This movement, combined with the observation that H195 coordinates the γ-phosphate in the pre-hydrolysis complex, suggests that this residue might help move the γ-phosphate from the active site into the acidic channel, from which it is ejected by electrostatic repulsion. This shift of the conserved histidine near a negatively charged surface is also observed in a structure of MJ0796, a homolog of LolD, which powers lipoprotein extraction from the IM (10). Such a role is consistent with the low-level ATPase activity observed for LptB-H195A in complex with the other Lpt IM components.

The LptB crystal structures reveal a groove that undergoes movement upon ATP hydrolysis. A hypothesis is that this groove is involved in the interaction with the TMDs LptF and LptG and that its movement is essential for connecting ATP hydrolysis by LptB with LPS extraction by LptFG. Biochemical and genetic studies implicate groove residue F90 as an important binding site for LptFG. The crystal structures suggest that this residue is critical because its aromatic side chain faces the inside of the groove that likely interacts with the

coupling helices of the TMDs. Structural alignments with other NBDs, both in isolation and in complex with their TMDs, reveal that, despite being part of a structurally diverse region, there is often an aromatic residue at the same location as F90 in LptB. For example, F90 in LptB aligns with F429 in *S. typhimurium* MsbA (PDB ID: 3b60), with Y87 in MalK (PDB ID: 2r6g), and with Y94 in *Sulfolobus solfataricus* GlcV (PDB ID: 1oxx). In the structure of multidrug exporter Sav1866 bound to AMP-PNP (PDB ID: 2onj), the guanidinium group of R206 in the TMD is in close enough proximity to make a π-cation interaction with the aromatic ring of F427 in the NBD, which aligns with F90 in LptB, suggesting that this residue is critical for interaction with the TMDs (Figure 2.8). For LptB, affinity purifications and genetic analyses have established the importance of residue F90: LptB-F90A results in destabilization of the ABC transporter. The aromatic character of this residue is critical for mediating the interaction of LptB with LptFG because the F90Y substitution only results in a partial loss of function *in vivo*, suggesting that the interaction is specific. Further studies are necessary to examine how this key interaction with the TMDs might be important for linking ATP hydrolysis to the extraction of LPS from the opposite side of the membrane via the conformational changes in the groove region.

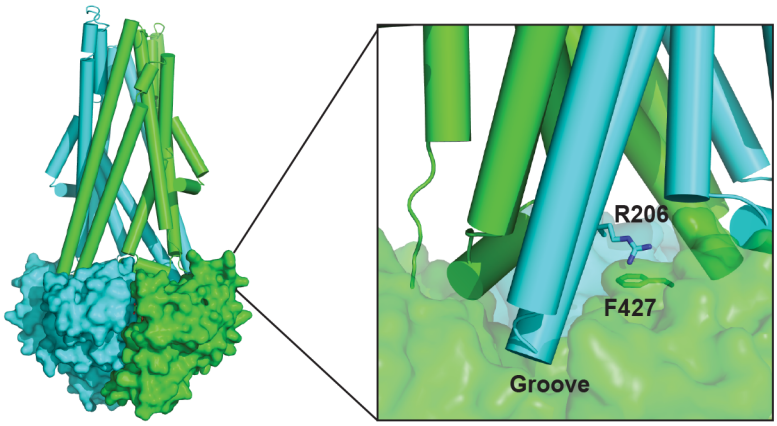

Figure 2.8. Crystal structure of Sav1866 bound to AMP-PNP (PDB ID: 2onj) indicates a TMD-NBD interaction in the groove. Overall structure of the homodimeric multidrug exporter with one chain shown in green and the other shown in cyan. NBDs are depicted as surfaces, and TMDs are depicted as cylinders. The inset shows a close-up view of the side of the transporter, highlighting a π-cation interaction between R206 in one TMD and F427 in one NBD. F427 structurally aligns with F90 in LptB.

2.6 Conclusion

Several LptB residues were identified that are important for ATP hydrolysis (E163), assembly with LptFG (F90), and the function of the complex (H195). High-resolution crystallographic snapshots of LptB pre- and post-hydrolysis reveal that residues involved in binding ATP and catalyzing γ-phosphate hydrolysis reorganize to stabilize the product, ADP. These crystal structures suggest that movement of residues around the LptB active site is coupled to movement of regions at the interface with LptFG that might be essential for LPS transport. In addition, using a catalytically inactive LptB-E163Q variant, we demonstrated that ATP hydrolysis by LptB is essential for cell viability; in contrast, ATP hydrolysis is not required for the formation of the Lpt IM complex.

LptBFG is a unique ABC transporter that powers the extraction of LPS from the opposite side of the IM from the NBD, LptB. Phylogenetic analysis of ABC modules indicates that this

protein family branched fairly early into functional groups (importers, exporters, and "others"), prior to the differentiation of prokaryotes and eukaryotes (1, 31). LptB phylogenetically clusters with import systems, and it is highly related to the NBDs of hydrophobic amino acid update systems (31). Although the structure of LptBFG resembles that of bacterial importers, which largely have NBDs and TMDs as separate polypeptide chains (2), its role is not to import its cargo. It also does not function as a flippase, such as MsbA (see Chapter 1). LptB is not close in proximity to LPS. Therefore, large conformational changes must be necessary to couple ATP binding and hydrolysis to Lpt function. Additionally, there must be different regulatory and feedback systems in place for this transporter than for traditional importers or exporters (2). Overall, further studies of LptBFG and the role of its associated protein LptC will lead to more insights into the mechanism of this unusual transporter. At this point, nothing is known about the roles of LptF and LptG in LPS transport. Very little is known about LptC, aside from its ability to bind LPS (8, 9). These crystal structures of LptB have provided clues as to how to trap LptBFGC in different conformations along the catalytic cycle. Structural studies of *E. coli* LptBFGC are underway to try to obtain snapshots of the full IM complex, which is an essential next step to understand the mechanism of this transporter and how LptC interacts with LptFG.

Clearly, interfering with catalytic activity and coupling with other Lpt components are viable strategies for the development of new antibiotics targeting LPS biogenesis. Although inhibitors of ABC transporters have been used to treat cancer (32), to the best of our knowledge only one ABC transporter inhibitor with antimicrobial activity has been reported (33). As the only enzyme in the seven-protein pathway, a logical starting point for finding inhibitors of LPS transport was to screen for LptB ATPase inhibitors (4, 8). However, it is apparent from this study that discovery of LptB inhibitors that do not compete directly with ATP might prove quite

valuable. To validate such inhibitors, tools must be in place that report on LPS transport directly and not just ATPase activity by LptB. In order to study the mechanism of the Lpt pathway, it is essential to understand the role of the power source, LptB, in relation to other Lpt components. Chapter 3 describes the development of a reconstitution of lipopolysaccharide extraction from proteoliposomes using purified Lpt components. This *in vitro* assay reports on both ATPase activity and LPS release catalyzed by the IM complex, and it will allow for a more comprehensive understanding of the mechanism, regulation, and inhibition of the IM complex as a whole.

2.7 Materials and Methods

2.7.1 Strains and Plasmids

Strains are listed in Table 2.1. Primers are listed in Tables 2.2 and 2.3. All restriction enzymes are from New England Biolabs.

Construction of plasmids pET22/42LptB-His_8 and pET23/42LptB-His_8 have already been reported (4, 7). Plasmid pET23/42LptB was constructed by mutagenizing pET23/42LptB-His_8 to insert a stop codon before the region encoding the His_8 tag using primers LptB-MinusCHis-f and LptB-MinusCHis-r. All *lptB-his* mutant alleles were constructed by mutagenizing pET22/42LptB-His_8 or pET23/42LptB-His_8 using site-directed mutagenesis (SDM) with KOD Hot Start Polymerase (Novagen). The PCR product of the SDM reaction was digested with DpnI (New England Biolabs) and introduced into NovaBlue competent cells by heat-shock. Transformants were selected in media containing carbenicillin (50 μg/mL). After confirming plasmid DNA sequence, mutagenized plasmids were introduced into NR754, BL21(λDE3), and KRX strains.

To construct pCDFDuetLptCAB-His_6-LptFG, the DNA fragment encoding LptFG was amplified by PCR from MC4100 genomic DNA using primers N-NdeI-LptF and LptG-KpnI-C. The amplified fragment encoding LptFG was digested with restriction enzymes NdeI and KpnI and ligated into pCDFDuet-1 (Novagen) between the respective restriction sites to make pCDFDuetLptFG. The DNA fragment encoding LptCAB-His_6 was amplified by PCR from MC4100 genomic DNA using primers N-NcoI-LptC and LptB-His6-EcoRI-C. The amplified fragment was then digested with restriction enzymes NcoI and EcoRI and ligated into pCDFDuetLptFG to make pCDFDuetLptCAB-His_6-LptFG. In order to amplify the DNA fragment for LptCAB-His_6 with the correct restriction site, the amino acid at the second position of LptC was mutated from serine to glycine. The ligation product was transformed into NovaBlue competent cells by heat-shock, and transformants were selected in media containing spectinomycin (50 μg/mL). Plasmids were purified from individual colonies and sequenced.

Plasmid pCDFDuetHis_6-LptB-LptFG was constructed in three steps. First, the parent plasmid pCDFDuetLptFG was prepared by digesting pCDFDuetLptCAB-His_6-LptFG with NcoI and EcoRI enzymes to remove the DNA segment encoding *lptCAB-his* from the first multiple cloning site. The parent plasmid, pCDFDuetLptFG, was gel-purified and used for subsequent steps. A digested PCR product generated using primers N-NcoI-His_6LptB and C-LptB-EcoRI, and pET23/42LptB as template was used to ligate a *his-lptB* allele into the first multiple cloning site of the parent plasmid. The ligation product was transformed into NovaBlue competent cells by heat-shock, and transformants were selected in media containing spectinomycin (50 μg/mL). Plasmids were purified from individual colonies and sequenced.

pET22/42LptC was constructed by amplifying the *lptC* allele using primers N-NdeI-LptC and C-LptC-HindIII and pCDFDuet-LptCABHis_6-LptFG as template. The amplified fragment

was digested with NdeI and HindIII enzymes and inserted into a digested pET22/42 expression vector (34).

All variants of the Lpt IM complex were made by mutagenizing pCDFDuetHis$_6$LptB-LptFG using SDM, as described above.

Table 2.1. Strains used in this study.

Strain	Genotype	Reference
BL21(λDE3)	F$^-$ *omp*T *gal dcm lon hsd*S$_B$(r$_B^-$, m$_B^-$) λ(DE3)	Novagen
KRX	[F', *tra*D36, Δ*omp*P, *pro*A$^+$B$^+$, *lac*I^q, Δ(*lac*Z)M15] Δ*omp*T, *end*A1, *rec*A1, *gyr*A96, *thi*-1, *hsd*R17 (r$_K^-$, m$_K^+$), e14– (McrA–), *rel*A1, *sup*E44, Δ(*lac-pro*AB), Δ(*rha*BAD)::T7 gene 1	Promega
NovaBlue	*endA1 hsd*R17 (r$_K^-$, m$_K^+$) *sup*E44 *thi*-1 *rec*A1 *gyr*A96 *rel*A1 *lac* F′[*pro*A$^+$B$^+$ *lac*I^{q}ZΔM15::Tn*10*]	Novagen
MC4100	F$^-$ *araD139* Δ(*arg*F-*lac*)U169 *rpsL150 relA1 flbB5301 deoC1 ptsF25 rbsR*	(35)
NR754	MC4100 *ara*$^+$	(36)
NR1414	NR754 (pET23/42)	This study
NR2583	NR754 (pET23/42LptB)	This study
NR1872	NR754 (pET23/42LptB-His$_8$)	This study
NR2575	NR754 (pET23/42LptB-F90A)	This study
NR2576	NR754 (pET23/42LptB-F90A-His$_8$)	This study
NR2577	NR754 (pET23/42LptB-F90Y)	This study
NR2578	NR754 (pET23/42LptB-F90Y-His$_8$)	This study
NR2634	NR754 (pET23/42LptB-R91A)	This study
NR2675	NR754 (pET23/42LptB-R91A-His$_8$)	This study
NR2723	NR754 (pET23/42LptB-E163Q)	This study
NR2589	NR754 (pET23/42LptB-E163Q-His$_8$)	This study
NR2719	NR754 (pET23/42LptB-H195A)	This study
NR2670	NR754 (pET23/42LptB-H195A-His$_8$)	This study

Table 2.2. SDM primers.

aa change	Primer name	Primer sequence (5' to 3')
Stop Codon Insertion	LptB-MinusCHis-f	GAAGACTTCAGACTCTGAGAGCACCACCACCACCACCAC
	LptB-MinusCHis-r	GTGGTGGTGGTGGTGGTGCTCTCAGAGTCTGAAGTCTTC
F90A	5LptBF90A	GCCACAGGAAGCCTCCATTGCCCGTCGCCTC
	3LptBF90A	GAGGCGACGGGCAATGGAGGCTTCCTGTGGC
F90Y	5LptBF90Y	CCACAGGAAGCCTCCATTTACCGTCGCCTC
	3LptBF90Y	GAGGCGACGGTAAATGGAGGCTTCCTGTGG
R91A	5LptBR91A	ACAGGAAGCCTCCATTTTCGCTCGCCTCAGCGTT
	3LptBR91A	AACGCTGAGGCGAGCGAAAATGGAGGCTTCCTGT
E163Q	LptB-E163Q-f	TATTCTGCTCGACCAACCGTTTGCCGGGGTTGACCCG
	LptB-E163Q-r	CGGGTCAACCCCGGCAAACGGTTGGTCGAGCAGAATA
H195A	LptB-H195A-f	CAGTGTTTCACGCACGTTGGCGTCAGTGATCAGCACGCC
	LptB-H195A-r	GGCGTGCTGATCACTGACGCCAACGTGCGTGAAACACTG

Table 2.3. Other primers.

Primer name	Primer Sequence (5' to 3')
N-NdeI-LptF	GGAATTCCATATGATAATCATAAGATATCTGGTGCGG
LptG-KpnI-C	CGGGGTACCTTACGATTTTCTCATTAACAGCCACA
N-NcoI-LptC	CATGCCATGGGTAAAGCCAGACGTTGGGTT
LptB-His6-EcoRI-C	GGAATTCTTAATGATGATGATGATGATGCTCGAGTCTGAAGTCTTCCCCA AGG
N-NcoI-His_6LptB	TATACCATGGGCCATCATCATCATCATCACGGAATGGCAACATTAACTGC AAAGAACC
C-LptB-EcoRI	TATAGAATTCTCAGAGTCTGAAGTCTTCCCCAAGGTATACACG
N-NdeI-LptC	TATACATATGAGTAAAGCCAGACGTTGGG
C-LptC-HindIII	TATAAAGCTTTTAAGGCTGAGTTTGTTTGTTTTGAATTTC

2.7.2 Affinity Purifications

To perform affinity purifications of LptB variants, the reported method was slightly modified (7). Overnight cultures of NR2583, NR1872, NR2589, NR2576, NR2578, and NR2670 (Table 2.1) were inoculated 1 to 100 into fresh LB broth supplemented with 50 μg/mL carbenicillin. Cultures were grown at 37°C to mid-logarithmic phase. Cells were harvested by centrifugation at 5,000 x *g* for 10 min, as described. At this point, cells were frozen at -80°C. Thawed cells were resuspended in 20 mM Tris-HCl, pH 7.4 supplemented with 1 mM phenylmethanesulfonylfluoride (PMSF, Sigma), 100 μg/mL lysozyme (Sigma), and 50 μg/mL DNase I (Sigma). Cells were lysed by three passages through an EmulsiFlex-C3 high pressure cell disruptor (Avestin Inc.), and the lysate was centrifuged at 5,000 x *g* for 10 min to remove unbroken cells. The supernatant was centrifuged at 100,000 x *g* for 1 h to pellet membranes, as described. Resuspended membranes were solubilized in 50 mM Tris-HCl, pH 7.4, 300 mM NaCl, 10% glycerol, 5 mM $MgCl_2$, 1% *n*-dodecyl-β-D-maltopyranoside (DDM, Anatrace) at 4°C for 1 hour. Solubilized membranes were centrifuged again at 100,000 x *g* for 1 h, and the supernatant supplemented with 10 mM imidazole was passed twice over TALON metal affinity resin (Clontech) pre-equilibrated with 50 mM Tris-HCl, pH 7.4, 300 mM NaCl, 10% glycerol, 0.05% DDM, 10 mM imidazole. After washing with 40 column volumes of 50 mM Tris-HCl, pH 7.4, 300 mM NaCl, 10% glycerol, 0.05% DDM, 20 mM imidazole, protein was eluted with 50 mM Tris-HCl, pH 7.4, 300 mM NaCl, 10% glycerol, 0.05% DDM, 200 mM imidazole. Eluates were precipitated with 10% trichloroacetic acid (TCA), followed by a cold acetone wash. Precipitates were resuspended in 2x SDS-PAGE sample buffer supplemented with 5% β-mercaptoethanol. Samples were boiled for 10 min and loaded onto 4-20% SDS-polyacrylamide gels, and the proteins were transferred onto Immun-Blot® PVDF membranes (Bio-Rad) and

subjected to immunoblotting using anti-BamA (37), anti-LptC (38), anti-LptF (39), and anti-LptB polyclonal antisera (this study), followed by immunoblotting with a donkey anti-rabbit horseradish peroxidase (HRP) conjugate secondary antibody (GE Amersham). Bands were visualized using ECL™ Prime Western Blotting Detection Reagent (GE Amersham) and Biomax Light Film (Kodak).

Anti-LptB antisera were raised in a rabbit using the LptB peptide DDLSAEQREDRANE as immunogen (ProSci Inc.).

2.7.3 ATPase Assays

ATPase activity was measured using a modified molybdate method for detecting inorganic phosphate release (5, 40). The LptB reaction mixture contained 7 μM LptB in 50 mM Tris-HCl, pH 8.0, 500 mM NaCl, 10% glycerol. The LptBFGC reaction mixture contained 0.2 μM LptBFGC in 50 mM Tris-HCl, pH 8.0, 500 mM NaCl, 10% glycerol, 0.05% *n*-dodecyl-β-D-maltopyranoside (DDM, Anatrace). Reactions were initiated at 25°C with the addition of the indicated amount of ATP. If not indicated, 5 mM ATP/5 mM $MgCl_2$ (final concentrations) were used. The linear time range of activity was determined for both LptB and LptBFGC. Reactions were stopped within the linear range by the addition of an equal volume of 12% SDS. Inorganic phosphate was measured using the reported method (40). Absorbance values were measured using a Spectramax Plus 384 plate reader (Molecular Devices). Data was analyzed and kinetic parameters were determined using GraphPad Prism 5 (GraphPad Software, Inc., La Jolla, CA, USA).

2.7.4 Protein Overexpression and Purification

2.7.4.1 LptB and LptBFGC for ATPase Assays

pET22/42LptB-His_8, pET22/42LptB-E163Q-His_8, pET22/42LptB-H195A-His_8, pET23/42LptB-F90A-His_8, and pET23/42LptB-F90Y-His_8 were each transformed into KRX cells. Cultures were grown at 37°C after diluting overnight cultures 1 to 100 into fresh LB broth supplemented with 50 μg/mL carbenicillin. LptB-His variant expression was induced with 0.2% L-rhamnose at OD_{600} ~ 1, and cultures were grown for 16 h at 16°C. Proteins were purified as described in Section 2.7.4.2 below.

LptB-His_6-LptFGC was used to compare the ATPase activity of LptB alone and in complex (Figure 2.7A), as well as to test for compound inhibition (data not shown). pCDFDuetLptCAB-His_6-LptFG was transformed into BL21(λDE3) cells, which were grown in LB broth supplemented with 50 μg/mL spectinomycin at 37°C until they reached OD_{600} ~ 1. At this time, 50 μM isopropyl β-D-1-thiogalactopyranoside (IPTG; Gold Biotechnology) was added to the media to induce expression of LptBFGC. Cells were grown for an additional 2 h at 37°C, at which point they were harvested by centrifugation at 5,200 x *g* for 10 min. Cells were resuspended in 50 mM Tris-HCl, pH 7.4, supplemented with 1 mM PMSF, 100 μg/mL lysozyme, and 50 μg/mL DNase I. Harvested cells were lysed by three passages through a French pressure cell (Thermo Electron) at 16,000 psi. After removal of unbroken cells, membranes were recovered by centrifugation at 100,000 x *g* for 1 h. Membranes were resuspended in 20 mM Tris-HCl, pH 7.4, 10% glycerol. At this point, membranes were flash frozen in liquid nitrogen and stored at -80°C. Thawed membranes were solubilized with 20 mM Tris-HCl, pH 7.4, 5 mM $MgCl_2$, 300 mM NaCl, 1% DDM, 10% glycerol, and 2 mM ATP at 4°C

for 1 h, followed by centrifugation at 100,000 x *g* for 30 min. The remainder of the purification is the same as the reported protocol (5).

To overexpress and purify His_6-LptBFGC (to test the ATPase activity of LptB variants), KRX cells were transformed with pCDFDuetHis_6LptB-LptFG and pET22/42LptC. Cultures were grown at 37°C after diluting overnight cultures 1 to 100 into fresh LB broth supplemented with 50 μg/mL spectinomycin and 50 μg/mL carbenicillin. Complex expression was induced with 0.02% L-rhamnose at OD_{600} ~ 1, and cultures were grown for 3 h at 37°C. Cells were harvested by centrifugation at 5200 x *g* for 15 min and resuspended in 50 mM Tris-HCl, pH 7.4, supplemented with 1 mM 0.5 mM PMSF, 100 μg/mL lysozyme, and 50 μg/mL DNase I. Harvested cells were lysed by three passages through an EmulsiFlex-C3 high pressure cell disruptor. After removal of unbroken cells, membranes were recovered by centrifugation at 100,000 x *g* for 1 h. Membranes were resuspended and subsequently solubilized in 20 mM Tris-HCl, pH 7.4, 5 mM $MgCl_2$, 300 mM NaCl, 1% DDM, 10% glycerol, and 2 mM ATP at 4°C for 1 h, followed by centrifugation at 100,000 x *g* for 30 min. The supernatant was applied to TALON metal affinity resin, followed by elution with 20 mM Tris-HCl, pH 7.4, 300 mM NaCl, 0.05% DDM, 10% glycerol, and 25 mM imidazole. The eluate was concentrated with an Amicon centrifugation filter, 50 kDa MWCO (Amicon Ultra, Millipore), and then subjected to size exclusion chromatography on a Superdex 200 10/300 GL column (GE Healthcare) in 20 mM Tris-HCl, pH 7.4, 300 mM NaCl, 0.05% DDM, 10% glycerol. Fractions were pooled and concentrated to ~ 2.5 mg/mL.

2.7.4.2 LptB for Crystallography

Full-length LptB with a C-terminal His_8 tag (referred to as LptB-His) was overexpressed as previously described, with a few notable changes (4). Cultures of BL21(λDE3) cells containing the plasmid with LptB-His were grown at 37°C after diluting an overnight culture 1 to 100 in fresh LB broth supplemented with 50 μg/mL carbenicillin. Cells were grown to OD_{600} ~ 1, and the temperature was reduced to 16°C. Overexpression was induced by addition of 100 μM IPTG, and the cells were grown for 16 h at 16°C. Cells were harvested by centrifugation at 5,000 x *g* for 20 min. Cells were resuspended in Tris-buffered saline (TBS; 20 mM Tris, pH 8.0, 150 mM NaCl), 20% glycerol, 0.5 mM Tris(hydroxypropyl)phosphine (THP, EMD Millipore) supplemented with 0.5 mM PMSF, 50 μg/mL lysozyme, and 50 μg/mL DNase I. Cells were lysed by three passages through a French pressure cell at 16,000 psi and centrifuged at 6,000 x *g* for 10 min to remove unbroken cells. The supernatant was centrifuged at 100,000 x *g* for 30 min to remove membranes. Imidazole was then added to the supernatant to a final concentration of 10 mM. Ni-NTA Superflow resin (Qiagen) was pre-washed with TBS supplemented with 20% glycerol and 10 mM imidazole in preparation for batch nickel affinity chromatography. The supernatant was then incubated with the pre-washed Ni-NTA resin at 4°C for 60 min. Following removal of the flow-through, the resin was washed with 20 column volumes of TBS with 20% glycerol and 20 mM imidazole. The protein was then eluted in one batch with 2 column volumes of TBS with 20% glycerol, 0.5 mM THP, and 200 mM imidazole. The eluate was concentrated with an Amicon centrifugation filter, 10 kDa MWCO to ~ 20 mg/mL. The concentrated protein was further purified by size exclusion chromatography on a Superdex 200 10/300 GL column in TBS, 20% glycerol, 0.5 mM THP. The fractions with pure LptB-His were collected, pooled, and concentrated to 15 – 20 mg/mL using a centrifugal filter.

LptB-E163Q-His was overexpressed in KRX cells in LB medium supplemented with 50 μg/mL carbenicillin. Overexpression was induced with 0.2% L-rhamnose. Cells were harvested and the protein was purified as described above for the wild-type protein with one notable difference. Following elution from the Ni-NTA Superflow resin and prior to concentration, ethylenediaminetetraacetic acid (EDTA) was added to the eluate to a final concentration of 1 mM.

A selenomethionine derivative of LptB-His (hereby called SeMet-LptB-His) was overexpressed in BL21(λDE3) from the same pET22/42 vector as the wild-type variant but overexpressed in SeMet minimal medium, using a previously reported method (41). The cells were harvested and the protein was purified as described above for the wild-type protein.

2.7.5 LptB Crystallization

2.7.5.1 Native Crystals

Prior to crystallization, LptB-His or LptB-E163Q-His was diluted to 7 – 10 mg/mL with TBS to yield a final glycerol content of 10%. Crystals were grown with the hanging drop method at room temperature. Prior to setting up hanging drops, LptB-His was incubated with 2.5 mM ATP, 2.5 mM $MgCl_2$ and LptB-E163Q-His was incubated with 2.5 mM ATP at 4°C for 60 min. After screening many conditions, the optimal condition for obtaining Mg^{2+}-ADP co-complex crystals was mixing 1 μL protein with 1 μL reservoir solution containing 0.1 M MES, pH 6.5, 30% PEG 4000. After several days, triangular plate-like crystals appeared. Crystals were flash-frozen with liquid nitrogen after cryoprotecting with a solution containing 0.1 M MES, pH 6.5, 33% PEG 4000, 24% glycerol. After screening conditions to crystallize LptB-E163Q-His in complex with ATP, the best condition was found to be mixing 1 μL protein with 1

μL reservoir solution containing 0.6 M NaCl, 0.1 M MES, pH 7.0, 26.5% PEG 4000. After several days, large crystals were obtained. Crystals were flash-frozen using a cryoprotectant containing 0.6 M NaCl, 0.09 M MES, pH 7.0, 28% PEG 4000, 23% glycerol, and 2.5 mM ATP.

2.7.5.2 Selenomethionine Derivative Crystals

As described above, the final SeMet-LptB-His solution was diluted to 7 – 10 mg/mL with a final glycerol content of 10%. Optimal crystals were obtained with 2 μL protein mixed with 1 μL reservoir solution comprised of 0.1 M MES, pH 6.5, 31% PEG 4000. These flat, plate-like crystals were flash-frozen using a cryoprotectant containing 0.1 M MES, pH 6.5, 35% PEG 4000, 20% glycerol.

2.7.5.3 Heavy Metal Soak

A tantalum derivative of the native LptB-His crystals was prepared in order to obtain additional phasing information. Crystals were soaked overnight with tantalum clusters (Jena) and then frozen in tantalum-free cryoprotectant, as described above.

2.7.6 Crystallography Data Collection

X-ray diffraction data were collected at the National Synchrotron Light Source beamlines X29 or X25 at Brookhaven National Laboratory, except for the SeMet dataset, which was collected at 24-ID-E of the Advanced Photon Light Source at Argonne National Laboratory by Dr. Seong-Joo Lee. SeMet-LptB-His crystals were collected at 0.97917 Å, and the crystals soaked with tantalum clusters were collected at 1.2548 Å. All other crystals were collected at

1.075 Å. LptB-His and all of its derivatives belong to the space group *C*121. LptB-E163Q-His belongs to the space group $C222_1$.

2.7.7 Crystallography Data Processing and Structure Determination

2.7.7.1 SeMet-LptB-ADP Complex

All data sets were indexed and integrated using iMosflm and scaled using Scala (42, 43). Heavy atom sites in the SeMet and tantalum structures were determined using HKL2MAP (44). The top occupancy sites for each of the two derivatives were then input into the CCP4 program Phaser to refine and find additional sites using single-wavelength anomalous diffraction (SAD) (45, 46). Initially, only a low-resolution (3.25 Å) native data was obtained, and this dataset was merged with the 2.05 Å SeMet data set truncated to 2.5 Å and the tantalum dataset. Phases going out to 2.5 Å were obtained by multiple isomorphous replacement with anomalous scattering (MIRAS) using SHARP with the merged dataset and the Phaser-refined heavy atom sites for the two derivatives (47). After obtaining the phases from SHARP and performing density modification using DM, a map that looked protein-like was obtained, but it was not sufficiently clear to facilitate model building (48). Therefore, Phenix Autobuild was used to build a model after inputting the experimental phases, the HLDM coefficients and 2.05 Å SeMet structure factors, and the amino acid sequence of the construct (49). After this initial Autobuild run, a model with an R_{work} of 36.3% and an R_{free} of 40.0% was obtained. The density was much improved, but there were still several gaps in the backbone of the model. At this point, a homology model was used to fill in the gaps. Using the Wide Search Molecular Replacement server (50), the optimal homology model was determined to be PDB entry 1GAJ. After superposition in Coot (51, 52), the missing parts of the model were manually added from the

homology structure. Then, a second round of Autobuild was performed using the latest SeMet-LptB-His model to generate the map along with the Hendrickson-Lattman coefficients from SHARP to guide the building and refinement. At this stage, a model with an R_{work} of 25.2% and an R_{free} of 30.3% was obtained. Next, the model was refined with CNS by doing rounds of *B*-factor refinement and simulated annealing (53, 54). The refinement was then completed with Phenix, by doing cycles of minimization, ADP (atomic displacement parameter or *B*-factor) refinement, and TLS refinement using TLS parameters determined by the TLSMD server (55), interspersed with manual adjustments using Coot. The final R_{work} and R_{free} were 21.3% and 25.2%, respectively for the SeMet structure.

2.7.7.2 Native LptB-ADP Complex

After determining the structure of the SeMet-LptB-Mg^{2+}-ADP complex, a high-resolution dataset of native LptB-Mg^{2+}-ADP was obtained. The structure of the native Mg^{2+}-ADP co-complex was obtained by molecular replacement using the SeMet structure as the search model and doing rigid body refinement in Phenix (56), after copying and extending the free-*R* column from the SeMet dataset. The structure was then refined in Phenix as described above. The final R_{work} and R_{free} values were 19.8% and 21.8%, respectively.

2.7.7.3 LptB-E163Q-ATP Complex

The LptB-E163Q-ATP structure was solved by molecular replacement using Phaser with the native LptB-Mg^{2+}-ADP structure as the search model. The search model had to be broken up into the RecA-like ATPase domain and the α-helical domain in order to obtain a solution. Each domain was searched for twice, leading to an initial dimer model of the full protein. The model

was then refined using Phenix as described above. Final R_{work} and R_{free} values of 18.8% and 21.0%, respectively, were obtained.

Table 2.4. Data collection and refinement statistics.

Data Set	LptB-ADP	LptB-ATP
Space Group	C121	$C222_1$
Unit Cell		
Dimensions (a, b, c) (Å)	191.90, 36.02, 64.51	66.62, 138.36, 101.28
Angles (α, β, γ) (°)	90.00, 96.16, 90.00	90, 90, 90
Data Collection[a]		
Wavelength (Å)	1.075	1.075
Resolution Range (Å)	40.41-1.55 (1.63-1.55)	40.86-1.65 (1.74-1.65)
R_{merge}	0.074 (0.570)	0.139 (0.806)
Completeness, %	98.6 (94.7)	99.2 (98.5)
Mean $I/\sigma(I)$	9.8 (2.1)	9.2 (2.8)
Unique Reflections	63317	56004
Multiplicity	3.9 (3.4)	7.9 (8.0)
Refinement		
R_{work} (%) / R_{free} (%)	19.76 / 21.76	18.81 / 21.00
Number of LptB molecules/asymmetric unit	2	2
Number of modeled LptB residues / chain	234 (A) / 230 (B)	235 (A) / 235 (B)
Number of water molecules	168	149
Number of ions	2	2
Average B factor (Å^2)		
Nucleotide-metal	25.876	14.869
Solvent	32.795	28.792
Protein	29.666	25.95
Ramachandram plot		
Favored (%)	99.8	98.3
Disallowed (%)	0	0
Rmsd from ideal geometry		
Bond lengths (Å)	0.004	0.007
Bond angles (°)	0.95	0.965

[a] Values in parentheses are for highest-resolution shell.

Table 2.5. Data collection and phasing statistics.

Data Set	LptB-ADP (SeMet)	LptB-ADP (Tantalum)	LptB-ADP (Low-resolution native)
Space Group	C121	C121	C121
Unit Cell			
Dimensions (a, b, c) (Å)	192.60, 35.88, 64.34	192.31, 36.79, 64.43	194.55, 35.39, 65.15
Angles (α, β, γ) (°)	90, 95.83, 90	90, 95.08, 90	90, 95.37, 90
Data Collection[a]			
Wavelength (Å)	0.97917	1.2548	1.075
Resolution Range (Å)	40-2.05 (2.16-2.05)	47.89-2.80 (2.95-2.80)	48.42-3.25 (3.43-3.25)
R_{merge}	0.074 (0.498)	0.097 (0.378)	0.182 (0.380)
Completeness, %	99.2 (97.8)	99.6 (99.6)	98.8 (99.3)
Mean $I/\sigma(I)$	8.7 (2.3)	8.3 (3.0)	3.8 (2.2)
Unique Reflections	27803	11391	7169
Multiplicity	3.3 (3.2)	3.7 (3.7)	3.0 (3.1)
Overall isomorphous phasing power acentric	1.073	0.689	0
Overall isomorphous phasing power centric	0.906	0.673	0
Overall anomalous phasing power	0.919	0.426	0

[a] Values in parentheses are for highest-resolution shell.

2.7.8 Data Deposition

The atomic coordinates and structure factors for the structures described in this chapter have been deposited in the Protein Data Bank, www.pdb.org (PDB ID codes 4p31, 4p32, and 4p33).

2.8 References

1. Dassa E & Bouige P (2001) The ABC of ABCS: a phylogenetic and functional classification of ABC systems in living organisms. *Research in microbiology* 152(3-4):211-229.

2. Davidson AL, Dassa E, Orelle C, & Chen J (2008) Structure, function, and evolution of bacterial ATP-binding cassette systems. *Microbiology and molecular biology reviews : MMBR* 72(2):317-364, table of contents.

3. Dean M, Rzhetsky A, & Allikmets R (2001) The human ATP-binding cassette (ABC) transporter superfamily. *Genome research* 11(7):1156-1166.

4. Gronenberg LS & Kahne D (2010) Development of an activity assay for discovery of inhibitors of lipopolysaccharide transport. *J Am Chem Soc* 132(8):2518-2519.

5. Narita S & Tokuda H (2009) Biochemical characterization of an ABC transporter LptBFGC complex required for the outer membrane sorting of lipopolysaccharides. *FEBS Lett* 583(13):2160-2164.

6. Sherman DJ*, et al.* (2014) Decoupling catalytic activity from biological function of the ATPase that powers lipopolysaccharide transport. *Proc Natl Acad Sci U S A* 111(13):4982-4987.

7. Chng SS, Gronenberg LS, & Kahne D (2010) Proteins required for lipopolysaccharide assembly in Escherichia coli form a transenvelope complex. *Biochemistry* 49(22):4565-4567.

8. Okuda S, Freinkman E, & Kahne D (2012) Cytoplasmic ATP hydrolysis powers transport of lipopolysaccharide across the periplasm in E. coli. *Science* 338(6111):1214-1217.

9. Tran AX, Dong C, & Whitfield C (2010) Structure and functional analysis of LptC, a conserved membrane protein involved in the lipopolysaccharide export pathway in Escherichia coli. *J Biol Chem* 285(43):33529-33539.

10. Smith PC*, et al.* (2002) ATP binding to the motor domain from an ABC transporter drives formation of a nucleotide sandwich dimer. *Mol Cell* 10(1):139-149.

11. Hung LW*, et al.* (1998) Crystal structure of the ATP-binding subunit of an ABC transporter. *Nature* 396(6712):703-707.

12. Walker JE, Saraste M, Runswick MJ, & Gay NJ (1982) Distantly related sequences in the alpha- and beta-subunits of ATP synthase, myosin, kinases and other ATP-requiring enzymes and a common nucleotide binding fold. *EMBO J* 1(8):945-951.

13. Oswald C, Holland IB, & Schmitt L (2006) The motor domains of ABC-transporters. What can structures tell us? *Naunyn-Schmiedeberg's archives of pharmacology* 372(6):385-399.

14. Hopfner KP*, et al.* (2000) Structural biology of Rad50 ATPase: ATP-driven conformational control in DNA double-strand break repair and the ABC-ATPase superfamily. *Cell* 101(7):789-800.

15. Krissinel E & Henrick K (2004) Secondary-structure matching (SSM), a new tool for fast protein structure alignment in three dimensions. *Acta Crystallogr D Biol Crystallogr* 60(Pt 12 Pt 1):2256-2268.

16. Moody JE, Millen L, Binns D, Hunt JF, & Thomas PJ (2002) Cooperative, ATP-dependent association of the nucleotide binding cassettes during the catalytic cycle of ATP-binding cassette transporters. *J Biol Chem* 277(24):21111-21114.

17. Zaitseva J, Jenewein S, Jumpertz T, Holland IB, & Schmitt L (2005) H662 is the linchpin of ATP hydrolysis in the nucleotide-binding domain of the ABC transporter HlyB. *EMBO J* 24(11):1901-1910.

18. Ernst R*, et al.* (2008) A mutation of the H-loop selectively affects rhodamine transport by the yeast multidrug ABC transporter Pdr5. *Proc Natl Acad Sci U S A* 105(13):5069-5074.

19. Karpowich N*, et al.* (2001) Crystal structures of the MJ1267 ATP binding cassette reveal an induced-fit effect at the ATPase active site of an ABC transporter. *Structure* 9(7):571-586.

20. Oldham ML & Chen J (2011) Snapshots of the maltose transporter during ATP hydrolysis. *Proc Natl Acad Sci U S A* 108(37):15152-15156.

21. Davidson AL & Sharma S (1997) Mutation of a single MalK subunit severely impairs maltose transport activity in Escherichia coli. *J Bacteriol* 179(17):5458-5464.

22. Nikaido K & Ames GF (1999) One intact ATP-binding subunit is sufficient to support ATP hydrolysis and translocation in an ABC transporter, the histidine permease. *J Biol Chem* 274(38):26727-26735.

23. Schneider E & Hunke S (1998) ATP-binding-cassette (ABC) transport systems: functional and structural aspects of the ATP-hydrolyzing subunits/domains. *FEMS microbiology reviews* 22(1):1-20.

24. Shyamala V, Baichwal V, Beall E, & Ames GF (1991) Structure-function analysis of the histidine permease and comparison with cystic fibrosis mutations. *J Biol Chem* 266(28):18714-18719.

25. Janas E*, et al.* (2003) The ATP hydrolysis cycle of the nucleotide-binding domain of the mitochondrial ATP-binding cassette transporter Mdl1p. *J Biol Chem* 278(29):26862-26869.

26. Zaitseva J*, et al.* (2006) A structural analysis of asymmetry required for catalytic activity of an ABC-ATPase domain dimer. *EMBO J* 25(14):3432-3443.

27. McNicholas S, Potterton E, Wilson KS, & Noble ME (2011) Presenting your structures: the CCP4mg molecular-graphics software. *Acta Crystallogr D Biol Crystallogr* 67(Pt 4):386-394.

28. Sherman DJ, Okuda S, Denny WA, & Kahne D (2013) Validation of inhibitors of an ABC transporter required to transport lipopolysaccharide to the cell surface in Escherichia coli. *Bioorg Med Chem* 21(16):4846-4851.

29. Hollenstein K, Frei DC, & Locher KP (2007) Structure of an ABC transporter in complex with its binding protein. *Nature* 446(7132):213-216.

30. Mourez M, Hofnung M, & Dassa E (1997) Subunit interactions in ABC transporters: a conserved sequence in hydrophobic membrane proteins of periplasmic permeases defines an important site of interaction with the ATPase subunits. *EMBO J* 16(11):3066-3077.

31. Saurin W, Hofnung M, & Dassa E (1999) Getting in or out: early segregation between importers and exporters in the evolution of ATP-binding cassette (ABC) transporters. *Journal of molecular evolution* 48(1):22-41.

32. Szakacs G, Paterson JK, Ludwig JA, Booth-Genthe C, & Gottesman MM (2006) Targeting multidrug resistance in cancer. *Nature reviews. Drug discovery* 5(3):219-234.

33. Swoboda JG*, et al.* (2009) Discovery of a small molecule that blocks wall teichoic acid biosynthesis in Staphylococcus aureus. *ACS Chem Biol* 4(10):875-883.

34. Sklar JG*, et al.* (2007) Lipoprotein SmpA is a component of the YaeT complex that assembles outer membrane proteins in Escherichia coli. *Proc. Natl. Acad. Sci. U.S.A.* 104(15):6400-6405.

35. Casadaban MJ (1976) Transposition and fusion of the lac genes to selected promoters in Escherichia coli using bacteriophage lambda and Mu. *J Mol Biol* 104(3):541-555.

36. Ruiz N, Gronenberg LS, Kahne D, & Silhavy TJ (2008) Identification of two inner-membrane proteins required for the transport of lipopolysaccharide to the outer membrane of Escherichia coli. *Proc. Natl. Acad. Sci. U. S. A.* 105(14):5537-5542.

37. Kim S*, et al.* (2007) Structure and function of an essential component of the outer membrane protein assembly machine. *Science* 317(5840):961-964.

38. Freinkman E, Okuda S, Ruiz N, & Kahne D (2012) Regulated Assembly of the Transenvelope Protein Complex Required for Lipopolysaccharide Export. *Biochemistry* 51(24):4800-4806.

39. Villa R*, et al.* (2013) The Escherichia coli Lpt Transenvelope Protein Complex for Lipopolysaccharide Export Is Assembled via Conserved Structurally Homologous Domains. *J Bacteriol* 195(5):1100-1108.

40. Chifflet S, Torriglia A, Chiesa R, & Tolosa S (1988) A method for the determination of inorganic phosphate in the presence of labile organic phosphate and high concentrations of protein: application to lens ATPases. *Anal Biochem* 168(1):1-4.

41. Van Duyne GD, Standaert RF, Karplus PA, Schreiber SL, & Clardy J (1993) Atomic structures of the human immunophilin FKBP-12 complexes with FK506 and rapamycin. *J. Mol. Biol.* 229(1):105-124.

42. Leslie AGW & Powell HR (2007) Processing Diffraction Data with Mosflm. *Evolving Methods for Macromolecular Crystallography*), Vol 235, pp 41-51.

43. Evans P (2006) Scaling and assessment of data quality. *Acta Crystallographica Section D-Biological Crystallography* 62:72-82.

44. Pape T & Schneider TR (2004) HKL2MAP: a graphical user interface for macromolecular phasing with SHELX programs. *Journal of Applied Crystallography* 37:843-844.

45. Bailey S (1994) The Ccp4 Suite - Programs for Protein Crystallography. *Acta Crystallographica Section D-Biological Crystallography* 50:760-763.

46. Mccoy AJ*, et al.* (2007) Phaser crystallographic software. *Journal of Applied Crystallography* 40:658-674.

47. Bricogne G, Vonrhein C, Flensburg C, Schiltz M, & Paciorek W (2003) Generation, representation and flow of phase information in structure determination: recent developments in and around SHARP 2.0. *Acta Crystallographica Section D-Biological Crystallography* 59:2023-2030.

48. Cowtan K (1994) Joint CCP4 and ESF-EACBM Newsletter on Protein Crystallography. pp 34-38.

49. Terwilliger TC*, et al.* (2008) Iterative model building, structure refinement and density modification with the PHENIX AutoBuild wizard. *Acta Crystallographica Section D-Biological Crystallography* 64:61-69.

50. Stokes-Rees I & Sliz P (2010) Protein structure determination by exhaustive search of Protein Data Bank derived databases. *Proceedings of the National Academy of Sciences of the United States of America* 107(50):21476-21481.

51. Emsley P & Cowtan K (2004) Coot: model-building tools for molecular graphics. *Acta Crystallographica Section D-Biological Crystallography* 60:2126-2132.

52. Emsley P, Lohkamp B, Scott WG, & Cowtan K (2010) Features and development of Coot. *Acta Crystallographica Section D-Biological Crystallography* 66:486-501.

53. Brunger AT*, et al.* (1998) Crystallography & NMR system: A new software suite for macromolecular structure determination. *Acta Crystallographica Section D-Biological Crystallography* 54:905-921.

54. Brunger AT (2007) Version 1.2 of the Crystallography and NMR system. *Nature Protocols* 2(11):2728-2733.

55. Painter J & Merritt EA (2006) Optimal description of a protein structure in terms of multiple groups undergoing TLS motion. *Acta Crystallographica Section D-Biological Crystallography* 62:439-450.

56. Adams PD*, et al.* (2010) PHENIX: a comprehensive Python-based system for macromolecular structure solution. *Acta Crystallogr D Biol Crystallogr* 66(Pt 2):213-221.

Chapter Three

Reconstitution of the Lpt Inner Membrane Complex from Purified Components

---

All data in this chapter was generated by me. However, this project was largely a collaborative effort with Dr. Suguru Okuda, who made significant contributions to the methodology and assay development.

3.1 How to Study LPS Transport

A pure biochemical reconstitution of LPS transport that recapitulates what is observed *in vivo* is necessary to understand how the Lpt components function together to transport LPS. As described in Chapter 1, genetic depletion of any Lpt component does not result in observable intermediate LPS localizations, such as accumulation in the inner leaflet of the OM, and the essentiality of this pathway makes it impossible to make genetic knockouts of individual components (1, 2). Only recently have on-pathway intermediates of LPS transport been identified in cells (3). In order to observe these intermediates, the levels of specific Lpt proteins had to be modulated in the cell to create a bottleneck, beyond which LPS could not move. Therefore, LPS could be observed accumulating in Lpt components. The ability to observe transport intermediates in broken Lpt bridges made it possible to analyze the ATP requirement of the early steps of LPS transport in membrane vesicles derived from cells. These studies established the "PEZ" model for LPS transport through the transenvelope bridge. The limitations of genetic perturbations of the Lpt pathway due to its essentiality, however, and the lack of homogeneity in cell-derived membrane vesicles make it difficult to study the mechanism of LPS transport in these systems. A reconstitution from purified Lpt components is therefore essential to assess the minimal requirements for LPS transport without the confounding factors present in a cell or membrane vesicle. A pure reconstitution can also be used to assess the roles of individual components. LptC is closely associated with the ABC transporter LptBFG, and its specific role in the transport process is unclear. This chapter describes the development of a biochemical reconstitution of the Lpt IM complex from purified components that recapitulates how the process works in cells and was used to identify a potential role of LptC in IM complex activity.

The structural and biochemical studies of LptB described in Chapter 2 demonstrate the need to study Lpt components in complexes instead of individually to gain a better understanding of their cellular functions. It is clear that the ATPase activity of LptB alone differs drastically from that of the full IM complex purified in detergent (4). Additionally, ATP hydrolysis by LptB causes conformational changes in a region of the protein that is essential for interacting with other Lpt components (5). The activity of LptB has to be tightly coupled to other Lpt proteins in order to extract LPS from the IM. LptB is convenient to study individually because it has a measurable enzymatic activity (ATP hydrolysis). The other Lpt components do not have activities that can be detected using standard enzyme assays. Therefore, methods had to be developed to monitor LPS movement through the Lpt components.

Reconstituting LPS transport poses a particular challenge because the process involves transporting a large glycolipid out of one membrane, through an aqueous compartment and into another membrane. Reconstitution of the IM complex, however, was a good starting point for building up to a complete reconstitution of LPS transport. A reconstitution of the Lpt IM complex would help us understand how LptBFG function in combination with LptC to extract LPS from the IM. To study membrane transport processes, membrane protein machinery required to carry out the function of interest are purified in detergent solutions and often incorporated into liposomes, which mimic the cellular membrane environment (6). Therefore, the first step in developing a reconstitution of the Lpt IM complex was to find the most stable, active construct of LptBFGC that can be overexpressed, purified, and incorporated into liposomes. Once obtaining the optimal construct, tools to reconstitute the early steps of LPS transport were developed to begin to learn about how the IM complex works.

Like the reconstitution of bacterial lipoprotein transport (7), a reconstitution of the Lpt IM complex involves release of a lipid substrate from proteoliposomes to a soluble carrier protein. Although LptA is believed to form a transenvelope bridge *in vivo*, addition of soluble LptA to membrane vesicles overexpressing LptBFGC can receive LPS in an ATP-dependent manner (3). LptBFGC had previously been overexpressed and purified in detergent (4, 5, 8), but it was unclear when we started this project if this was the best construct to use for an *in vitro* reconstitution to recapitulate how the transporter works in the cell. Section 3.2 describes how highly active, functional IM complex components were obtained for use in a biochemical reconstitution. We then describe our approach to reconstituting the activity of this complex in proteoliposomes.

3.2 Overexpression and Purification of LptBFGC

Previously, all LptBFGC overexpression and purification methods involved affinity purification using a C-terminal hexahistidine tag on LptB (4, 8). During efforts to overexpress and purify LptB for crystallography (see Chapter 2), only LptB constructs with a C-terminal polyhistidine tag could be successfully obtained. Attempts to overexpress and purify LptB with an N-terminal polyhistidine tag resulted in large amounts of inclusion bodies and very little pure, soluble protein (data not shown). It was unclear, however, whether the full IM complex with a C-terminal hexahistidine tag on LptB is the most stable, active, and highest yielding construct to use for the reconstitution. The structure of LptB indicates that the N-terminus is farther from the dimer interface that is responsible for ATP hydrolysis in ABC systems than the C-terminus (5, 9, 10). This suggested that perhaps a complex with an N-terminal instead of a C-terminal affinity tag might have increased ATPase activity. Collaborator Natividad Ruiz at The Ohio State

University found that *E. coli* haploid strains expressing the C-terminally polyhistidine tagged LptB construct that we were using (LptB-His) show OM permeability defects, suggestive of an LPS assembly defect (data not shown). However, cells harboring a *his-lptB* allele (encoding LptB with an N-terminal polyhistidine tag, His-LptB) are phenotypically wild-type, indicating that the N-terminal polyhistidine tag does not interfere with cellular function. This suggested that the C-terminal tag interferes with the efficiency of LptB dimerization, as predicted by the crystal structure, resulting in less active Lpt machines.

Remarkably, although we could not overexpress and purify His-LptB as an NBD alone, we developed a method to overexpress and purify His-LptBFG and His-LptBFGC (with N-terminal polyhistidine tags on LptB) as stable complexes (Figure 3.1A). This result suggested that the presence of the TMDs (LptF and LptG) protects His-LptB from aggregation. This construct was used to evaluate LptB variants in Chapter 2 (see Figure 2.6). A complex containing His-LptB-E163Q was also overexpressed and purified. A comparison of the ATPase activities of these complexes in detergent indicated that an N-terminal polyhistidine tag on LptB does not interfere as much with activity as a C-terminal tag (Figure 3.1B). For both N- and C-terminally tagged complexes, the ATPase activity was reproducibly a little higher for LptBFGC than for LptBFG. Because of the increase in activity of the N-terminally tagged complexes, a reconstitution of LPS release from proteoliposomes would be done with the new constructs containing His-LptB. The fact that both LptBFG and LptBFGC can be overexpressed and purified allowed for the opportunity to study the role of LptC in a pure reconstitution. Additionally, we are very interested in obtaining a crystal structure of LptBFGC to learn about the interactions of these components during the catalytic cycle. With methods described in Chapter 2 to obtain pre- and post-hydrolysis states of LptB, we these wild-type-complexes to

find conditions in which LptBFGC can crystallize with ATP and ADP bound for structural studies.

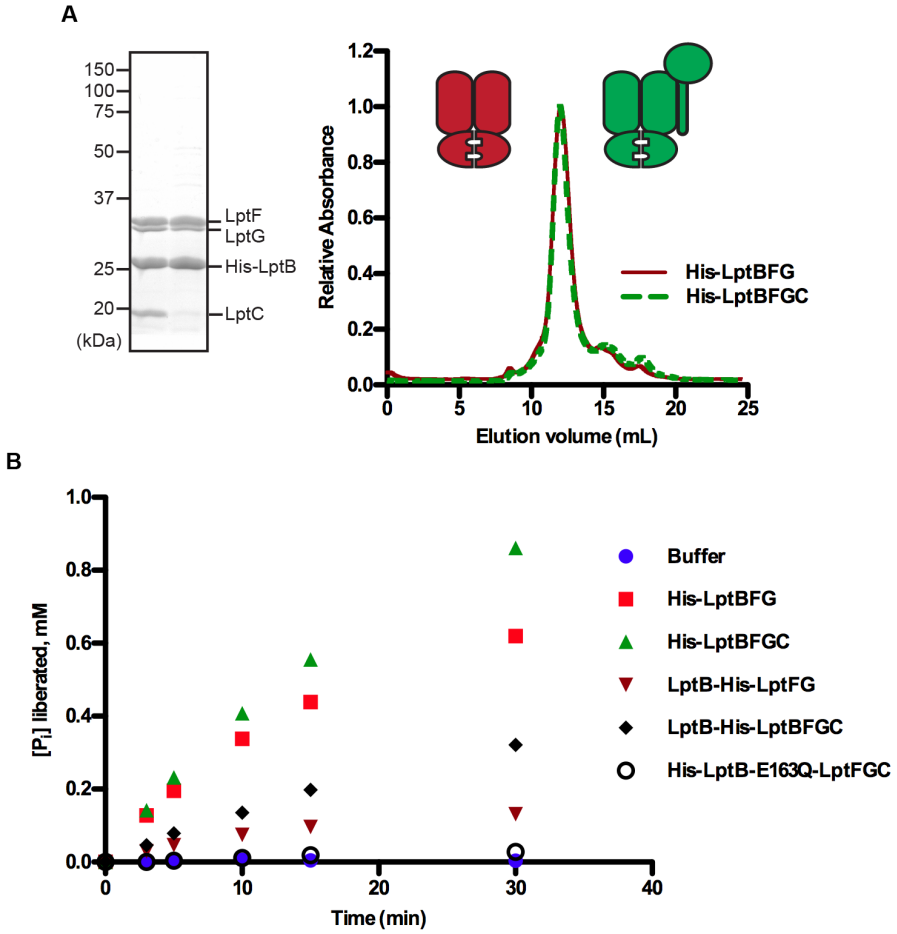

Figure 3.1. His-LptBFGC is more active than previous IM complex constructs. *(A)* Sodium dodecyl sulfate polyacrylamide gel electrophoresis (SDS-PAGE) and size exclusion chromatograms of purified LptBFG and LptBFGC. *(B)* ATPase activities of purified complexes in 0.05% DDM using 5 mM ATP/$MgCl_2$ were measured using a modified molybdate method for detecting inorganic phosphate release.

3.3 Incorporation of LptBFGC into Liposomes

In order to develop a reconstitution from purified components, we needed methods to incorporate LptBFG and LptBFGC into liposomes. The reported *in vitro* system for monitoring LPS release from cell-derived membrane vesicles made use of a heterogeneous system in which

the cell produced and assembled the proteins (3). It was unlikely that transport activity could be detected in detergent solution, and preliminary evidence for this was that the ATPase activities of the complexes in detergent were unaffected by the presence of LPS or lipid A (8). It is unclear if LPS can even interact with the complex in detergent. Therefore, a challenge was to incorporate purified Lpt complexes into liposomes without affecting complex the stability or conformation of the proteins such they lose function.

Dr. Suguru Okuda successfully incorporated equivalent molar concentrations of LptB-His-LptFG and LptB-His-LptFGC into liposomes using a detergent dilution method similar to that previous used in the Kahne lab to incorporate the Bam complex into liposomes (11, 12). Liposomes were prepared from *E. coli* phospholipids and rough LPS (lacking the O-antigen). LPS was added to detergent-destabilized liposomes to avoid adding aggregates of LPS exogenously during the assay. The method originally used by Dr. Okuda to incorporate LptB-His-LptFGC into liposomes was adapted to incorporate His-LptBFG and His-LptBFGC (see Section 3.8.3). We optimized an ATPase assay to measure the activities of these proteoliposomes. To begin, we tested the activities with a range of magnesium chloride concentrations to find the concentration that gave maximal activity, as was initially done with the reconstitution of the IM LPS flippase, MsbA (Figure 3.2A) (13). The same modified molybdate assay for determining inorganic phosphate release in detergent solution was adapted for this purpose (4, 5, 8, 14). The optimal concentration of magnesium chloride was found to be 2 mM for His-LptBFGC, which would be used for reconstitution experiments. The activity of LptB-His-LptFGC proteoliposomes reached a plateau around 1 mM magnesium chloride, but this complex had overall lower activity and would not be used for subsequent experiments (Figure 3.2A). The concentration of ATP was kept at 5 mM for all assays, as this is the maximum that

can be used for the molybdate assay (14). The heterogeneity of the *E. coli* lipid extracts and the presence of LPS in the proteoliposomes presumably result in different magnesium requirements than in DDM solution.

Using proteoliposomes with just His-LptBFGC variants, we measured ATP hydrolysis over time (Figure 3.2B). We found that the activity remained linear for at least two hours, which is much longer than the ~ 5 minute linear range for the complexes in DDM (see Figure 3.1B). This could be the result of having the complex in a more stable, membrane-like environment, rather than in less ordered detergent micelles. Additionally, we found that LptB-E163Q-LptFGC had no ATPase activity over time, as expected. Proteoliposomes containing LptBFGC were also made with just phospholipids and no LPS to determine if activity in this system was dependent on the presence of LPS, which will be discussed more in Section 3.6. The ATPase activity of the complex in these proteoliposomes was also linear for at least two hours (see Figure 3.5). Therefore, LptBFGC is stable in a proteoliposome system and can be used to develop an assay to detect LPS transport.

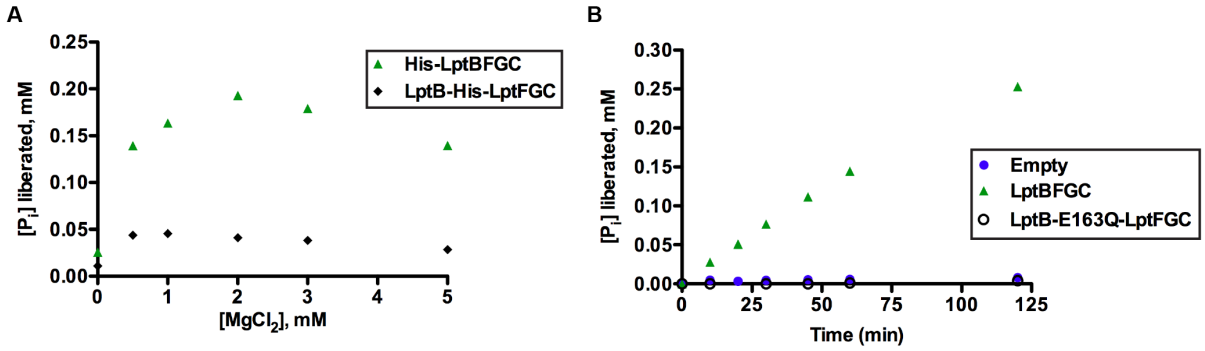

Figure 3.2. LptBFGC shows ATP hydrolysis activity in proteoliposomes containing phospholipids and LPS. *(A)* ATPase activity was measured using a modified molybdate method for detecting inorganic phosphate release. Concentrations of magnesium chloride ranged from 0 mM to 5 mM, while ATP was kept constant at 5 mM. Data represent 60 min time points. *(B)* Time course of ATPase activity for proteoliposomes with His-LptBFGC, His-LptB-E163Q-LptFGC, and no protein ("Empty"). Reactions were initiated with the addition of 5 mM ATP, 2 mM $MgCl_2$. In both *(A)* and *(B)*, assays were done at 30°C.

3.4 Monitoring LPS Extraction from Proteoliposomes

The next challenge in developing this reconstitution was to monitor LPS transport out of proteoliposomes into the periplasmic bridge component LptA to see if the reconstitution recapitulate what is observed *in vivo*. The stable ATPase activity for LptBFGC and the lack of any activity for LptB-E163Q-LptFGC initially demonstrated that this system recapitulates what is observed in the cell. A major advantage of using a pure system is that ATPase activity can be measured without the presence of contaminating ATPases, which was not the case with the cell-derived membrane vesicle reconstitution (3). To reconstitute LPS transport in proteoliposomes, we adapted techniques used to detect LPS crosslinking to LptC and LptA *in vivo* (3). Technology developed by Peter Schultz at The Scripps Research Institute was utilized to site-specifically incorporate an unnatural amino acid, *p*BPA, at positions of LptC and LptA (see Chapter 1) (15-18). Upon irradiation at 365 nm, a wavelength that typically does not damage proteins, the benzophenone group of *p*BPA reacts with nearby carbon-hydrogen bonds (19). Specific sites of LptC and LptA were found to be binding sites for LPS along the transport pathway. It was found that LPS crosslinks to LptC most strongly at position 47 (20). Therefore, crosslinking at this position of LptC was used to monitor LPS extraction from proteoliposomes by LptC.

In order to reconstitute LPS extraction from proteoliposomes, we overexpressed and purified LptBFGC-T47*p*BPA. This complex eluted as a single peak in size-exclusion chromatography, like the wild-type complex. We incorporated this complex into liposomes containing phospholipids and LPS. Samples were irradiated at 365 nm at specific time points after starting the assay to determine the time-dependence of LPS extraction. We analyzed samples by SDS-PAGE followed by immunoblotting with anti-LPS and anti-LptC antisera to

detect crosslinked LptC-LPS adducts. The results indicate that LPS can crosslink to LptC in an ATP- and time-dependent manner (Figure 3.3). LptC-LPS crosslinking occurred rather quickly in the presence of ATP (within five minutes after initiating the reaction). Crosslinking appears to saturate by ten minutes after adding ATP. A little crosslinking is detected immediately after adding ATP to initiate the assay (zero minute time point), and this is likely due to LPS interacting with LptC in the proteoliposome preparation procedure (the complex is inserted into detergent-destabilized phospholipid/LPS liposomes to make the proteoliposomes). These data demonstrate that LPS extraction from the IM is due to ATP hydrolysis by LptB and is independent of MsbA, the ABC transporter responsible for flipping LPS from the inner leaflet of the IM to the outer leaflet (see Chapter 1). Although it is possible that flipping by MsbA feeds LPS into the Lpt pathway *in vivo*, ATP hydrolysis by LptBFG powers LPS binding to LptC along the transport pathway. Because nothing is known about LPS interactions with LptFG, this is a reconstitution of the first known step of LPS transport.

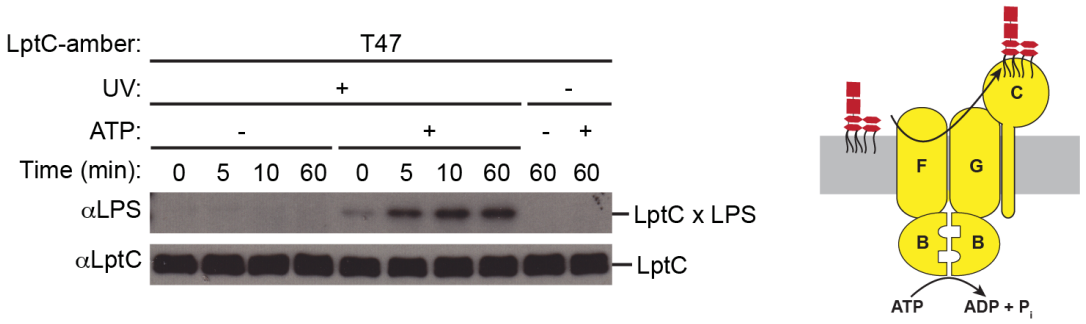

Figure 3.3. LPS can be extracted from proteoliposomes containing LptBFGC. Assays were initiated by adding 5 mM ATP or buffer ("- ATP") to proteoliposomes containing LPS and LptBFGC-T47*p*BPA. At specific time points, aliquots were removed and UV-irradiated. Samples were then subject to SDS-PAGE followed by immunoblotting with anti-LptC and anti-LPS antisera to detect crosslinked adducts (LptC x LPS). Assays were done at 30°C.

3.5 Monitoring LPS Release from Proteoliposomes

LPS is transferred to LptA following extraction by LptC (3, 20). In order to detect LPS release from proteoliposomes to LptA, LptA-I36*p*BPA-His was overexpressed in the periplasm and purified by nickel-affinity chromatography from *E. coli* spheroplasts (see Section 3.8.2.2). Position I36 was found to crosslink to LPS *in vivo* and in cell-derived membrane vesicles in a time-, ATP-, and LptBFGC-dependent manner (3). To evaluate LPS release in a pure reconstitution, proteoliposomes containing LPS and wild-type LptBFGC were mixed with purified LptA-I36*p*BPA-His. LPS release was initiated by addition of 5 mM ATP to the assay mixtures. Aliquots were taken at different time points and UV-irradiated prior to analysis by SDS-PAGE and immunoblotting.

As shown in Figure 3.4, LPS accumulates in LptA near position 36 over time when LptBFGC is present in the proteoliposomes, as there is nowhere else for LPS to go. As was previously shown in membrane vesicles (3), soluble LptA can likely exchange with LptA associated with the proteoliposomes, allowing for time-dependent buildup of LPS in LptA. Such a result is not observed with LPS crosslinking to LptC (Figure 3.3), as LptC always remains in the proteoliposomes and cannot exchange. To evaluate the specificity of release to Lpt components, we also monitored LPS release in proteoliposomes containing only LptBFG. Very little LPS is released without LptC, consistent with the finding that a full IM complex is required to transport LPS. It was initially unclear if purified LptA would be able to associate properly with LptBFGC incorporated into proteoliposomes. Dr. Suguru Okuda previously found that the soluble C-terminal domain of LptC can extract LPS from LptBFG in membrane vesicles (data not shown). Because the C-terminus of LptC and LptA share a similar β-jellyroll fold, it was possible that there would be high background transfer in a purified system. These data indicate

that LptA must interact specifically with LptC in this reconstitution, as it does in cells. Very little LPS is released to LptA by LptBFG after sixty minutes. The periplasmic regions of LptFG have been predicted to have a β-jellyroll fold (21); therefore, it would not be surprising if a very low level of LPS release can be achieved without LptC. It is clear, however, that LptC is essential for efficient LPS release from proteoliposomes to LptA.

Proteoliposomes containing the LptB-E163Q variant could not transfer LPS to LptA. It has been shown that LptB-E163Q can bind ATP without hydrolyzing it, and this LptB variant was used to demonstrate that ATP hydrolysis by LptB is essential for cell viability (see Chapter 2) (5). These results show that ATP hydrolysis and not just binding is necessary to obtain any transport into the periplasmic bridge. This reconstitution of the IM complex in proteoliposomes demonstrates ATPase and LPS transport activities that recapitulate the cellular process.

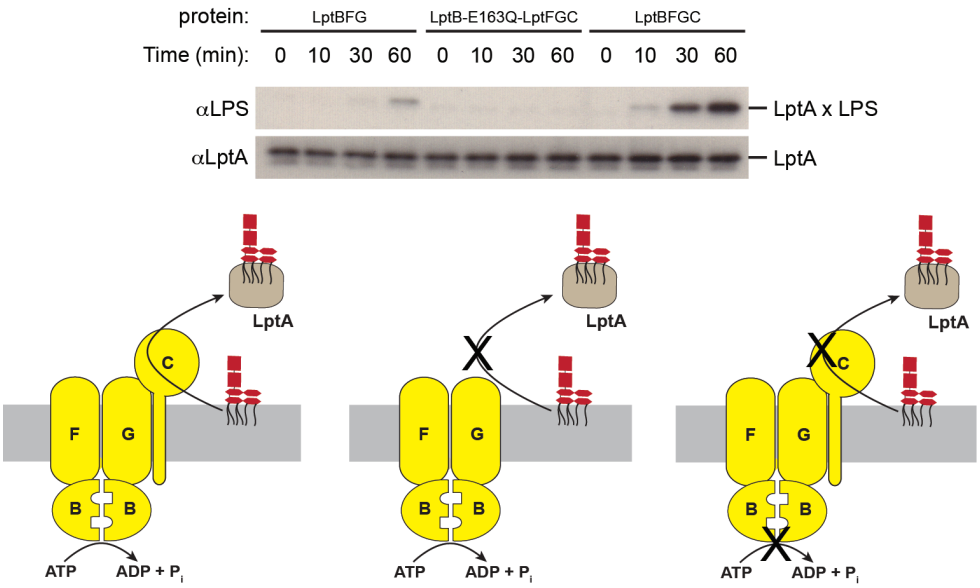

Figure 3.4. LPS is released to LptA from proteoliposomes in an ATP- and LptBFGC-dependent manner. Assays were initiated by adding 5 mM ATP to proteoliposomes containing LPS and LptBFG, LptB-E163Q-LptFGC, or LptBFGC, mixed with soluble LptA-I36*p*BPA. Aliquots were removed at different time points and UV-irradiated, then subject to SDS-PAGE followed by immunoblotting with anti-LptA and anti-LPS antisera to detect crosslinked adducts (LptA x LPS). Assays were done at 30°C.

3.6 LptC Reduces the ATPase Activity of LptBFG in the Presence of LPS

The development of a reconstitution of the Lpt IM complex from purified components allowed for the evaluation of the role of LptC. It is known that the ATPase activities of many well-characterized ABC transporters are stimulated by the presence of their substrates (22-24). For many bacterial importers, activation relies on the presence of a substrate-binding protein that interacts with the TMDs of the ABC transporter (9, 25). One hypothesis for the role of LptC is that it serves as a "sensor" for the presence of LPS, like a substrate-binding protein, and this activates the ABC transporter. The tools were now in place to begin to understand the role of LptC.

Proteoliposomes containing LptBFG and LptBFGC, both with and without LPS, were prepared simultaneously. A representative time course of the ATPase activity of proteoliposomes containing LptBFGC and LPS is shown in Figure 3.2. All sets of proteoliposomes (containing LptBFG or LptBFGC, with or without LPS) showed linear ATPase activity for at least two hours (Figure 3.5). Interestingly, the rates of ATPase activity (determined by the slope of the line through the data points in the time course) are similar for LptBFGC in proteoliposomes with and without LPS. This rate is also similar to that of LptBFG in proteoliposomes without LPS. As observed for other ABC transporters, there is low-level activation of LptBFG in the presence of LPS, suggesting that LPS stimulates the activity of LptBFG. However, the presence of LptC reduces the activity to around the same level as proteoliposomes prepared without LPS (the basal activity). The ATPase activities of LptBFG and LptBFGC were previously found to be unstimulated in a detergent solution (8). However, as noted above, reconstituting these complexes in proteoliposomes more closely resembles their activities in a membrane.

The finding that LptBFGC reduces the ATPase activity of ABC transporter LptBFG in the presence of LPS suggests a potential role for LptC in regulating the activity of the transporter. It would not be surprising if a mechanism were in place to reduce efflux of LPS when there is a buildup in the IM. If LPS stimulates LptBFG, similar to the substrate activation of other transporters, then LptC can serve the role of regulating activity so that too much LPS does not get pumped into the transenvelope bridge. This also ensures that LPS does not get pumped if there is a defect in any component of the pathway such that LPS builds up in the IM. Further studies are necessary to specifically assign a role to LptC, but the tools are in place to begin to understand its function.

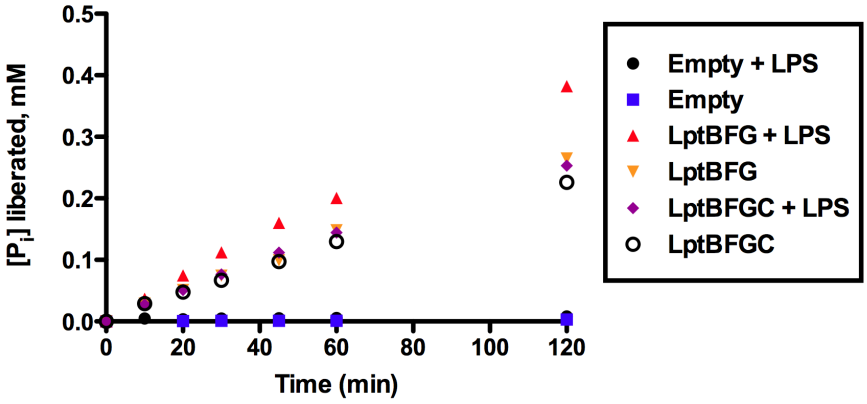

Figure 3.5. LptC reduces the ATPase activity of LptBFG in the presence of LPS. Time course of ATPase activity for proteoliposomes containing LptBFG and LptBFGC, with and without LPS. "Empty" denotes liposomes without incorporated protein. Reactions were initiated with the addition of 5 mM ATP, 2 mM $MgCl_2$. ATPase activity was measured using a modified molybdate method for detecting inorganic phosphate release. Assays were done at 30°C.

3.7 Conclusion

In order to understand how the individual components of the LptBFGC IM complex work, a pure reconstitution of LPS transport is necessary. Obtaining an active, wild-type LptBFGC complex was necessary to develop the reconstitution. This complex was successfully

incorporated into liposomes containing phospholipids and LPS. With the addition of ATP, we demonstrate that LPS can be extracted from proteoliposomes containing LptBFGC and bind to LptC near position 47. The time- and ATP-dependence of this process demonstrate that LPS extraction is not spontaneous. We would not expect lipid extraction from a membrane to be spontaneous, as it involves removal of acyl chains from a stable lipid bilayer. Nonetheless, the state of LPS bound to LptC and its orientation relative to the membrane remain unknown.

We demonstrate that LPS can be released to LptA in an LptBFGC-, time-, and ATP-dependent manner. LptC is required for efficient transfer of LPS to LptA. The inability of LptB-E163Q-LptFGC to release LPS to LptA indicates that ATP hydrolysis by LptB is required for LPS transport, irrespective of the presence of MsbA. These findings support the model that LptBFG serve as an independent ABC transporter with associated LptC required to transduce the signal of ATP hydrolysis in the cytoplasm to LPS transport through the periplasmic bridge. Importantly, studies of the ATPase activities of proteoliposomes with and without LptC suggest that LPS slightly stimulates the activity of LptBFG, and LptC counteracts this activation. Therefore, it is possible that LptC serves a regulatory role in transducing signal from the outer leaflet of the IM back to LptB, too.

As discussed in Chapter 2, LptB is a promising antibiotic target because of its role as the power source for LPS transport. The tools described here will allow for more detailed studies of IM complex inhibition and serve as a way of validating inhibitors found in screening efforts. The development of this pure reconstitution of LPS extraction and release from a membrane by Lpt components provided confidence that a reconstitution of all Lpt components might be possible, and the next major challenge was to reconstitute the later steps of LPS transport. This process requires transit of LPS from LptA to a different membrane. Chapter 4 describes the

development of a reconstitution of LPS transport from one proteoliposome containing LptBFGC through LptA to another proteoliposome containing the Lpt OM complex, LptDE. This system will ultimately allow for mechanistic studies of the full Lpt pathway. It will also allow for the development of inhibitors of any step of the transport pathway.

3.8 Materials and Methods

3.8.1 Strains and Plasmids

Construction of all plasmids used for overexpression of the Lpt IM complex was described in Chapter 2. Construction of plasmid pET22bLptA-I36*p*BPA-His_6 was previously reported (3). Strains used in this study are listed in Table 3.1.

Plasmid pET22/42LptC-T47*p*BPA was constructed using site-directed mutagenesis (SDM). Plasmid pET22/42LptC wias mutagenized with KOD Hot Start Polymerase (Novagen) using primers T47-amber-f (5'-TATAAAAGCGAGCATTAGGACACGCTCGTCTAT-3') and T47-amber-r (5'-ATAGACGAGCGTGTCCTAATGCTCGCTTTTATA-3'). The PCR product of the SDM reaction was digested with DpnI (New England Biolabs) and introduced into NovaBlue competent cells by heat-shock. Transformants were selected in media containing carbenicillin (50 μg/mL). After confirming plasmid DNA sequence, the mutagenized plasmid was introduced into NovaBlue and KRX strains.

Table 3.1. Strains used in this study.

Strain	Genotype	Reference
BL21(λDE3)	F^- *omp*T *gal dcm lon hsd*S_B(r_B^-, m_B^-) λ(DE3)	Novagen
KRX	[F', *tra*D36, Δ*omp*P, *pro*A^+B^+, *lac*I^q, Δ(*lac*Z)M15] Δ*omp*T, *end*A1, *rec*A1, *gyr*A96, *thi*-1, *hsd*R17 (r_K^-, m_K^+), e14– (McrA–), *rel*A1, *sup*E44, Δ(*lac-pro*AB), Δ(*rha*BAD)::T7 gene 1	Promega
NovaBlue	*endA1 hsd*R17 (r_K^-, m_K^+) *sup*E44 *thi*-1 *rec*A1 *gyr*A96 *rel*A1 *lac* F'[*pro*A^+B^+ *lac*I^qZΔM15::Tn*10*]	Novagen

3.8.2 Protein Overexpression and Purification

3.8.2.1 Lpt IM Complexes

To overexpress His_6-LptBFG, His_6-LptBFGC, and His_6-LptB-E163Q-LptFGC, KRX cells were transformed with plasmid pCDFDuetHis_6LptBFG or pCDFDuetHis_6LptB-E163Q-LptFG. When LptC was co-overexpressed with LptBFG, this strain was also transformed with pET22/42LptC. The overexpression and purification protocols are described in Chapter 2, Section 2.7.4.1.

To overexpress His_6-LptBFGC-T47*p*BPA, KRX cells were transformed with three plasmids: pCDFDuetHis_6LptBFG, pET22/42LptC-T47*p*BPA, and pSupBpaRS-6TRN (17), which encodes an orthogonal tRNA and aminoacyl-tRNA synthetase to incorporate unnatural amino acid *p*BPA at amber (TAG) stop codons. Cultures were grown at 37°C after diluting overnight cultures 1 to 100 into fresh LB broth supplemented with 50 μg/mL spectinomycin, 50 μg/mL carbenicillin, 30 μg/mL chloramphenicol, and 0.5 mM *p*BPA (Bachem). Complex expression was induced with 0.02% L-rhamnose at OD_{600} ~ 1, and cultures were grown for 3 h at 37°C. The purification protocol is the same as described in Chapter 2, Section 2.7.4.1.

To assess purity following size-exclusion chromatography, all complexes were analyzed by SDS-PAGE using 14% resolving polyacrylamide gels.

3.8.2.2 LptA-I36pBPA-His

LptA-I36*p*BPA-His was overexpressed in the periplasm and purified by making spheroplasts, as originally reported (3).

3.8.3 Proteoliposome Preparation

First, a 30 mg/mL sonicated aqueous suspension of *E. coli* polar lipid extract (Avanti Polar Lipids, Inc.) was prepared. If not used immediately to prepare proteoliposomes, aliquots were flash frozen in liquid nitrogen and stored at -80°C. A 2 mg/mL aqueous suspension of LPS from *E. coli* EH100 (Ra mutant, Sigma) was prepared, flash frozen in liquid nitrogen, and stored in aliquots at -80°C. When ready for use, aliquots of liposomes and LPS were thawed. Proteoliposomes containing the Lpt IM complex were prepared by a detergent dilution method (11, 12). Prior to dilution, a mixture with the following final concentrations was prepared in Tris-buffered saline (TBS; 20 mM Tris, pH 8.0, 150 mM NaCl): 7.5 mg/mL liposomes, 0.5 mg/mL LPS, 0.25% *n*-dodecyl-β-D-maltopyranoside (DDM, Anatrace), and 0.86 μM purified IM complex. While making this mixture, first the DDM was added to the liposomes to make detergent-destabilized liposomes. LPS was added to this mixture, which was subsequently kept on ice for 10 min to allow for mixed detergent-phospholipid-LPS micelles to form. The protein complex was added, and the mixture was left on ice for 20 min. The mixture was then transferred to an ultracentrifuge tube and diluted 100x with cold TBS. After letting the dilute mixture sit on ice for 30 min, the proteoliposomes were pelleted by ultracentrifugation at 300,000 x *g* for 2 h at 4°C. The proteoliposomes were resuspended in TBS and diluted 100x again, then pelleted by ultracentrifugation at 300,000 x *g* for 2 h at 4°C. Finally, for every 100 μL original mixture (prior to the first dilution step), 250 μL cold TBS, 10% glycerol was added. If the resuspended proteoliposomes were not used immediately, they were flash frozen in liquid nitrogen and stored at -80°C.

3.8.4 ATPase Assays

ATPase activity of the purified Lpt IM complex in DDM was measured using the same modified molybdate method described in Chapter 2, Section 2.7.3. ATPase assays of proteoliposomes were done using essentially the same method, without the detergent. All assays were done in 50 mM Tris-HCl, pH 8.0, 500 mM NaCl, 10% glycerol (final concentrations). Reactions contained 60% proteoliposomes by volume (prepared as described in Section 3.8.3, thawed on ice). The remaining volume was composed of Tris-HCl, NaCl, and glycerol such that the final concentrations would be the values listed above. Reactions were initiated at 30°C with the addition of ATP/$MgCl_2$ (final concentrations were 5 mM ATP, 2 mM $MgCl_2$ unless otherwise specified). Reaction aliquots were taken at specified time points and quenched with an equal volume of 12% SDS. Inorganic phosphate was measured using the reported method (14). Absorbance values were measured using a Spectramax Plus 384 plate reader (Molecular Devices).

3.8.5 Reconstitution of LPS Extraction by LptC

The reconstitution of LPS extraction by LptC in proteoliposomes was done similarly to the ATPase assay described above. All assays were done in 50 mM Tris-HCl, pH 8.0, 500 mM NaCl, 10% glycerol (final concentrations). Reactions contained 60% LptBFGC-T47*p*BPA proteoliposomes by volume (prepared as described in Section 3.8.3, thawed on ice). The remaining volume was composed of Tris-HCl, NaCl, and glycerol such that the final concentrations would be the values mentioned above. Reactions were initiated at 30°C with the addition of ATP/$MgCl_2$ or just $MgCl_2$ (final concentrations were 5 mM ATP, 2 mM $MgCl_2$). At specified time points, 30 μL aliquots were removed from the reactions and added to a microtiter

plate, which was subsequently irradiated with UV light (365 nm) on ice for five minutes using a B-100AP lamp (UVP). Following UV-irradiation, samples were added to 220 µL cold TBS, 0.2% DDM. To each sample, 250 µL 20% trichloroacetic acid (TCA) was added. The proteins were precipitated on ice, followed by a cold acetone wash. Precipitates were resuspended in 30 µL 2x SDS-PAGE sample buffer supplemented with 5% β-mercaptoethanol. Samples were boiled for 10 min and loaded onto 4-20% polyacrylamide gradient gels. The proteins were transferred onto Immun-Blot® PVDF membranes (Bio-Rad) and subjected to immunoblotting using polyclonal anti-LptC antiserum (26) and anti-LPS mouse monoclonal antiserum (Hycult Biotech). Membranes were subsequently immunoblotted with donkey anti-rabbit and sheep anti-mouse horseradish peroxidase (HRP) conjugate secondary antibodies (GE Amersham) for LptC and LPS blots, respectively. Bands were visualized using ECL™ Prime Western Blotting Detection Reagent (GE Amersham) and Biomax Light Film (Kodak).

3.8.6 Reconstitution of LPS Release to LptA

The reconstitution of LPS release from proteoliposomes to LptA was done similarly to the LPS extraction reconstitution described in Section 3.8.5. All assays were done in 50 mM Tris-HCl, pH 8.0, 500 mM NaCl, 10% glycerol (final concentrations). Reactions contained 60% IM proteoliposomes by volume (prepared as described in Section 3.8.3, thawed on ice). The remaining volume was composed of Tris-HCl, NaCl, and glycerol such that the final concentrations would be the values mentioned above. LptA-I36*p*BPA-His was added to a final concentration of 2 µM prior to starting the assay. Reactions were initiated at 30°C with the addition of ATP/$MgCl_2$ (final concentrations were 5 mM ATP, 2 mM $MgCl_2$). At specified time points, 25 µL aliquots were removed from the reactions and added to a microtiter plate, which

was subsequently irradiated with UV light (365 nm) on ice for three minutes using a B-100AP lamp. Following UV-irradiation, samples were added to 225 μL cold TBS, 0.2% DDM. To each sample, 250 μL 20% trichloroacetic acid (TCA) was added. The proteins were precipitated and gel samples prepared as described above. Immunoblotting was done using polyclonal anti-LptA antiserum (27) and anti-LPS mouse monoclonal antiserum. Immunoblotting with secondary antibodies and band visualization were the same as above.

3.9 References

1. Sperandeo P*, et al.* (2008) Functional analysis of the protein machinery required for transport of lipopolysaccharide to the outer membrane of Escherichia coli. *J Bacteriol* 190(13):4460-4469.

2. Ruiz N, Gronenberg LS, Kahne D, & Silhavy TJ (2008) Identification of two inner-membrane proteins required for the transport of lipopolysaccharide to the outer membrane of Escherichia coli. *Proc. Natl. Acad. Sci. U. S. A.* 105(14):5537-5542.

3. Okuda S, Freinkman E, & Kahne D (2012) Cytoplasmic ATP hydrolysis powers transport of lipopolysaccharide across the periplasm in E. coli. *Science* 338(6111):1214-1217.

4. Sherman DJ, Okuda S, Denny WA, & Kahne D (2013) Validation of inhibitors of an ABC transporter required to transport lipopolysaccharide to the cell surface in Escherichia coli. *Bioorg Med Chem* 21(16):4846-4851.

5. Sherman DJ*, et al.* (2014) Decoupling catalytic activity from biological function of the ATPase that powers lipopolysaccharide transport. *Proc Natl Acad Sci U S A* 111(13):4982-4987.

6. Rigaud JL & Levy D (2003) Reconstitution of membrane proteins into liposomes. *Methods Enzymol* 372:65-86.

7. Yakushi T, Masuda K, Narita S, Matsuyama S, & Tokuda H (2000) A new ABC transporter mediating the detachment of lipid-modified proteins from membranes. *Nat Cell Biol* 2(4):212-218.

8. Narita S & Tokuda H (2009) Biochemical characterization of an ABC transporter LptBFGC complex required for the outer membrane sorting of lipopolysaccharides. *FEBS Lett* 583(13):2160-2164.

9. Davidson AL, Dassa E, Orelle C, & Chen J (2008) Structure, function, and evolution of bacterial ATP-binding cassette systems. *Microbiology and molecular biology reviews : MMBR* 72(2):317-364, table of contents.

10. Oswald C, Holland IB, & Schmitt L (2006) The motor domains of ABC-transporters. What can structures tell us? *Naunyn-Schmiedeberg's archives of pharmacology* 372(6):385-399.

11. van der Does C, de Keyzer J, van der Laan M, & Driessen AJ (2003) Reconstitution of purified bacterial preprotein translocase in liposomes. *Methods Enzymol.* 372:86-98.

12. Hagan CL, Kim S, & Kahne D (2010) Reconstitution of outer membrane protein assembly from purified components. *Science* 328(5980):890-892.

13. Doerrler WT & Raetz CR (2002) ATPase activity of the MsbA lipid flippase of Escherichia coli. *J Biol Chem* 277(39):36697-36705.

14. Chifflet S, Torriglia A, Chiesa R, & Tolosa S (1988) A method for the determination of inorganic phosphate in the presence of labile organic phosphate and high concentrations of protein: application to lens ATPases. *Anal Biochem* 168(1):1-4.

15. Wang L, Brock A, Herberich B, & Schultz PG (2001) Expanding the genetic code of Escherichia coli. *Science* 292(5516):498-500.

16. Chin JW, Martin AB, King DS, Wang L, & Schultz PG (2002) Addition of a photocrosslinking amino acid to the genetic code of Escherichiacoli. *Proc Natl Acad Sci U S A* 99(17):11020-11024.

17. Ryu Y & Schultz PG (2006) Efficient incorporation of unnatural amino acids into proteins in Escherichia coli. *Nat Methods* 3(4):263-265.

18. Liu CC & Schultz PG (2010) Adding new chemistries to the genetic code. *Annu Rev Biochem* 79:413-444.

19. Dorman G & Prestwich GD (1994) Benzophenone photophores in biochemistry. *Biochemistry* 33(19):5661-5673.

20. Tran AX, Dong C, & Whitfield C (2010) Structure and functional analysis of LptC, a conserved membrane protein involved in the lipopolysaccharide export pathway in Escherichia coli. *J Biol Chem* 285(43):33529-33539.

21. Villa R*, et al.* (2013) The Escherichia coli Lpt Transenvelope Protein Complex for Lipopolysaccharide Export Is Assembled via Conserved Structurally Homologous Domains. *J Bacteriol* 195(5):1100-1108.

22. Davidson AL, Shuman HA, & Nikaido H (1992) Mechanism of maltose transport in Escherichia coli: transmembrane signaling by periplasmic binding proteins. *Proc Natl Acad Sci U S A* 89(6):2360-2364.

23. Liu CE, Liu PQ, & Ames GF (1997) Characterization of the adenosine triphosphatase activity of the periplasmic histidine permease, a traffic ATPase (ABC transporter). *J Biol Chem* 272(35):21883-21891.

24. van Veen HW*, et al.* (1998) A bacterial antibiotic-resistance gene that complements the human multidrug-resistance P-glycoprotein gene. *Nature* 391(6664):291-295.

25. Biemans-Oldehinkel E, Doeven MK, & Poolman B (2006) ABC transporter architecture and regulatory roles of accessory domains. *FEBS Lett* 580(4):1023-1035.

26. Freinkman E, Okuda S, Ruiz N, & Kahne D (2012) Regulated Assembly of the Transenvelope Protein Complex Required for Lipopolysaccharide Export. *Biochemistry* 51(24):4800-4806.

27. Chng SS, Gronenberg LS, & Kahne D (2010) Proteins required for lipopolysaccharide assembly in Escherichia coli form a transenvelope complex. *Biochemistry* 49(22):4565-4567.

Chapter Four

Reconstitution of LPS Transport
from Purified Components

4.1 Reconstituting a Transenvelope Process

This chapter describes the reconstitution of LPS transport between two membranes. A major challenge to developing a reconstitution of LPS transport is that it is a transenvelope process with Lpt components in the IM (LptB), IM (LptC/F/G), periplasm (LptA), and OM (LptD/E) (see Figure 2.1A). The Lpt components are believed to form a transenvelope bridge spanning these cellular compartments, solving the problem of specifically and efficiently transporting LPS unidirectionally against a concentration gradient (1-5). The lack of soluble intermediates in the periplasm allows for direct passage to the cell surface.

Transenvelope processes solve complex problems in the cell but are difficult to study *in vitro* because they involve connecting two membranes. Another example of an important transenvelope process is Gram-negative multidrug efflux (6). Efflux systems of the resistance-nodulation-division (RND) transporter superfamily are known to form tripartite complexes with different proteins in the periplasm and the OM (7). *E. coli* AcrB was the first member of this family to be reconstituted in proteoliposomes (8). This reconstitution demonstrated that pure AcrB functions as a proton antiporter that transports lipid substrates out of the membrane. The presence of its associated periplasm-spanning protein AcrA increased the rate of transport. However, this system was not reconstituted with its associated OM efflux channel, TolC, and it was never confirmed that AcrA bound to AcrB in a manner such that can bridge two membranes. It would be very useful to study complete multidrug efflux systems *in vitro* to identify intermediates in the efflux process and to find ways to block these pumps. The challenge of connecting two membranes in a physiologically relevant way has made the development of such reconstitutions difficult.

A full reconstitution of LPS transport is necessary to understand the mechanism of the entire transenvelope process and to develop ways of inhibiting its function. A pure biochemical system would allow for questions to be answered about the role of LptDE in the transport process, which has largely remained a mystery thus far. Therefore, we needed to develop methods to overcome the challenges of connecting separate membranes *in vitro*. Proper connection of LptC to LptA and LptA to LptD is essential for LPS transport to occur (4). Therefore, nonspecific interactions between two sets of proteoliposomes and liposome fusion events must be minimized. Additionally, at the start of this project, there was no suitable readout to monitor transport to a second proteoliposome. Identification of *in vivo* intermediates in LptC and LptA allowed for photocrosslinking at specific positions in these proteins to serve as a readout in the reconstitution (9). However, there were no known LPS binding sites in LptD or LptE to indicate that LPS interacts with these OM components. The first challenge to reconstituting the full Lpt pathway was to develop a method for detecting LPS at the second membrane. Once we had a way to detect where LPS ends up, we would develop methods to assemble the Lpt transenvelope bridge *in vitro*.

4.2 Identification of an LPS Binding Site in LptD

Dr. Suguru Okuda, who developed the methodology to identify *in vivo* intermediates of LPS transport using site-specific photocrosslinking, screened for positions in LptD that crosslink to LPS *in vivo* (data not shown). At the time, there was no crystal structure of LptD available; however, the N-terminal periplasmic position of LptD was predicted to contain a similar β-jellyroll fold to the C-terminus of LptC and LptA (4, 5, 10, 11). Dr. Okuda found that LPS crosslinks to LptD at position 112 in the N-terminal domain.

Since this initial finding, the crystal structure of full-length *S. flexneri* LptDE has been solved, which confirms previous predictions about the plug-and-barrel structure of the OM translocon (12-14). The *S. flexneri* and *E. coli* LptD orthologs share ninety-nine percent sequence identity; therefore, the deposited crystal structure can be used to interpret data about *E. coli* LptD. As predicted, the N-terminus of LptD (residues 24 – 232) contains a β-jellyroll with a highly hydrophobic interior cavity. We reproduced the LPS crosslink to LptD in cells using amber codon suppression (described in Chapter 3) with the unnatural amino acid *p*BPA incorporated at position 112 (normally tyrosine) (Figure 4.1). This position in the N-terminal domain is located inside the β-jellyroll; previously, all positions that crosslinked to LptA *in vivo* were also in the hydrophobic lumen of the β-jellyroll (9). A structural alignment of the N-terminus of LptD and LptA indicates that position Y112 in LptD aligns with F95 in LptA. LptA-F95*p*BPA was found to crosslink to LPS *in vivo* in a UV-dependent manner (9). Therefore, it is not surprising that there is a binding site for LPS in LptD near this location. This result was encouraging because it provided the potential to detect LPS crosslinking to LptD at position 112 *in vitro*.

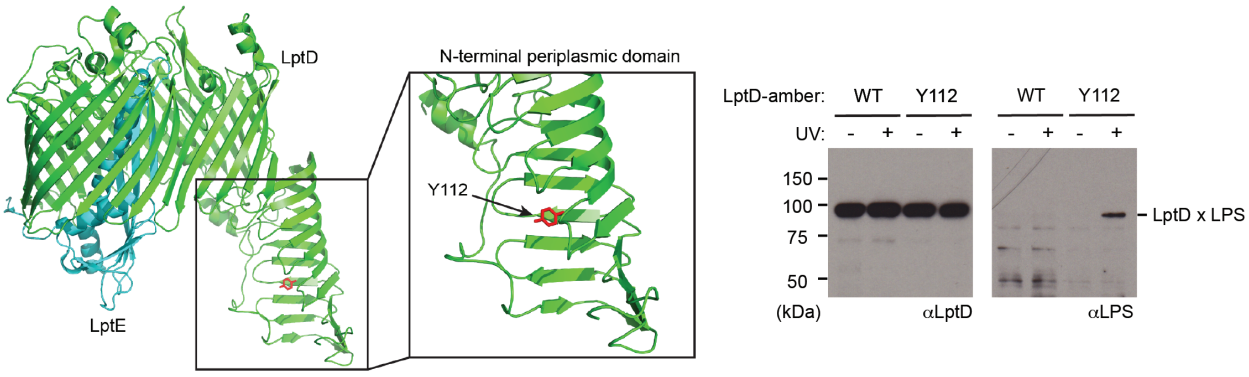

Figure 4.1. LptD crosslinks to LPS *in vivo* inside its N-terminal β-jellyroll. Polyhistidine-tagged LptD was mutated to incorporate unnatural amino acid *p*BPA at position 112. This position crosslinks to LPS upon UV-irradiation of the cells (right). The wild-type His-tagged protein ("WT") does not contain *p*BPA. The crystal structure of *S. flexneri* LptDE (PDB ID: 4q35) shows amino acid Y112 in LptD facing the interior of the hydrophobic β-jellyroll of LptD (left), supporting the model that the N-terminus of LptD accepts LPS from LptA in the transenvelope bridge. The crosslinked adduct (LptD x LPS) was detected by nickel-affinity chromatography followed by immunoblotting with anti-LPS antiserum.

4.3 Experimental Design of a Reconstitution of LPS Transport

A reconstitution of LPS transport involves movement of LPS from a proteoliposome containing LptBFGC and LPS (described in Chapter 3), through LptA to a proteoliposome containing LptDE. Crosslinking of LPS to LptD at position 112 can be used to monitor LPS transfer to the second proteoliposome, although it was unclear initially if LPS would reside in LptD long enough to trap this intermediate. In order to try this experiment, LptD-Y112*p*BPA/LptE had to be overexpressed and purified. In the crystal structure of LptDE, the C-terminus of LptD is inside the lumen of the β-barrel. Although LptD with a C-terminal polyhistidine tag was used for the *in vivo* photocrosslinking experiment described above, as LptD-Y112*p*BPA needed to be enriched on nickel affinity resin, it seemed like a less ideal construct to overexpress and purify for a reconstitution. Therefore, LptD-Y112*p*BPA/LptE-His (with a C-terminal polyhistidine tag on LptE) was overexpressed and purified using a reported method (Figure 4.2A) (13). This complex was pure as judged by SDS-PAGE and was

subsequently incorporated into liposomes containing *E. coli* polar lipids by a detergent dilution method similar to that used to make the IM proteoliposomes (see Section 4.7.5; Figure 4.2B).

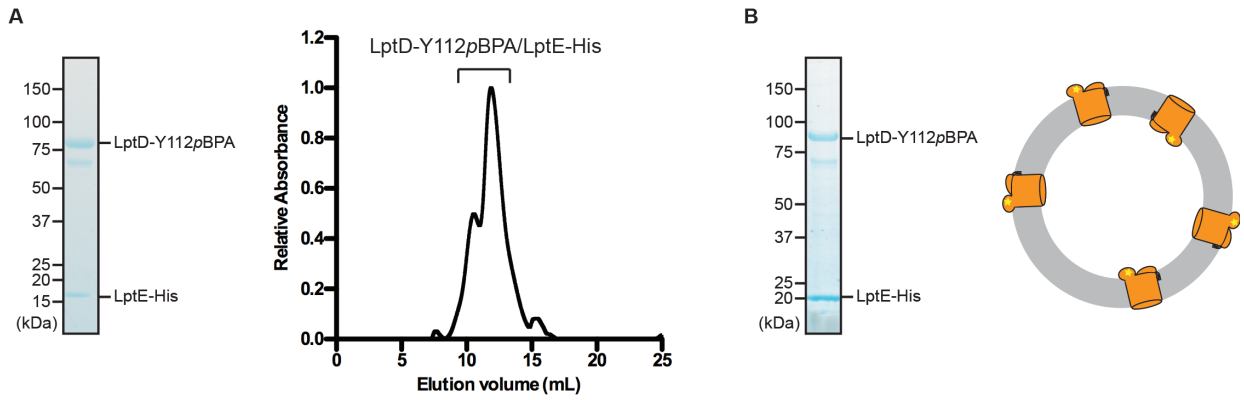

Figure 4.2. LptD-Y112*p*BPA/LptE-His can be overexpressed and purified as a stable complex and incorporated into liposomes. *(A)* SDS-PAGE and size-exclusion chromatogram of LptD-Y112*p*BPA/LptE-His. Fractions from size-exclusion chromatography were pooled and concentrated prior to making proteoliposomes. *(B)* SDS-PAGE of proteoliposomes containing OM complex, incorporated by a detergent dilution method. In both *(A)* and *(B)*, gel samples were boiled at 100°C for 10 min to unfold the β-barrel of LptD.

Now that we had access to proteoliposomes containing the IM complex with LPS and proteoliposomes containing the OM complex, the next challenge was to demonstrate transit from the IM proteoliposomes to the OM proteoliposomes through LptA. In the IM complex reconstitution, an LptA-His construct was used to assay for LPS release from LptBFGC-containing proteoliposomes. However, it is likely that the C-terminal polyhistidine tag in this construct will interfere with interactions with LptD, as the C-terminus of LptA is believed to interact with the N-terminus of LptD (3, 4). Additionally, various constructs of LptA tend to aggregate in solution (data not shown). Therefore, a fusion construct of LptA with an N-terminal solubility tag followed by a polyhistidine tag designed by Dr. Shu Sin Chng was used. Tagless, mature LptA is liberated by cleaving the N-terminal tags with the protease thrombin following nickel affinity chromatography.

After obtaining cleaved LptA, we could have chosen from two approaches to conduct the reconstitution. One is first to pre-load LptA with LPS released from IM proteoliposomes in an ATP-dependent manner. Then, LPS-LptA complexes would be separated from the proteoliposomes by ultracentrifugation. Soluble, LPS-loaded LptA would then be incubated with OM proteoliposomes. If transfer to LptD does not rely on an intact bridge and, therefore, ATP hydrolysis, LPS should be transferred from LptA to LptD (similarly to how lipoprotein delivery to the OM works, as described in Chapter 1). A second approach to performing the reconstitution is to form an Lpt bridge with both IM and OM proteoliposomes present in one assay mixture. Considering the aggregation issues with pure LptA, it seemed reasonable to pre-form bridges so that LptA does not have an opportunity to aggregate in solution, potentially preventing transport. It was previously found using sucrose density gradient centrifugation that LptA without any affinity tag preferentially associates with the OM and is not found in the soluble fraction (3). This lent support to attempting the second approach (pre-forming bridges). Incubation of the LptA cleavage reaction mixture with OM proteoliposomes should allow for association of mature LptA with LptD in complexes with the N-terminus of LptD outside of the proteoliposome lumen. Subsequent ultracentrifugation of this mixture should result in a pellet containing OM proteoliposomes and any associated, cleaved LptA. This was the approach that we used to reconstitute LPS transport.

4.4 Reconstituting LPS Transport to LptD

We had to ensure that our reconstituted Lpt system monitors specific transport of LPS instead of random LPS-binding events. As described in Section 4.3, we first incubated OM proteoliposomes with the LptA cleavage reaction mixture. Following ultracentrifugation, the

LptA-OM proteoliposomes were resuspended and incubated with proteoliposomes containing LptBFGC and LPS. The reasoning for this step is that during this short incubation period, bridges between the two liposomes could have a chance to form. The assay was initiated with the addition of ATP/$MgCl_2$. After one hour of incubation at 30°C, an LptD x LPS crosslink was observed (Figure 4.3). Importantly, crosslinking was time-dependent (no crosslinking was observed immediately upon addition of ATP). Crosslinking was also dependent on individual Lpt components. OM proteoliposomes without any LptA were pelleted alongside proteoliposomes pre-incubated with LptA to use in a parallel control assay. LPS crosslinking to LptD could not be observed in the reaction lacking LptA. Therefore, the crosslinking event is not a result of random proteoliposome fusion with LPS from the IM proteliposomes interacting nonspecifically with LptD. Crosslinking was also dependent on the presence of LptBFGC, as empty liposomes containing only phospholipids and LPS could not transport LPS to LptD. Finally, LPS crosslinking to LptD was dependent on the addition of ATP and on UV-irradiation. Therefore, LPS transport to LptD in a time-, LptBFGCA-, and ATP-dependent manner can be reconstituted *in vitro* from purified components.

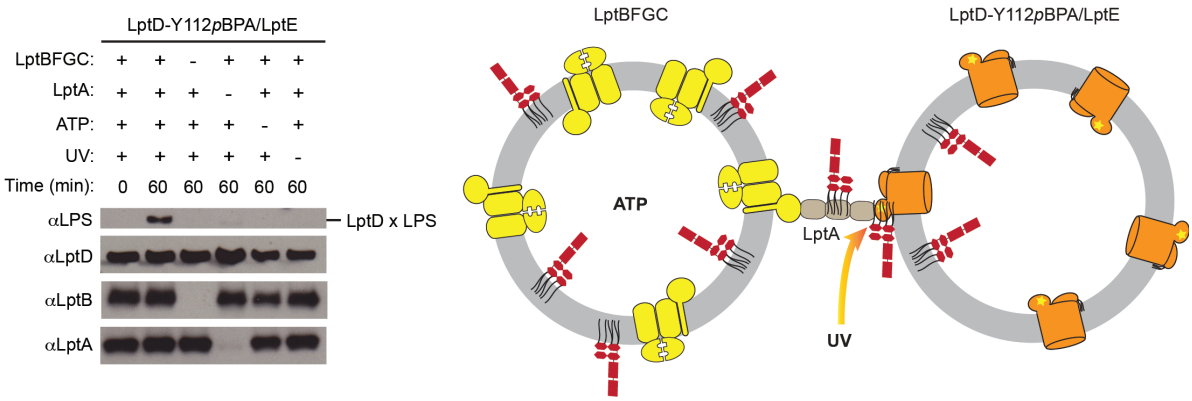

Figure 4.3. LPS transport to LptD can be reconstituted *in vitro*. Proteoliposomes containing LptD-Y112*p*BPA/LptE and *E. coli* phosopholipids were pre-incubated with wild-type, mature LptA (or buffer). Following ultracentrifugation, these proteoliposomes and any associated LptA were resuspended and incubated with proteoliposomes containing *E. coli* phospholipids and LPS with or without LptBFGC. The assay was initiated with addition of 5 mM ATP/2 mM $MgCl_2$ (or buffer). At the indicated time points, aliquots were removed and UV-irradiated. Samples were then subject to SDS-PAGE followed by immunoblotting with anti-LPS antiserum to detect crosslinked adducts (LptD x LPS). Assays were done at 30°C.

4.5 LPS Transport to LptD Stops When LPS Accumulates in the OM

We observed that LPS crosslinking to LptD has a very unusual time dependence (Figure 4.4). We do not observe LPS accumulation in LptD over time, as we do in LptC and LptA in the IM reconstitution. Rather, there is a buildup of LPS in LptD after a relatively short amount of time (ten minutes) followed by a decrease in LPS binding. The main difference between this reconstitution and the IM complex reconstitution is that we are using a complete Lpt complex this time, whereas we previously used broken bridges that allowed for accumulation of LPS in LptC or LptA. This result indicates that LPS does not get trapped in LptD, which was not apparent when looking at just the zero and sixty minute time points (Figure 4.3). If the OM complex were nonfunctional, then we would expect to observe buildup of LPS in LptD.

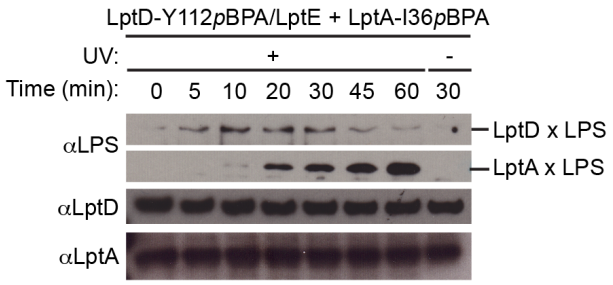

Figure 4.4. LPS transport to LptD *in vitro* decreases with time with a concomitant buildup in LptA. Proteoliposomes containing LptD-Y112*p*BPA/LptE and *E. coli* phospholipids were pre-incubated with mature LptA-I36*p*BPA. Following ultracentrifugation, these proteoliposomes and any associated LptA were resuspended and incubated with proteoliposomes containing LptBFGC, *E. coli* phospholipids, and LPS. The assay was initiated with addition of 5 mM ATP/2 mM $MgCl_2$. At specific time points, aliquots were removed and UV-irradiated. Samples were then subject to SDS-PAGE followed by immunoblotting with anti-LPS antiserum to detect crosslinked adducts (LptD x LPS and LptA x LPS). Assays were done at 30°C.

While observing crosslinking to LptD, we also used a construct of LptA with *p*BPA incorporated at position 36 (the position used in the IM complex reconstitution for photocrosslinking). We noticed that LPS crosslinking to LptA also changes with time. It appears that LPS accumulates in LptA after about twenty minutes, around the time that LPS crosslinking to LptD starts to decrease. A possible explanation for this observation is that, in all previous experiments, LPS accumulates in LptA because it has nowhere else to go (the OM complex is not present). In this experiment, LPS is being transported through LptA to LptD, and therefore it is unlikely that LPS will reside in LptA long enough to photocrosslink. Additionally, the fact that LPS builds up in LptA after it decreases in LptD demonstrates that the decrease in LPS transport to LptD is not due to depletion of LPS or ATP. It appears, however, that LPS is not transported past LptA to LptD after about thirty minutes and instead accumulates in LptA.

These results suggest that in the total reconstitution, the observable bottleneck in the transport process is initially binding to the N-terminus of LptD near position 112. Therefore, LPS is transported through LptA and then more slowly through LptD. This would explain why

LPS crosslinking to LptA cannot be observed at early time points. The fast kinetics of this transport to the OM are consistent with early observations by Mary Jane Osborn and colleagues that newly synthesized LPS rapidly reaches the OM in pulse-chase experiments (15).

One hypothesis to explain the observed time dependence of LPS crosslinking to LptD is that changes in the amount of LPS in the membrane affect the state of LptDE, and the decrease in crosslinking to LptD is a result of the translocon "turning off." This would explain the buildup in LptA after this point; if the LptDE complex is no longer functioning, a bottleneck is created at LptA. This is similar to the observation that LPS builds up in LptA in the IM complex reconstitution when there is no LptDE present. It is unclear whether the bridges are connected at this point or whether a buildup of LPS in the OM proteoliposomes results in disassembly of the bridges.

To test this hypothesis, we prepared two sets of OM proteoliposomes simultaneously: one containing just the OM complex and phospholipids, and the other containing the OM complex, phospholipids, and LPS (the same amount incorporated into the IM proteoliposomes). We observed that crosslinking to LptD with time in the full reconstitution differed between the two sets of proteoliposomes (Figure 4.5). There is a sharper decrease in crosslinking to LptD at an earlier time point when OM proteoliposomes are pre-loaded with LPS. These results suggest that the presence of LPS around LptDE changes the state of the translocon, as a different LPS composition in the proteoliposome alters the kinetics of LPS transport. To further explore this possibility, experiments are underway using different concentrations of ATP to determine if this can also alter the kinetics of transport through LptD. If our hypothesis is correct, we would expect to observe that slower transport rates lead to a later accumulation of LPS in LptD, and consequently a delayed decrease in crosslinking.

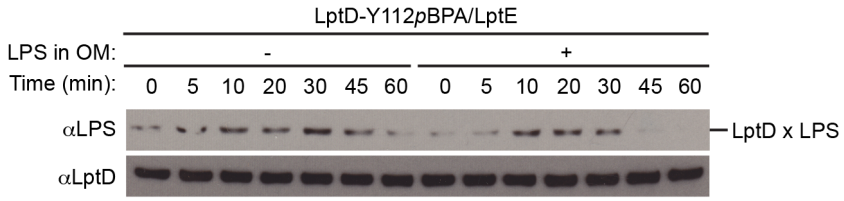

Figure 4.5. LPS transport through LptD *in vitro* stops as LPS accumulates in the membrane. Proteoliposomes containing LptD-Y112*p*BPA/LptE were prepared using *E. coli* phospholipids with or without LPS. These proteoliposomes were pre-incubated with mature LptA. Following ultracentrifugation, these proteoliposomes and any associated LptA were resuspended and incubated with proteoliposomes containing LptBFGC, *E. coli* phospholipids, and LPS. The assay was initiated with addition of 5 mM ATP/2 mM $MgCl_2$. At specific time points, aliquots were removed and UV-irradiated. Samples were then subject to SDS-PAGE followed by immunoblotting with anti-LPS antiserum to detect crosslinked adducts (LptD x LPS). Assays were done at 30°C.

4.6 Conclusion

In this chapter, we have demonstrated that we can reconstitute LPS transport by the Lpt proteins spanning two proteoliposomes. Monitoring LPS transport over time led us to propose a hypothesis about a potential regulatory mechanism at the OM. This reconstitution works when LptA is pre-incubated with OM proteoliposomes; it is unclear whether this reconstitution can be made to work with a broken bridge, but preliminary experiments did not demonstrate clear crosslinking to LptD when the two sets of preoliposomes were separated. This observation lends further support for the "PEZ" model of LPS transport.

This reconstitution provides the first biochemical tools to study the full process of LPS transport, including the OM translocon, LptDE. Although this reconstitution reports on crosslinking to LptD at position 112, it is possible to overexpress and purify different LptDE complexes with *p*BPA at other positions. This assay can also be used to study interactions of LPS with LptE. The observation that LPS in the OM might signal a change in LptDE suggests that the current crystal structures of LptDE, which likely represent a "resting state" that can

crystallize, might not be the only state of the translocon (12, 16). It would not be surprising if interactions with LPS alter the conformation of the OM complex to reflect different stages of transport and assembly.

The described method for bridging two proteoliposomes *in vitro* can be used to develop assays that directly detect LPS insertion into proteoliposomes by LptDE. LPS insertion into the membrane can perhaps be detected by incorporating probes into the lumen of the OM proteoliposomes that create a signal when LPS is present. The described method for bridging proteoliposomes can also be used for structural studies, such as cryo-electron microscopy, to investigate macroscopic features of the Lpt bridge structure.

Finally, the reconstitution has taught us about a potential regulatory mechanism of the Lpt pathway. The "PEZ" model proposes that multiple rounds of ATP hydrolysis are required to push LPS through the transenvelope bridge. Therefore, ATP is required to transport LPS in the forward direction. This model does not explain how the cell knows to stop transporting LPS when enough has been assembled in the OM. The development of this pure reconstitution of LPS transport indicates a potential mechanism by which LPS transport can be "turned off." It is possible that once enough LPS has been transported to the OM, the conformation of LptDE changes, making it unable to receive more LPS. We observe buildup of LPS in LptA at this point. We previously observed that LptC reduces the activity of LptBFG in proteoliposomes containing LPS (see Chapter 3). This is consistent with a model by which a full OM causes LptDE to "turn off," causing LPS to accumulate in LptA and LptC until the entire pathway eventually shuts down. This model suggests that the Lpt pathway might be able to communicate forward from the IM (the "PEZ" model) and backward from the OM when enough LPS has reached its destination.

4.7 Materials and Methods

4.7.1 Strains and Plasmids

Strains used in this study are listed in Table 4.1. Primers are listed in Table 4.2. All restriction enzymes are from New England Biolabs.

Construction of plasmid pET23/42LptD-His_8 has been previously reported (17). Plasmid pET23/42LptD-Y112Am-His_8 was made by mutagenizing plasmid pET23/42LptD-His_8 with KOD Hot Start Polymerase (Novagen) and primers LptD-Y112Am-f and LptD-Y112Am-r. The PCR product of the site-directed mutagenesis (SDM) reaction was digested with DpnI (New England Biolabs) and introduced into NovaBlue competent cells by heat-shock. Transformants were selected in media containing carbenicillin (50 μg/mL). After confirming plasmid DNA sequence, mutagenized plasmids were introduced into NovaBlue cells.

Construction of plasmid pET23/42LptD-Y112Am was done by mutagenizing plasmid pET23/42LptD, which has previously been reported (13), using SDM with primers LptD-Y112Am-f and LptD-Y112Am-r.

Plasmid pET43.1b(+)LptA was constructed by Dr. Shu Sin Chng. To make this plasmid, the DNA fragment encoding mature LptA (amino acids 28 – 185) was amplified by PCR from MC4100 genomic DNA using primers yhbNN-SmaI and yhbNC-AvrII. The amplified fragment encoding mature LptA was digested with restriction enzymes SmaI and AvrII and ligated into pET43.1b(+) (Novagen) between the respective restriction sites to make pET43.1b(+)LptA. The ligation product was transformed into NovaBlue competent cells by heat-shock, and transformants were selected in media containing carbenicillin (50 μg/mL). Plasmids were purified from individual colonies and sequenced.

Plasmid pET43.1b(+)LptA-I36Am was constructed by mutagenizing plasmid pET43.1b(+)LptA using SDM with primers LptA-I36Am-f and LptA-I36Am-r.

Table 4.1. Strains used in this study.

Strain	Genotype	Reference
BL21(λDE3)	F^- *ompT gal dcm lon hsd*$S_B(r_B^-, m_B^-)$ λ(DE3)	Novagen
NovaBlue	*endA1 hsd*R17 (r_K^-, m_K^+) *sup*E44 *thi*-1 *rec*A1 *gyr*A96 *rel*A1 *lac* F′[*pro*A^+B^+ *lac*I^qZΔM15::Tn*10*]	Novagen
MC4100	F^- *araD139* Δ(*arg*F-*lac*)U169 *rpsL150 relA1 flbB5301 deoC1 ptsF25 rbsR*	(18)

Table 4.2. Primers.

Primer name	Primer Sequence (5' to 3')
LptD-Y112Am-f	CTCGGTAATGTCCATTAGGACGATAACCAGGTG
LptD-Y112Am-r	GGACATTACCGAGCGCATCAACGGTAC
yhbNN-SmaI	ATATCCCGGGTAACCGGAGACACTGATCAG
yhbNC-AvrII	ATATCCTAGGTTAATTACCCTTCTTCTGTGCCG
LptA-I36Am-f	CACTGATCAGCCGTAGCACATTGAATCG
LptA-I36Am-r	CGATTCAATGTGCTACGGCTGATCAGTG

4.7.2 *In Vivo* Photocrosslinking

To photocrosslink LptD to LPS in *E. coli*, the previously reported method was followed (9). To make the strains used for photocrosslinking, MC4100 harboring pSup-BpaRS-6TRN (described in Chapter 3) was transformed with plasmid pET23/42LptD-His_8 or pET23/42LptD-Y112Am-His_8 and grown in LB broth supplemented with carbenicillin (50 μg/mL), chloramphenicol (30 μg/mL), and 0.8 mM *p*BPA (Bachem). To detect photocrosslinked adducts, final gel samples were boiled for 10 min and loaded onto 4-20% polyacrylamide gradient gels. The proteins were transferred onto Immun-Blot® PVDF membranes (Bio-Rad) and subjected to immunoblotting using polyclonal anti-LptD antiserum and anti-LPS mouse monoclonal antiserum (Hycult Biotech). Anti-LptD antiserum was provided by Shin-ichi Matsuyama

(Rikkyo University, Tokyo, Japan). Membranes were subsequently immunoblotted with donkey anti-rabbit and sheep anti-mouse horseradish peroxidase (HRP) conjugate secondary antibodies (GE Amersham) for LptD and LPS blots, respectively. Bands were visualized using ECL™ Prime Western Blotting Detection Reagent (GE Amersham) and Biomax Light Film (Kodak).

4.7.3 Overexpression and Purification of LptD-Y112*p*BPA/LptE-His

To overexpress LptD-Y112*p*BPA/LptE-His, BL21(λDE3) harboring pSup-BpaRS-6TRN were transformed with plasmids pET23/42LptD-Y112Am and pCDFLptE-His_6 (13). The reported protocol was followed for overexpressing and purifying this complex, with the inclusion of 30 μg/mL chloramphenicol and 0.5 mM *p*BPA in the LB broth in addition to the other reported additives (13). Protein was flash frozen in liquid nitrogen and stored at -80°C until use. Purity was assessed by SDS-PAGE using 4-20% polyacrylamide gradient gels.

4.7.4 Preparation of LptA

4.7.4.1 Overexpression and Purification of Nus-His-LptA

To overexpress and purify Nus-His-LptA for use in the reconstitution, BL21(λDE3) cells were transformed with pET43.1b(+)LptA. Cultures were grown at 37°C after diluting overnight cultures 1 to 100 into fresh LB broth supplemented with 50 μg/mL carbenicillin. Cells were grown to OD_{600} ~ 0.5, and the temperature was reduced to 16°C. Overexpression was induced by addition of 50 μM isopropyl-β-D-1-thiogalactopyranoside (IPTG), and the cells were grown for 16 h at 16°C. Cells were harvested by centrifugation at 5,000 x *g* for 20 min. Cells were resuspended in Tris-buffered saline (TBS; 20 mM Tris, pH 8.0, 150 mM NaCl), 10% glycerol supplemented with 1 mM phenylmethanesulfonylfluoride (PMSF, Sigma), 100 μg/mL lysozyme

(Sigma), and 50 μg/mL DNase I (Sigma). Cells were lysed by two passages through an EmulsiFlex-C3 high pressure cell disruptor (Avestin Inc.) and centrifuged at 5,000 x *g* for 10 min to remove unbroken cells. The supernatant was centrifuged at 100,000 x *g* for 30 min to remove membranes. Imidazole was then added to the supernatant to a final concentration of 10 mM. Ni-NTA Superflow resin (Qiagen) was pre-washed with TBS, 10% glycerol in preparation for batch nickel affinity chromatography. The supernatant was then flowed over the pre-washed Ni-NTA resin three times at 4°C. The resin was subsequently washed with 20 column volumes of TBS with 10% glycerol and 20 mM imidazole. The protein was then eluted in one batch with 4 column volumes of TBS with 10% glycerol and 200 mM imidazole. The eluate was concentrated with an Amicon centrifugation filter, 10 kDa MWCO to ~ 10 mg/mL. The concentrated protein was either cleaved immediately with thrombin (see Section 4.7.4.2) or flash frozen in liquid nitrogen and stored at -80°C in aliquots until use.

Nus-His-LptA-I36*p*BPA was purified as described for the wild-type construct, but the overexpression strain was BL21(λDE3) harboring both pET43.1b(+)LptA-I36Am and pSup-BpaRS-6TRN. Cultures were grown at 37°C after diluting overnight cultures 1 to 100 into fresh LB broth supplemented with 50 μg/mL carbenicillin, 30 μg/mL chloramphenicol, and 0.8 mM *p*BPA. Cells were grown to OD_{600} ~ 1, and the temperature was reduced to 16°C. Overexpression was induced by addition of 10 μM isopropyl-β-D-1-thiogalactopyranoside (IPTG), and the cells were grown for 16 h at 16°C. The purification procedure was the same as above.

4.7.4.2 Thrombin Cleavage of Nus-His-LptA

Nus-His-LptA was cleaved with Restriction Grade Thrombin (EMD Millipore) for 16 h at room temperature (~ 22°C). Nus-His-LptA was either cleaved immediately after purification, or an aliquot was thawed on ice and cleaved. For the cleavage reaction, 0.00396 U enzyme was used per μg Nus-His-LptA. The cleavage mixture was either used immediately for the reconstitution or flash frozen in liquid nitrogen and stored at -80°C until use.

4.7.5 Proteoliposome Preparation

Proteoliposomes containing LptBFGC and LPS were prepared as described in Chapter 3. To make proteoliposomes containing LptD-Y112*p*BPA/LptE, a similar method was used. First, a 30 mg/mL sonicated aqueous suspension of *E. coli* polar lipid extract (Avanti Polar Lipids, Inc.) was prepared. If not used immediately to prepare proteoliposomes, aliquots were flash frozen in liquid nitrogen and stored at -80°C. When ready for use, aliquots of liposomes were thawed at room temperature. A mixture with the following final concentrations was prepared in Tris-buffered saline (TBS; 20 mM Tris, pH 8.0, 150 mM NaCl): 9 mg/mL liposomes, 1.25% *n*-octyl-β-D-glucopyranoside (OG, Anatrace), and 1.5 μM purified LptD-Y112*p*BPA/LptE. While making this mixture, first the OG was added to the liposomes to make detergent-destabilized liposomes. The mixture was kept on ice for 10 min. The protein complex was added, and the mixture was left on ice for 20 min. The mixture was then added to an ultracentrifuge tube and diluted 100x with cold TBS. After letting the dilute mixture sit on ice for 30 min, the proteoliposomes were pelleted by ultracentrifugation at 300,000 x *g* for 2 h at 4°C. For every 100 μL original mixture (prior to the dilution step), 200 μL cold TBS, 10% glycerol was added.

If the resuspended proteoliposomes were not used immediately, they were flash frozen in liquid nitrogen and stored at -80°C.

To prepare OM proteoliposomes containing LPS, a 2 mg/mL sonicated aqueous suspension of Ra-LPS (Sigma) was added to the initial mixture to a final concentration of 0.5 mg/mL, as for the IM proteoliposomes (see Chapter 3).

4.7.6 Reconstitution of LPS Transport

4.7.6.1 Preparation of OM Proteoliposomes with LptA

Prior to reconstitution experiments, 100 µL proteoliposomes containing LptD-Y112*p*BPA/LptE were incubated with 113 µg protein from the LptA thrombin cleavage reaction for 30 min at 4°C (volumes were scaled to account for assay volumes, described in Section 4.7.6.2). The proteoliposomes and any associated LptA were pelleted by ultracentrifugation at ~ 300,000 x *g* for 3 h at 4°C in an Optima™ MAX-E (Beckman Coulter Inc.). After removing the supernatant, the pellet was resuspended in 36.5 µL cold TBS, 10% glycerol and either used immediately or flash frozen in liquid nitrogen and stored at -80°C until use.

4.7.6.2 Assay for LPS Transport to LptD

All assays were done in 50 mM Tris-HCl, pH 8.0, 500 mM NaCl, 10% glycerol (final concentrations). Assay mixtures contained 60% LptBFGC proteoliposomes by volume (prepared as described in Section 3.7.3, thawed on ice) and 10% resuspended OM proteoliposomes (with any associated LptA) by volume (prepared as described in Section 4.7.6.1). This allowed for approximately equimolar amounts of IM and OM complexes in the final assay mixture. The remaining volume was composed of Tris-HCl, NaCl, and glycerol such

that the final concentrations would be the values mentioned above. The mixture was kept at 4°C for 15 min prior to initiating the reactions. Reactions were initiated at 30°C with the addition of ATP/$MgCl_2$ or just $MgCl_2$ (final concentrations were 5 mM ATP, 2 mM $MgCl_2$). At specified time points, 25 µL aliquots were removed from the reactions and added to a microtiter plate, which was subsequently irradiated with UV light (365 nm) on ice for five minutes using a B-100AP lamp (UVP). Following UV-irradiation, aliquots were added to 225 µL cold TBS, 0.1% Anzergent 3-14 (Anatrace). To each sample, 250 µL 20% trichloroacetic acid (TCA) was added. The proteins were precipitated on ice, followed by a cold acetone wash. Precipitates were resuspended in 30 µL 2x SDS-PAGE sample buffer supplemented with 5% β-mercaptoethanol. Samples were boiled for 10 min and loaded onto 4-20% gradient SDS-polyacrylamide gels. The proteins were transferred onto Immun-Blot® PVDF membranes and subjected to immunoblotting using polyclonal anti-LptD antiserum and anti-LPS mouse monoclonal antiserum. Membranes were subsequently immunoblotted with donkey anti-rabbit and sheep anti-mouse HRP conjugate secondary antibodies for LptD and LPS blots, respectively. Bands were visualized as described in Section 4.7.2.

4.8 References

1. Ruiz N, Kahne D, & Silhavy TJ (2009) Transport of lipopolysaccharide across the cell envelope: the long road of discovery. *Nat Rev Microbiol* 7(9):677-683.

2. Tefsen B, Geurtsen J, Beckers F, Tommassen J, & de Cock H (2005) Lipopolysaccharide transport to the bacterial outer membrane in spheroplasts. *J Biol Chem* 280(6):4504-4509.

3. Chng SS, Gronenberg LS, & Kahne D (2010) Proteins required for lipopolysaccharide assembly in Escherichia coli form a transenvelope complex. *Biochemistry* 49(22):4565-4567.

4. Freinkman E, Okuda S, Ruiz N, & Kahne D (2012) Regulated Assembly of the Transenvelope Protein Complex Required for Lipopolysaccharide Export. *Biochemistry* 51(24):4800-4806.

5. Villa R*, et al.* (2013) The Escherichia coli Lpt Transenvelope Protein Complex for Lipopolysaccharide Export Is Assembled via Conserved Structurally Homologous Domains. *J Bacteriol* 195(5):1100-1108.

6. Nikaido H (2009) Multidrug resistance in bacteria. *Annu Rev Biochem* 78:119-146.

7. Nikaido H & Takatsuka Y (2009) Mechanisms of RND multidrug efflux pumps. *Biochim Biophys Acta* 1794(5):769-781.

8. Zgurskaya HI & Nikaido H (1999) Bypassing the periplasm: reconstitution of the AcrAB multidrug efflux pump of Escherichia coli. *Proc Natl Acad Sci U S A* 96(13):7190-7195.

9. Okuda S, Freinkman E, & Kahne D (2012) Cytoplasmic ATP hydrolysis powers transport of lipopolysaccharide across the periplasm in E. coli. *Science* 338(6111):1214-1217.

10. Suits MD, Sperandeo P, Deho G, Polissi A, & Jia Z (2008) Novel structure of the conserved gram-negative lipopolysaccharide transport protein A and mutagenesis analysis. *J Mol Biol* 380(3):476-488.

11. Tran AX, Dong C, & Whitfield C (2010) Structure and functional analysis of LptC, a conserved membrane protein involved in the lipopolysaccharide export pathway in Escherichia coli. *J Biol Chem* 285(43):33529-33539.

12. Qiao S, Luo Q, Zhao Y, Zhang XC, & Huang Y (2014) Structural basis for lipopolysaccharide insertion in the bacterial outer membrane. *Nature* 511(7507):108-111.

13. Chng SS, Ruiz N, Chimalakonda G, Silhavy TJ, & Kahne D (2010) Characterization of the two-protein complex in Escherichia coli responsible for lipopolysaccharide assembly at the outer membrane. *Proc. Natl. Acad. Sci. U. S. A.* 107(12):5363-5368.

14. Freinkman E, Chng SS, & Kahne D (2011) The complex that inserts lipopolysaccharide into the bacterial outer membrane forms a two-protein plug-and-barrel. *Proc. Natl. Acad. Sci. U. S. A.* 108(6):2486-2491.

15. Osborn MJ, Gander JE, & Parisi E (1972) Mechanism of assembly of the outer membrane of Salmonella typhimurium. Site of synthesis of lipopolysaccharide. *J Biol Chem* 247(12):3973-3986.

16. Dong H*, et al.* (2014) Structural basis for outer membrane lipopolysaccharide insertion. *Nature* 511(7507):52-56.

17. Wu T*, et al.* (2006) Identification of a protein complex that assembles lipopolysaccharide in the outer membrane of Escherichia coli. *Proc. Natl. Acad. Sci. U. S. A.* 103(31):11754-11759.

18. Casadaban MJ (1976) Transposition and fusion of the lac genes to selected promoters in Escherichia coli using bacteriophage lambda and Mu. *J Mol Biol* 104(3):541-555.